

11-00

108046

p. 79

---

# Comparison of Three Controllers Applied to Helicopter Vibration

---

Jane A. Leyland

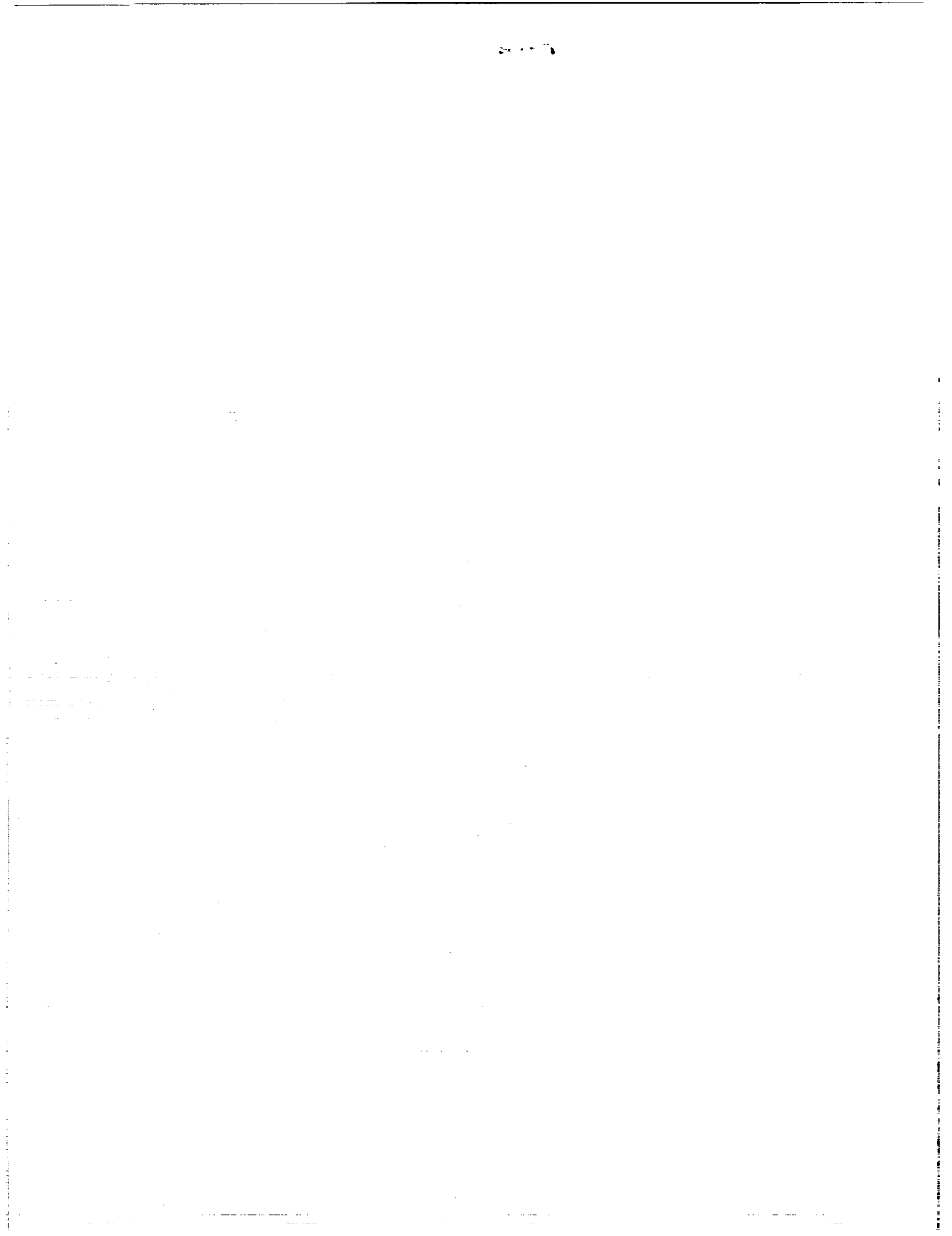
---

(NASA-TM-102192) COMPARISON OF THREE  
CONTROLLERS APPLIED TO HELICOPTER VIBRATION  
(NASA) 79 p

N92-28457

Unclas  
G3/08 0108046

May 1992



---

# Comparison of Three Controllers Applied to Helicopter Vibration

---

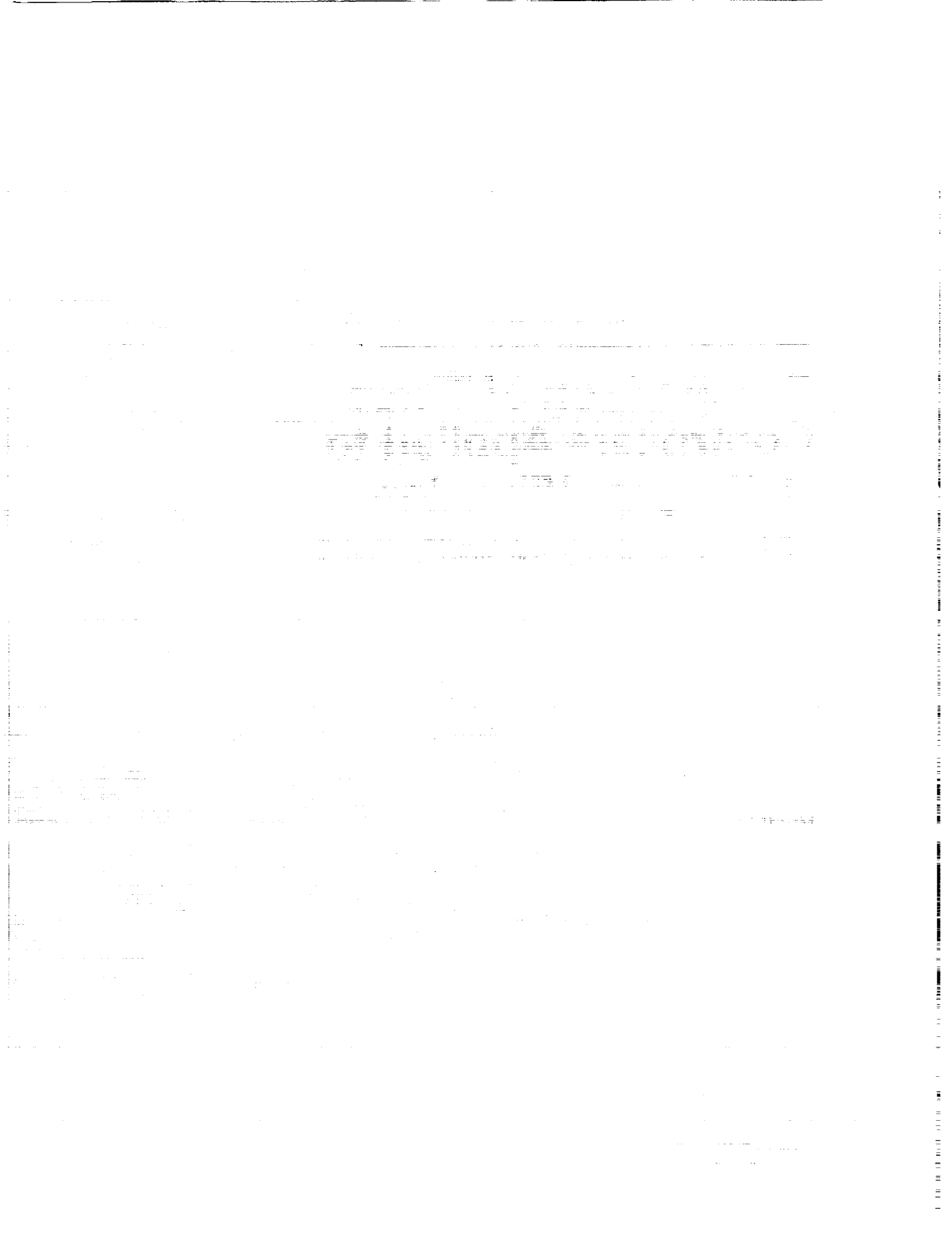
Jane A. Leyland, Ames Research Center, Moffett Field, California

May 1992



National Aeronautics and  
Space Administration

**Ames Research Center**  
Moffett Field, California 94035-1000



# CONTENTS

<b>NOMENCLATURE</b>	v
<b>SUMMARY</b>	1
<b>1 INTRODUCTION</b>	1
<b>2 TECHNICAL CONSIDERATIONS</b>	2
2.1 Systems Models . . . . .	2
2.1.1 Local Model . . . . .	2
2.1.2 Global Model . . . . .	2
2.2 Plant Model and Propagation . . . . .	3
2.2.1 Plant Initialization . . . . .	3
2.2.2 Initial Estimate of the Plant for the Identification Algorithm . . . . .	3
2.2.3 Plant Propagation . . . . .	4
2.2.4 Actual Vibration Response . . . . .	5
2.2.5 Measured Vibration Response . . . . .	5
2.3 General Controller Definition . . . . .	6
2.3.1 Vibration Minimization as a Trajectory Optimal Control Problem . . . . .	6
2.3.2 Kalman Filter Plant Matrix Identification . . . . .	9
2.4 Description of Controllers . . . . .	11
2.4.1 Deterministic Controller . . . . .	12
2.4.2 Stochastic Controllers . . . . .	13
2.4.2.1 Cautious Controller . . . . .	13
2.4.2.2 Dual Controller . . . . .	15
<b>3 COMPARISON STUDY</b>	16
3.1 Baseline Controller . . . . .	16
3.1.1 Initial Random Number Generator Seed . . . . .	16
3.1.2 Control Limiting . . . . .	16
3.1.2.1 External Limiting . . . . .	17
3.1.2.2 Internal Limiting . . . . .	17
3.1.3 Plant Matrix Propagation Rate . . . . .	19
3.2 Effect of the Initial Estimate of the $T$ -Matrix on Controller Performance . . . . .	19

3.3	Effect of the Plant Matrix Propagation Rate on Controller Performance . . . . .	20
3.4	Effect of Measurement Noise on Controller Performance . . . . .	21
3.4.1	Random Nonperiodic Measurement Noise . . . . .	21
3.4.2	Random Periodic Measurement Noise . . . . .	22
3.4.3	Nonrandom Periodic Measurement Noise . . . . .	23
<b>4</b>	<b>RESULTS</b>	<b>23</b>
4.1	Results Obtained from the Comparison Study . . . . .	25
4.2	Identification of Possible Causes of the Results of this Study . . . . .	26
4.2.1	Random Plant Model Versus Detailed Simulations Used on Previous Studies . . . . .	27
4.2.2	Plant Matrix Identification . . . . .	27
4.2.3	Stochastic Term in Performance Index . . . . .	27
4.2.4	Coalescence of Stochastic Controllers with the Deterministic Controller . . . . .	28
4.3	Theoretical Limitations of These Controllers . . . . .	29
4.3.1	Definition of the Optimal Control Problem . . . . .	29
4.3.1.1	Deterministic Part . . . . .	29
4.3.1.2	Stochastic Part . . . . .	30
4.3.2	Limitations of the Plant Matrix Identification Algorithm . . . . .	30
<b>5</b>	<b>FUTURE CONTROLLER DEVELOPMENT</b>	<b>30</b>
5.1	Theoretical Considerations . . . . .	31
5.1.1	Deterministic Part . . . . .	31
5.1.2	Stochastic Part . . . . .	31
5.1.3	Plant Matrix Identification . . . . .	32
5.2	Cockpit Application . . . . .	32
	<b>REFERENCES</b>	<b>33</b>
	<b>TABLES</b>	<b>34</b>
	<b>FIGURES</b>	<b>44</b>

## NOMENCLATURE

<i>A</i>	the square of a constraint bound
<i>C<sub>C</sub></i>	a coefficient in equation (2-6) which can either be identically equal to one for nonperiodic cases, or equal to the required periodic function for periodic cases
<i>C<sub>E</sub></i>	scaling coefficient for the random increment matrix term in equation (2-3) ( <i>C<sub>E</sub></i> = 0.001 for this study)
<i>C<sub>M</sub></i>	scaling coefficient for the random increment matrix term in equation (2-6). The baseline value of <i>C<sub>M</sub></i> selected for this study is 0.2000
<i>C<sub>ρ</sub></i>	scaling coefficient for the random increment matrix term in equation (2-4)
<i>f(Z)</i>	the probability density function <i>Z</i>
<i>f[Z(θ)]</i>	the performance index, which is a scalar function of <i>Z(θ)</i>
<i>F[Z(θ), Θ]</i>	augmented performance index, which is a scalar function of <i>Z(θ)</i> and <i>Θ</i>
<i>g.l.b.</i>	greatest lower bound
<i>HHC</i>	higher harmonic control
<i>J</i>	scalar performance index
<i>J<sub>Z</sub></i>	that part of the scalar performance index dependent on <i>Z</i>
<i>J<sub>θ</sub></i>	that part of the scalar performance index dependent on <i>θ</i>
<i>K</i>	Kalman filter gain vector
<i>L</i>	number of accelerometers used to measure the vibration ( <i>L</i> = 6 for this study)
<i>l.u.b.</i>	least upper bound
<i>M</i>	principal dimension of the Theta-vector equal to 6 for the local model and 7 for the global model, also the number of inequality constraints
<i>N</i>	number of blades in the rotor system ( <i>N</i> = 4 for this study)
<i>P</i>	covariance of the <i>T</i> -Matrix row currently being identified, evaluated after the measurement of the <i>Z</i> -Vector during the current cycle. The dimension is ( <i>M</i> × <i>M</i> ) for the matrix and ( <i>M</i> × <i>M</i> × 2 <i>L</i> ) for the rank 3 tensor
<i>Q</i>	covariance of the <i>j</i> -th row of the forcing function part of the <i>T</i> -Matrix. The dimension is ( <i>M</i> × <i>M</i> ) for the matrix and ( <i>M</i> × <i>M</i> × 2 <i>L</i> ) for the rank 3 tensor
<i>R</i>	(1 × 1) scalar covariance of the measurement noise
<i>R<sub>Δθ</sub></i>	external limiting envelope bound for <i>Δθ</i>
<i>R<sub>θ</sub></i>	external limiting envelope bound for <i>θ</i>
<i>S<sub>i</sub></i>	<i>P<sub>i</sub></i> + <i>Q<sub>i</sub></i> . The dimension is ( <i>M</i> × <i>M</i> ) for the matrix and ( <i>M</i> × <i>M</i> × 2 <i>L</i> ) for the rank-3 tensor
<i>RTA</i>	Rotor Test Apparatus
<i>t</i>	time expressed in rotor revolutions
<i>T</i>	plant matrix, quasi-static transfer matrix, <i>T</i> -Matrix. The dimension is (2 <i>L</i> × <i>M</i> ) (i.e., (2 <i>L</i> × 6) for the local model and (2 <i>L</i> × 7) for the global model)
<i>T̂<sub>j</sub></i>	<i>j</i> -th row of the <i>T</i> -Matrix (for <i>j</i> = 1, 2, ..., 2 <i>L</i> ), a row vector with dimension (1 × <i>M</i> )
<i>T̂</i>	estimate of the <i>T</i> -Matrix
<i>VCS</i>	Vibration Control system
<i>W<sub>Z</sub></i>	diagonal ( <i>M</i> × <i>M</i> ) weighting matrix for the quadratic <i>Z</i> -Vector metric

$W_{\Delta\theta}$	diagonal ( $M \times M$ ) weighting matrix for the quadratic $\Delta\theta$ -Vector term in the performance index
$W_{\theta}$	diagonal ( $M \times M$ ) weighting matrix for the quadratic Theta-Vector term in the performance index
$Z$	a vector of the coefficients of the cosine and sine terms of the vibration output vector, the actual helicopter vibration response $Z$ -Vector defined by equation (2-5). $Z$ is a vector function of $\theta$ and, correspondingly, is also written $Z(\theta)$ . The dimension is ( $2L \times 1$ )
$\bar{Z}$	measured helicopter vibration response $Z$ -Vector defined by equation (2-6)
$\alpha$	a slack variable corresponding to an inequality constraint; a vector, Alpha-Vector, whose elements are the slack variables
$\Delta\theta$	change in $\theta$ during one revolution of the rotor (i.e., $\Delta\theta = \theta_i - \theta_{i-1}$ )
$\theta$	Theta-vector whose elements are the $N - 1$ , the $N$ , and the $N + 1$ harmonic cosine and sine Fourier coefficients of the blade pitch control as defined in the rotating system, and whose last element is identically equal to one for the global model. The dimension is ( $M \times 1$ ) (i.e., ( $6 \times 1$ ) for the local model and ( $7 \times 1$ ) for the global model)
$\Theta$	augmented Theta-Vector composed of the Theta-Vector and the Alpha-Vector
$\lambda$	adjoint coefficient, vector of adjoint coefficients, a Lagrangian multiplier, the adjoint vector composed of Lagrangian multipliers; also a parameter used to adjust the magnitude of the stochastic term relative to the nonstochastic terms in the performance index and control laws of the stochastic controllers
$\nu$	vector composed of uniform distribution random numbers $\in [0.0, 1.0]$ . $\nu$ has the same dimension as the $Z$ -Vector
$\xi$	matrix composed of uniform distribution random numbers $\in [0.0, 1.0]$ . $\xi$ has the same dimension as the $T$ -matrix
$\sigma$	phase of the sinusoidal coefficient of the random term in equation (2-6) expressed in a nondimensional fraction of a rotor revolution
$\tau$	period of the sinusoidal coefficient of the random term in equation (2-6) expressed in rotor revolutions
$\phi$	equality constraint function, a vector composed of equality constraint functions
$\psi$	inequality constraint function, a vector composed of inequality constraint functions

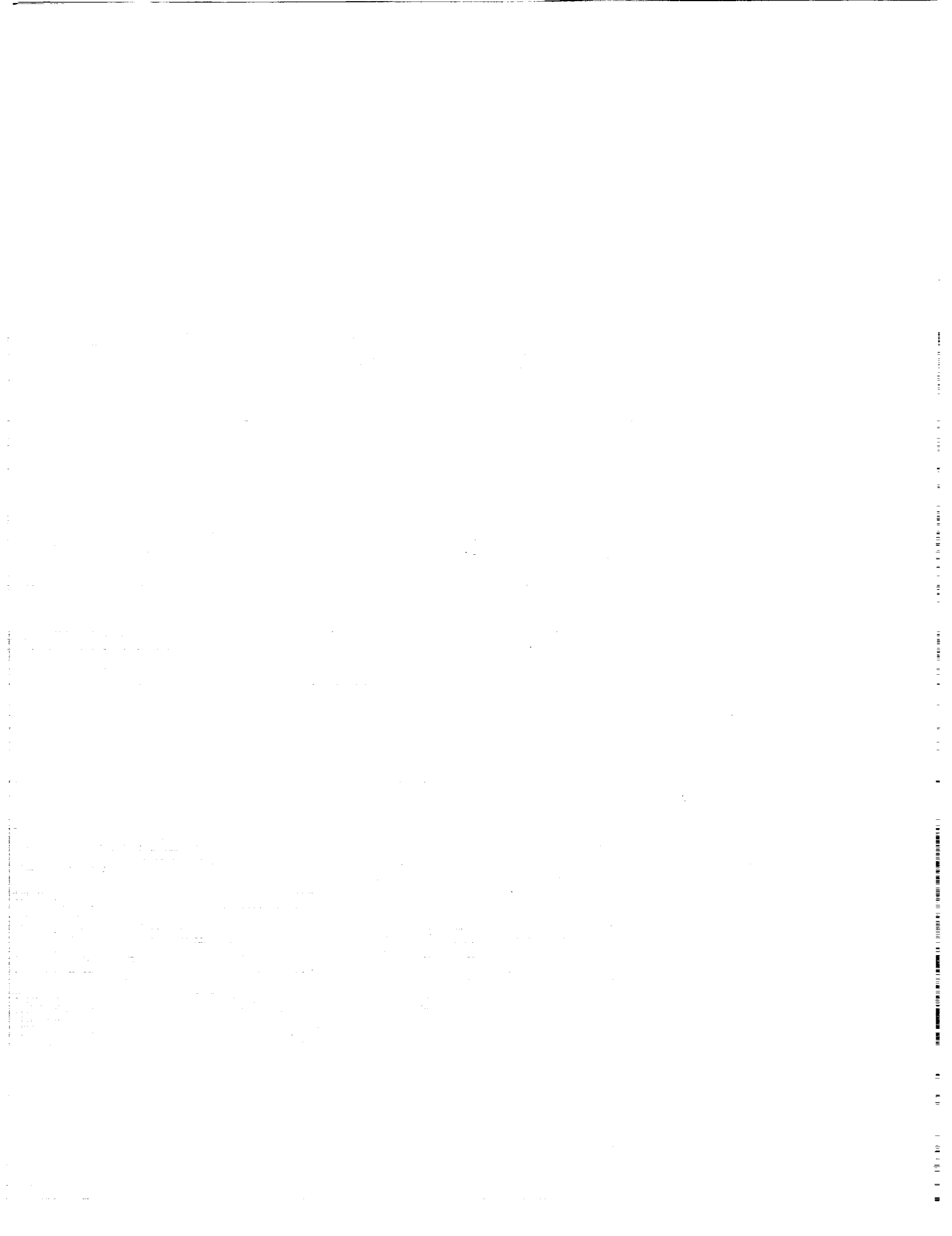
### Superscripts

$T$	transpose of a matrix
$-1$	inverse of a matrix
*	the solution (e.g., the optimal) value of a variable

### Subscripts

$i$	time point number (e.g., number of rotor revolutions)
$j$	$T$ -Matrix row number ( $j = 1, 2, \dots, 2L$ ), also constraint function index
$k$	constraint function and slack variable index

<i>L</i>	number of accelerometers used to measure the vibration ( $L = 6$ for this study)
<i>M</i>	number of inequality constraints
<i>N</i>	number of blades in the rotor system ( $N = 4$ for this study)
0	uncontrolled condition (i.e., evaluated for a zero Theta-Vector)



## SUMMARY

A comparison was made of the applicability and suitability of the deterministic controller, the cautious controller, and the dual controller for the reduction of helicopter vibration by using higher harmonic blade pitch control. A randomly generated linear plant model was assumed and the performance index was defined to be a quadratic output metric of this linear plant. A computer code, designed to check out and evaluate these controllers, was implemented and used to accomplish this comparison. The effects of random measurement noise, the initial estimate of the plant matrix, and the plant matrix propagation rate were determined for each of the controllers. With few exceptions, the deterministic controller yielded the greatest vibration reduction (as characterized by the quadratic output metric) and operated with the greatest reliability. Theoretical limitations of these controllers were defined and appropriate candidate alternative methods, including one method particularly suitable to the cockpit, were identified.

## 1 INTRODUCTION

The reduction of rotorcraft vibration and loads is an important means to extend the useful life of the vehicle and to improve its ride quality. Although vibration reduction can be accomplished by using passive dampers and/or tuned masses, active control has the potential to reduce vibration throughout a wider flight regime while requiring less additional weight to the aircraft than would be required when employing either the passive dampers or the tuned masses.

Davis (ref. 1) investigated the use of the deterministic, cautious, and dual controllers to provide higher harmonic blade pitch control for the four-bladed H-34 rotor mounted on NASA's Rotor Test Apparatus (RTA) (ref. 2). For this investigation, Davis employed a detailed, nonlinear, aeroelastic helicopter vibration simulation, the G400 computer code (a detailed nonlinear aeroelastic helicopter vibration simulation, United Technologies Research Center), to determine the RTA vibration response to the higher harmonic blade pitch control defined by the controller being investigated. Davis concluded that the deterministic, cautious, and dual controllers provided excellent performance over a wide range of steady flight conditions for both the global model system and the local model system, and that there is no apparent advantage to using any particular subject controller or any particular model system for the conditions which were considered. Davis further concluded that these controllers exhibited good performance characteristics, when "properly tuned," for transient cases which result from sudden changes in thrust. The subject controllers employed two suboptimal methods, internal limiting and external limiting, to impose constraints on the control vector. Davis concluded that of the two constraint methods, internal limiting worked best for the deterministic controller.

This document discusses a comparison of the aforementioned controllers for a more general application than that considered by Davis; a randomly generated linear plant was employed rather than Davis's detailed helicopter simulation. Use of a randomly generated linear plant provides a convenient and relatively efficient means to evaluate the effectiveness as well as the robustness of the controller being considered. Care must be exercised, however, in the selection of the governing parameters for the random models which are employed by this scheme.

## 2 TECHNICAL CONSIDERATIONS

Helicopter vibration is, in general, a highly nonlinear phenomenon. As in Davis's investigation (ref. 1), it is assumed in this study that the relationship between the helicopter's vibration response (the  $Z$ -Vector) and its higher harmonic blade pitch control (the Theta-Vector) can be adequately modeled with a quasi-static transfer matrix (the  $T$ -Matrix) that linearly relates the two over the feasible range of control (i.e., the range of interest). This transfer matrix is the helicopter plant matrix for this assumed linear model. The objective of the subject controllers of this investigation (i.e., the deterministic, the cautious, and the dual controllers) is to minimize the helicopter's vibration response along the state trajectory by defining the optimal control vector, which is, in general, subject to constraints. In this case, the state trajectory is the time propagation of the  $T$ -Matrix, and the vibration is controlled via the control vector and is measured at closely spaced, discrete time points along the state trajectory.

### 2.1 Systems Models

Two principal systems models were considered by Davis, the local and the global models. For both models it is assumed that, at each of the discrete time points along the state trajectory at which the control is to be exercised, the relationship between the helicopter's vibration response and its higher harmonic blade pitch control can be adequately modeled with a  $T$ -Matrix that linearly relates the two over the feasible range of control (i.e., the control constraints are satisfied).

#### 2.1.1 Local Model

The local model defines the change in vibration response due to a change in the control vector between the current time and the previous time; specifically

$$Z_i = T(\theta_i - \theta_{i-1}) + Z_{i-1} \quad (2-1)$$

where

$T$	plant matrix, quasi-static transfer matrix, $T$ -Matrix; the dimension is $(2L \times 6)$
$Z$	a vector of the coefficients of the cosine and sine terms of the vibration output vector; the dimension is $(2L \times 1)$
$\theta$	a vector whose elements are the $N - 1$ , the $N$ , and the $N + 1$ harmonic cosine and sine Fourier coefficients of the blade pitch control as defined in the rotating system; the dimension is $(6 \times 1)$
$i$	time point number (e.g., number of rotor revolutions)
$L$	number of accelerometers used to measure the vibration ( $L = 6$ for this study)
$N$	number of blades in the rotor system ( $N = 4$ for this study)

#### 2.1.2 Global Model

The global model defines the vibration response due to the current control vector where the response is measured relative to that for which no control is applied; specifically

$$Z_i = T\theta_i + Z_0 \quad (2-2)$$

which in expanded form is

$$\begin{bmatrix} Z_1 \\ Z_2 \\ Z_3 \\ \vdots \\ \vdots \\ \vdots \\ Z_{12} \end{bmatrix} = \begin{bmatrix} T_{1,1} & T_{1,2} & T_{1,3} & T_{1,4} & T_{1,5} & T_{1,6} & Z_{01} \\ T_{2,1} & T_{2,2} & T_{2,3} & T_{2,4} & T_{2,5} & T_{2,6} & Z_{02} \\ T_{3,1} & T_{3,2} & T_{3,3} & T_{3,4} & T_{3,5} & T_{3,6} & Z_{03} \\ \vdots & \vdots & \vdots & \vdots & \vdots & \vdots & \vdots \\ \vdots & \vdots & \vdots & \vdots & \vdots & \vdots & \vdots \\ \vdots & \vdots & \vdots & \vdots & \vdots & \vdots & \vdots \\ T_{12,1} & T_{12,2} & T_{12,3} & T_{12,4} & T_{12,5} & T_{12,6} & Z_{012} \end{bmatrix} \begin{bmatrix} \theta_1 \\ \theta_2 \\ \theta_3 \\ \theta_4 \\ \theta_5 \\ \theta_6 \\ \frac{1}{i} \end{bmatrix}$$

where

- $T$  augmented plant matrix, augmented quasi-static transfer matrix, augmented  $T$ -Matrix; the last column is the uncontrolled vibration output vector (i.e., the  $Z$ -Vector which corresponds to a zero Theta-Vector); the dimension is  $(2L \times 7)$
- $Z$  a vector of the coefficients of the cosine and sine terms of the vibration output vector; the dimension is  $(2L \times 1)$
- $\theta$  a vector whose first six elements are the  $N - 1$ , the  $N$ , and the  $N + 1$  harmonic cosine and sine Fourier coefficients of the blade pitch control as defined in the rotating system, and whose last element is identically equal to one; the dimension is  $(7 \times 1)$
- $0$  uncontrolled condition (i.e., evaluated for a zero Theta-Vector)
- $i$  time point number (e.g., number of rotor revolutions)
- $L$  number of accelerometers used to measure the vibration ( $L = 6$  for this study)
- $N$  number of blades in the rotor system ( $N = 4$  for this study)

## 2.2 Plant Model and Propagation

A randomly generated plant model, rather than a detailed helicopter simulation, was assumed for this study. The randomly generated model offers the advantage of rapid determination of state while having lower core requirements.

### 2.2.1 Plant Initialization

The  $T$ -Matrix is initialized with randomly selected elements such that the corresponding output response vector (the  $Z$ -Vector) has a norm equal to a specified value. First the initialization procedure randomly selects the elements of a reference control vector (the Theta-Vector) which has a norm equal to a specified value. Then the procedure randomly selects the elements of the  $T$ -Matrix. Using this first  $T$ -Matrix, the corresponding  $Z$ -Vector and its norm are computed. This first value of the  $Z$ -Vector norm is compared with its specified value and is then used to scale the first selected  $T$ -Matrix so that it will yield a  $Z$ -Vector with the specified norm.

### 2.2.2 Initial Estimate of the Plant for the Identification Algorithm

The controller algorithms that Davis studied (ref. 1) required that an initial estimate of the  $T$ -Matrix be provided in order to start the identification process. Accordingly, specification of an initial estimate of the  $T$ -Matrix was required in this comparison study. However, the ability of the identification algorithm

to converge to an acceptable  $T$ -Matrix in a reasonable number of iterations was strongly dependent on how close the initial estimate was to the actual  $T$ -Matrix for the cases which were examined. The obvious implication is that a priori knowledge of the  $T$ -Matrix is required in order to initiate the identification process. Such a priori knowledge of the  $T$ -Matrix can be obtained for  $T$ -Matrices computed by a detailed helicopter simulation such as the G400 utilized by Davis. However, when the initial  $T$ -Matrix is randomly defined, as in the cases reported herein, this a priori knowledge of the  $T$ -Matrix does not exist. The initial estimate of the  $T$ -Matrix is

$$\hat{T} = T + C_E \xi \quad (2-3)$$

where

- $C_E$  initial estimate scaling coefficient for the random increment matrix term (The nominal value of  $C_E$  used in this study is 0.001.)
- $T$  randomly generated reference  $T$ -Matrix (actual  $T$ -Matrix) which represents the actual helicopter plant
- $\hat{T}$  estimate of the  $T$ -Matrix
- $\xi$  matrix composed of uniform distribution random numbers  $\in [0.0, 1.0]$ .  $\xi$  has the same dimension as the  $T$ -Matrix

The numerical values for the elements of  $\xi$  are generated with a random number generator function, which generates a unique sequence of random numbers associated with a "starting seed" value. A starting seed value of 10691 was used throughout this study.

A typical actual  $T$ -Matrix ( $T$  in equation (2-3)) evaluated at the beginning of the fourth rotor revolution is shown below. If  $C_E$  has the value of 0.001 (the nominal value used in this study), each element of the estimated  $T$ -Matrix,  $\hat{T}$ , is within 0.001 of the corresponding element of  $T$ .

$$T = \begin{bmatrix} 0.007993 & -0.013754 & 0.003573 & -0.021985 & -0.005801 & -0.001251 & -0.003533 \\ -0.025252 & -0.000619 & -0.023625 & -0.016151 & -0.014406 & -0.017560 & 0.003986 \\ -0.021377 & -0.002089 & 0.013464 & -0.009670 & 0.007831 & -0.019800 & -0.007464 \\ -0.027889 & -0.004685 & 0.009947 & -0.022052 & -0.018997 & -0.027528 & -0.020086 \\ -0.020592 & -0.020647 & -0.015647 & 0.018364 & 0.024838 & 0.015331 & 0.011077 \\ -0.006769 & 0.023869 & -0.007284 & 0.002757 & -0.013934 & 0.011925 & 0.015603 \\ 0.014590 & 0.024039 & -0.000702 & -0.004288 & 0.023183 & 0.011904 & -0.013820 \\ 0.002893 & 0.026490 & 0.015204 & -0.000985 & -0.009007 & 0.007339 & -0.004398 \\ -0.005821 & -0.003604 & -0.011587 & 0.018989 & 0.002882 & -0.019509 & 0.011354 \\ 0.018340 & 0.009994 & -0.014521 & -0.020836 & 0.017659 & 0.015580 & -0.007720 \\ 0.016701 & -0.020694 & -0.026045 & -0.008956 & -0.029130 & 0.006915 & 0.002154 \\ 0.008342 & 0.021497 & -0.001494 & 0.011485 & 0.001207 & -0.027292 & 0.020534 \end{bmatrix}$$

### 2.2.3 Plant Propagation

The time history of the helicopter plant (i.e., the time history of the  $T$ -Matrix) is the state trajectory which is of concern in this study. Although use of a detailed helicopter simulation is a physically meaningful method to propagate the  $T$ -Matrix state trajectory, use of a random propagation scheme provides a more difficult test for the controller and has the advantage of computational rapidity with minimal core

requirements. Although several random propagation schemes were developed, the following defined method was used throughout this study. The reference  $T$ -Matrix, which represents the actual helicopter plant, was propagated in time according to

$$T_i = T_{i-1} + C_\rho \xi \quad (2-4)$$

where

- $C_\rho$  plant propagation scaling coefficient for the random increment matrix term
- $T$  randomly generated reference  $T$ -Matrix (actual  $T$ -Matrix) which represents the actual helicopter plant
- $\xi$  matrix composed of uniform distribution random numbers  $\in [0.0, 1.0]$ .  $\xi$  has the same dimension as the  $T$ -Matrix
- $i$  time point number (e.g., number of rotor revolutions)

The numerical values of the  $T$ -Matrix elements are generated with a random number generator function, which generates a unique sequence of random numbers associated with a starting seed value. The performance index reduction obtainable at the end of the first controlled step is dependent on the value of this seed, which was arbitrarily selected to be 7391 during the early computational checkout. For this value, however, the performance index only decreased 19.4% by the end of the first controlled step for the unconstrained deterministic controller. A larger first-step reduction is necessary to properly ascertain the effectiveness of the controller being investigated. Accordingly, a seed study was performed in which various values of the starting seed were tried until one was found which would yield an acceptable first-step reduction. As a result of this study, a starting seed value of 83298 was selected. Use of this value resulted in a first-step performance index decrease of 67.0% for the unconstrained deterministic controller. This value was used throughout the remainder of this study.

## 2.2.4 Actual Vibration Response

The actual helicopter vibration response (actual  $Z$ -Vector),  $Z$ , is determined from the actual  $T$ -Matrix,  $T$ , and the current control vector (current Theta-Vector), according to

$$Z = T\theta \quad (2-5)$$

where

- $T$  randomly generated reference  $T$ -Matrix which represents the actual helicopter plant
- $Z$  actual helicopter vibration response  $Z$ -Vector defined by equation (2-5)
- $\theta$  the current and/or most recently defined control Theta-Vector

## 2.2.5 Measured Vibration Response

The measured vibration response (measured  $Z$ -Vector) is the vibration response used by the identification algorithm to identify the  $T$ -Matrix. The measured  $Z$ -Vector differs from the actual  $Z$ -Vector in that it includes measurement noise. The measurement noise can be constrained by either constant bounds or by a sinusoidal envelope as required. The measured  $Z$ -Vector is defined according to

$$\bar{Z} = Z(1.0 + C_M C_C \nu) \quad (2-6)$$

where

$\bar{Z}$	measured helicopter vibration response $Z$ -Vector
$Z$	actual helicopter vibration response $Z$ -Vector
$\nu$	vector composed of uniform distribution random numbers $\in [0.0, 1.0]$ . $\nu$ has the same dimension as the $Z$ -Vector
$C_M$	measured response scaling coefficient for the random increment matrix term
$C_C$	$\begin{cases} 1.0 & \text{if } \tau \geq 1.0D + 10 \\ \cos(360.0^\circ[\sigma + t/\tau]) & \text{if } \tau < 1.0D + 10 \end{cases}$
$\sigma$	phase of the sinusoidal coefficient of the random term expressed in a nondimensional fraction of a rotor revolution
$t$	time expressed in rotor revolutions
$\tau$	period of the sinusoidal coefficient of the random term expressed in rotor revolutions

This technique for introducing random noise defines the numerical values for the elements of  $\nu$  using a random number generator function, which generates a unique sequence of random numbers associated with a starting seed value. A starting seed value of 49377 was used throughout this study.

## 2.3 General Controller Definition

The control acting on the helicopter plant produces a vibration response in accordance with the models presented in sections 2.2.4 and 2.2.5 figure 1. The objective of the subject controllers of this study is to determine an "optimal" Theta-Vector throughout the  $T$ -Matrix trajectory and to use it appropriately to control the plant in such a way that it "minimizes" some scalar measure of the vibration response (the performance index). The general scheme for the closed-loop vibration control system (VCS) employed by Davis (ref. 1) and used with the global model for this study is illustrated in figure 2. The general scheme used with the local model is slightly different than that shown in figure 2. During the operation of this system, the current  $Z$ -Vector is input to the identifier which uses it to estimate the current  $T$ -Matrix. The resulting estimate of the  $T$ -Matrix is then input to the controller which uses it to define an "optimal" change to the Theta-Vector. This increment to the Theta-Vector is, in turn, summed with the previous Theta-Vector to provide an updated control to the plant.

### 2.3.1 Vibration Minimization as a Trajectory Optimal Control Problem

The VCS operates throughout the trajectory. Specifically, the controller is engaged to determine the optimal control at closely spaced discrete time points along the state trajectory. The objective is to minimize the performance index as defined at each of these time points. This assumes that the performance index is dependent only on the currently defined  $T$ -Matrix; the currently defined control; and, in the case of the stochastic controllers, the currently defined covariance tensors that represent the measurement noise and  $T$ -Matrix identification statistics. Analytic solutions to this problem employ conventional max/min calculus (refs. 3, 4, and 5) rather than Pontryagin's Maximum Principle (refs. 6 and 7) or the calculus of variations (refs. 3 and 6). Pontryagin's Maximum Principle or the calculus of variations would be required if the value of the performance index and/or compliance with the constraints were dependent on finite segments of the trajectory (i.e., the state history over finite periods of time).

Typically, for the helicopter vibration problem, inequality constraints are imposed on the higher frequency blade pitch motions, blade loads, or other vehicle parameters, in addition to the basic requirement to minimize the vibration measure performance index. The standard max/min calculus formulation provides, however, for the imposition of equality constraints rather than inequality constraints. Equality constraints are imposed by adjoining a vector of corresponding constraint functions to the performance index using an adjoint vector. This adjoint vector is composed of a Lagrangian multiplier for each constraint function. The helicopter vibration reduction problem differs from this standard formulation in that inequality constraints, rather than equality constraints, are imposed. Consideration of the helicopter physics, for example, would more likely result in imposing an upper limit on the  $N$  per rev blade pitch angle rather than constraining the  $N$  per rev blade pitch angle to be exactly some nonzero value. This difference in constraint form can, however, be eliminated by a simple conversion of the inequality constraint functions to corresponding equality constraint functions. This is accomplished by defining a "slack variable" for each inequality constraint function. Specifically, the helicopter vibration reduction problem has the form:

$$\text{Minimize the performance index} \quad J = f[Z(\theta)] \quad (2-7)$$

$$\text{subject to inequality constraints} \quad \psi_k(\theta) \geq 0 \quad \text{for } k = 1, 2, \dots, M \quad (2-8)$$

Define a slack variable,  $\alpha_k$ , for each inequality constraint  $\psi_k(\theta)$ , such that

$$\alpha_k^2 = \psi_k(\theta) \quad \text{for } k = 1, 2, \dots, M \quad (2-9)$$

The slack variables are then treated as additional components of the Theta-Vector for the purpose of deriving necessary conditions for optimality. The Theta-Vector together with the slack variable vector, the Alpha-Vector, form the augmented Theta-Vector,  $\Theta$ , according to

$$\Theta = \begin{bmatrix} \theta \\ \alpha \end{bmatrix} \quad (2-10)$$

where

$$\alpha = \begin{bmatrix} \alpha_1 \\ \alpha_2 \\ \vdots \\ \alpha_M \end{bmatrix} \quad (2-11)$$

The equivalent equality constraints,  $\phi_k(\theta)$ , are defined

$$\phi_k(\theta) = \psi_k(\theta) - \alpha_k^2 \equiv 0 \quad \text{for } k = 1, 2, \dots, M \quad (2-12)$$

Using the slack variables defined by equation (2-9) and the corresponding equivalent equality constraints defined by equation (2-12), the helicopter vibration reduction problem can now be formulated in the standard max/min calculus form:

$$\text{Minimize the performance index} \quad J = f[Z(\theta)] \quad (2-13)$$

$$\text{subject to equality constraints} \quad \phi_k(\Theta) = 0 \quad \text{for } k = 1, 2, \dots, M \quad (2-14)$$

Necessary conditions for optimality can now be readily expressed using standard max/min calculus. The augmented performance function  $F[Z(\theta), \Theta]$  is formed by adjoining the constraint vector  $\phi$  to the original performance index  $f[Z(\theta)]$  using an adjoint vector,  $\lambda$ , whose elements are composed of Lagrangian multipliers, one for each constraint:

$$F[Z(\theta), \Theta] = f[Z(\theta)] + \lambda^T \phi \quad (2-15)$$

where

$$\lambda = \begin{bmatrix} \lambda_1 \\ \lambda_2 \\ \vdots \\ \lambda_M \end{bmatrix} \quad \text{and} \quad \phi = \begin{bmatrix} \phi_1 \\ \phi_2 \\ \vdots \\ \phi_M \end{bmatrix} \quad (2-16)$$

Necessary conditions for optimality are obtained by solving the  $6 + M$  simultaneous equations obtained by setting the first partial of  $F[Z(\theta), \Theta]$  with respect to the elements of  $\Theta$  equal to zero together with the  $M$  constraint equations (eq. (2-14)):

$$\frac{\partial F}{\partial \theta_j} = 0 \quad \text{for } j = 1, 2, \dots, 6 \quad (2-17)$$

$$\frac{\partial F}{\partial \alpha_j} = 0 \quad \text{for } j = 1, 2, \dots, M \quad (2-18)$$

$$\phi_j(\Theta) = 0 \quad \text{for } j = 1, 2, \dots, M \quad (2-19)$$

These  $6 + 2M$  simultaneous equations are, in general, nonlinear.

Up to this point, the performance index and the constraints have been presented in general form. One commonly used measure of vibration, employed by Davis (ref. 1), is a quadratic metric of the  $Z$ -Vector,  $Z^T W_Z Z$ . This metric is appropriate to use as the performance index:

$$J = f[Z(\theta)] = Z^T W_Z Z \quad (2-20)$$

where

$$\begin{array}{ll} f[Z(\theta)] & \text{performance index} \\ W_Z & \text{diagonal weighting matrix} \end{array}$$

It is emphasized that this choice of a performance index is but one of many possibilities. This performance index is relatively simple, representative of the control objective, and amenable to the pertinent mathematical derivations.

In general, constraints have to be imposed on the Theta-Vector in order to ensure that the higher harmonic control (HHC) motion of the blades does not result in excessive blade loads, excessive control system loads, and/or excessive power requirements. These constraints are inequality constraints and have the same general form as that defined by equation (2-8). A possible set of constraints can be defined by imposing a closed bound on the Fourier coefficients for the  $N - 1$ ,  $N$ , and  $N + 1$  harmonics as defined by the components of the Theta-Vector. Specifically

$$\psi_1(\theta) = A_1 - (\theta_1^2 + \theta_2^2) \geq 0 \quad \text{for the } (N - 1) \text{ harmonic} \quad (2-21)$$

$$\psi_2(\theta) = A_2 - (\theta_3^2 + \theta_4^2) \geq 0 \quad \text{for the } (N) \text{ harmonic} \quad (2-22)$$

$$\psi_3(\theta) = A_3 - (\theta_5^2 + \theta_6^2) \geq 0 \quad \text{for the } (N + 1) \text{ harmonic} \quad (2-23)$$

where  $A_1$ ,  $A_2$ , and  $A_3$  are the squares of the respective constraint bounds.

Although this choice of blade pitch constraints is the same as that used by Davis (ref. 1) to define his external limiting constraints, as used here they serve as an example only. In general, it is necessary to analyze each particular rotor system to determine the pertinent constraints for that system. In general, the mathematical form of the blade pitch constraints will differ for different types of rotor systems (e.g., articulated, teetering, hingeless) and even, possibly, for different rotor systems of the same type. Certainly in this latter case, the constraint bounds will, in general, differ for different rotor systems.

### 2.3.2 Kalman Filter Plant Matrix Identification

The identifier part of the VCS mentioned in section 2.3 employs a Kalman filter to identify the  $T$ -Matrix during each cycle. Equations (2-4) and (2-6) can be rewritten as

$$[T\text{-Matrix}]_i = [T\text{-Matrix}]_{i-1} + [\text{Random } \Delta T\text{-Matrix}]_{i-1} \quad (2-24)$$

$$[\text{Measured } Z\text{-Vector}] = [\text{Actual } Z\text{-Vector}] + [\text{Random Measurement Noise}] \quad (2-25)$$

where  $[T\text{-Matrix}]$  has dimension  $(2L \times M)$ ;  $[\text{Random } \Delta T\text{-Matrix}]$ , which has dimension  $(2L \times M)$ , is considered to be a zero mean random sequence forcing function which varies with flight condition; and  $[\text{Random Measurement Noise}]$ , which has dimension  $(2L \times M)$ , is assumed to be zero mean Gaussian.

The Kalman filter identification scheme used by Davis (ref. 1), and for this study, identifies each row of the  $T$ -Matrix ( $T_j$  for  $j = 1, 2, \dots, 2L$ ) individually. The principal steps in this Kalman filter identification scheme are

1. Compute the  $(M \times 1)$  Kalman filter gain vector  $K_i$ :

$$K_i = \frac{P_i \theta_i}{R_i} \quad (2-26)$$

where

$P$  is the  $(M \times M)$  covariance matrix of the  $T$ -Matrix row currently being identified, evaluated after the measurement of the  $Z$ -Vector during the current cycle

- $\theta$  is the Theta-Vector with dimension  $(M \times 1)$
- $R$  is the  $(1 \times 1)$  scalar covariance of the measurement noise
- $M$  is the principal dimension of the Theta-Vector;  $M = 6$  for the local model,  $M = 7$  for the global model
- $i$  time point number (e.g., number of rotor revolutions)

2. Update/identify the  $j$ -th row of the  $T$ -Matrix,  $\hat{T}_j$ :

$$[\hat{T}_j]_{i+1}^T = [\hat{T}_j]_i^T + K_i \{([\text{Measured } Z\text{-Vector}]_j)_i - \theta^T [\hat{T}_j]_i^T\} \quad (2-27)$$

where

- $T_j$  is the  $j$ -th row of the  $T$ -Matrix (for  $j = 1, 2, \dots, 2L$ ), a row vector with dimension  $(1 \times M)$
- $L$  is the number of accelerometers used to measure the vibration ( $L = 6$  for this study)
- $j$  is the  $T$ -Matrix row number ( $j = 1, 2, \dots, 2L$ )

3. Evaluate the  $(M \times M)$  matrix  $S$ , which is the covariance of the  $T_j$  being identified, for the conditions prior to the measurement of the  $Z$ -Vector during the current cycle, according to

$$S_i = P_i + Q_i \quad (2-28)$$

where  $Q$  is the  $(M \times M)$  covariance of the  $j$ -th row of the [Random  $\Delta T$ -Matrix] forcing function which is a term in the  $T_j$  being identified.

4. Update the  $(M \times M)$  matrix  $P$ , which is the covariance of the  $T_j$  being identified, for the conditions after the measurement of the  $Z$ -Vector during the current cycle, according to

$$P_{i+1} = S_i - \frac{S_i \theta_i \theta_i^T S_i}{\theta_i^T S_i \theta_i + R_i} \quad (2-29)$$

Step 4 completes the Kalman filter identification cycle. This process generates  $(M \times M)$   $S$ ,  $P$ , and  $Q$  covariance matrices for each  $(1 \times M)$  row of the  $T$ -Matrix. These covariance matrices, grouped according to type (the  $2L$   $S$ -Matrices, the  $2L$   $P$ -Matrices, and the  $2L$   $Q$ -Matrices), define their corresponding rank three covariance tensors (the  $S$ -Tensor, the  $P$ -Tensor, and the  $Q$ -Tensor). The individual  $(M \times M)$  covariance matrices are actually covariance lattices in their corresponding  $(M \times M \times 2L)$  rank three covariance tensors. Specifically, the covariance  $S$ -Tensor ( $P$ -Tensor,  $Q$ -Tensor) is composed of all the individual covariance  $S$ -Matrices ( $P$ -Matrices,  $Q$ -Matrices) generated for all the rows of the  $T$ -Matrix. These rank three covariance tensors are required to fully describe the statistics when the rows of the  $T$ -Matrix have little or no dependency. It was assumed by Davis (ref. 1), and for this study, that the  $S$ ,  $P$ , and  $Q$  covariance matrices, defined during the identification of a single row of the  $T$ -Matrix, would suffice for the identification of the other rows of the  $T$ -Matrix. This assumption may be adequate when there is some dependency between the rows of the  $T$ -Matrix as would likely be the case for the helicopter vibration problem. In that case, equations (2-28) and (2-29) need only

be evaluated once per cycle. These covariance matrices are not, in general, the same for each row of the  $T$ -Matrix. Use of the full rank three  $S$ ,  $P$ , and  $Q$  covariance tensors in the  $T$ -Matrix identification procedure simply requires the appropriate dimensioning of the associated  $S$ ,  $P$ , and  $Q$  arrays and the evaluation of equations (2-28) and (2-29) during the identification of each row of the  $T$ -Matrix.

## 2.4 Description of Controllers

The three controllers studied by Davis (ref. 1) were compared using the models presented in sections 2.1, 2.2, 2.3, and their subsections. Although the real or actual helicopter vibration reduction problem is as defined by equations (2-8) and (2-9), Davis (ref. 1) and his reference sources solved a somewhat different problem which, in general, neither minimizes the measure of vibration nor necessarily satisfies all the constraints. Indeed, the three controllers examined all use an external limiting scheme to adjust the solution control vector to yield a feasible solution (i.e., a solution which satisfies all the inequality constraints) in the event that the initial solution control vector results in a violation of one or more of the inequality constraints. Methodology of this type is usually used when the classical methods yield a problem which appears to be intractable or unsolvable.

Instead of directly addressing the problem defined by equations (2-7) and (2-8), the following problem is solved by each of the three subject controllers, at each of the discrete time points along the  $T$ -Matrix trajectory for which the controller is employed:

$$\begin{aligned} \text{Minimize} \quad & J = Z^T W_Z Z + \theta^T W_\theta \theta + \Delta\theta^T W_{\Delta\theta} \Delta\theta + [\text{Stochastic Term if defined}] \quad (2-30) \\ \text{Subject to} \quad & \text{No constraints for this optimization problem} \end{aligned}$$

where

$$\Delta\theta = \theta_i - \theta_{i-1} \quad (2-31)$$

In reality, however, constraints are imposed on the solution Theta-Vector after the fact. The optimal solution Theta-Vector is first determined from necessary conditions for the minimization of  $J$  as defined by equation (2-30). This first-cut optimal solution Theta-Vector is then checked for constraint violations and is adjusted, as required, to satisfy the constraints. In general, adjustments of this kind to the optimal solution Theta-Vector drive the solution away from optimality with a corresponding loss in performance (i.e., an increase in the value of  $J$ ). When using methodology of this type, it is advisable to have knowledge of the sensitivity of the performance to optimality. This after-the-fact imposition of constraints is referred to as "external limiting."

The motivation for this scheme is the use of the optimization process to prevent the control (and its rate) from becoming too large while attempting to minimize the vibration measure. The relative emphasis between the vibration measure and the control values is adjusted through the selection of the weighting matrices  $W_Z$ ,  $W_\theta$ , and  $W_{\Delta\theta}$ . Penalizing the control vector by incorporating it in the performance index in this manner is referred to as "internal limiting."

For stochastic controllers a stochastic term, which is a function of the  $T$ -Matrix row identification covariance  $P$ -Matrix, is added to the performance index. The principal idea here is to use the already generated statistical data (i.e., the covariance  $P$ -Matrix) to better estimate the solution Theta-Vector by using the optimization process to drive the covariance  $P$ -Matrix toward the zero matrix of the same

dimension. The implication is that better estimates of the solution Theta-Vector occur for better estimates of the  $T$ -Matrix. Controller schemes of this type will yield a suboptimal feasible solution if external limiting is imposed. Furthermore, if the sensitivity of performance to optimality is not too great and the weighting matrices are reasonable, this feasible suboptimal solution can yield a satisfactory value of the real part of the performance index (i.e., the  $Z^T W_Z Z$  term in equation (2-30)).

Necessary conditions for optimality are obtained by solving the six simultaneous equations resulting from setting the first partial derivative of  $J$  with respect to the Theta-Vector equal to zero:

$$\frac{\partial J}{\partial \theta_j} = 0 \quad \text{for } j = 1, 2, \dots, 6 \quad (2-32)$$

The external limiting scheme first checks for the constraint violations. These constraints are expressed as

$$R_{\theta_j} = \sqrt{\theta_{2j-1}^2 + \theta_{2j}^2} \leq [R_{\theta_j}]_{max} \quad \text{for } j = 1, 2, 3 \quad (2-33)$$

and

$$R_{\Delta\theta_j} = \sqrt{\Delta\theta_{2j-1}^2 + \Delta\theta_{2j}^2} \leq [R_{\Delta\theta_j}]_{max} \quad \text{for } j = 1, 2, 3 \quad (2-34)$$

In the event that the  $j$ -th  $\theta$  constraint is violated,  $\theta_{2j-1}$  and  $\theta_{2j}$  are adjusted according to

$$\theta_{2j-1} = \left( \frac{[R_{\theta_j}]_{max}}{R_{\theta_j}} \right) \theta_{2j-1} \quad \text{and} \quad \theta_{2j} = \left( \frac{[R_{\theta_j}]_{max}}{R_{\theta_j}} \right) \theta_{2j} \quad (2-35)$$

This process is repeated for the  $\Delta\theta$  constraints, which are adjusted in a similar manner as required. For example, in the event that the  $j$ -th  $\Delta\theta$  constraint is violated,  $\Delta\theta_{2j-1}$  and  $\Delta\theta_{2j}$  are adjusted according to

$$\Delta\theta_{2j-1} = \left( \frac{[R_{\Delta\theta_j}]_{max}}{R_{\Delta\theta_j}} \right) \Delta\theta_{2j-1} \quad \text{and} \quad \Delta\theta_{2j} = \left( \frac{[R_{\Delta\theta_j}]_{max}}{R_{\Delta\theta_j}} \right) \Delta\theta_{2j} \quad (2-36)$$

The three controllers that Davis (ref. 1) investigated (the deterministic, the cautious, and the dual controllers) were examined and compared as the object of this study. Davis's description of these controllers and the equations (ref. 1) is presented again here for the convenience of the reader.

#### 2.4.1 Deterministic Controller

The deterministic controller has the VCS general scheme, defined in section 2.3 and figure 2. The equations, which define the updated theta control vector for both the local and global models, are

determined by solving the problem defined by equations (2-30) and (2-31). In this case, the performance index is

$$J = Z_i^T W_Z Z_i + \theta_i^T W_\theta \theta_i + \Delta\theta_i^T W_{\Delta\theta} \Delta\theta_i \quad (2-37)$$

Provision is made for internal and external limiting in lieu of formal constraints on the theta control vector. Internal limiting can be applied via the last two terms in the performance index (eq. (2-37)), and external limiting can be imposed by the procedure defined by equations (2-33) through (2-36).

The theta control vector is updated according to

$$\theta_i^* = D\{(T^T W_Z T + W_{\Delta\theta})\theta_{i-1} - T^T W_Z Z_{i-1}\} \quad \text{for the local model} \quad (2-38)$$

$$\theta_i^* = D\{W_{\Delta\theta}\theta_{i-1} - T^T W_Z Z_0\} \quad \text{for the global model} \quad (2-39)$$

where

$$D = [T^T W_Z T + W_\theta + W_{\Delta\theta}]^{-1} \quad \text{for both models} \quad (2-40)$$

and

- $M$  is the principal dimension of the Theta-Vector and equals either 6 or 7 for the problems reported herein:  $M = 6$  if the local model is employed,  $M = 7$  if the global model is employed
- $W_Z$  is the  $(M \times M)$  diagonal weighting matrix for the  $Z$ -Vector terms
- $W_\theta$  is the  $(M \times M)$  diagonal weighting matrix for the Theta-Vector terms
- $W_{\Delta\theta}$  is the  $(M \times M)$  diagonal weighting matrix for the  $\Delta\theta$ -Vector terms
- $*$  denotes that this value of  $\theta$  is the solution to equation (2-32)
- $0$  denotes the uncontrolled condition (i.e., evaluated for a zero Theta-Vector)
- $i$  is the time point number (e.g., number of rotor revolutions)

## 2.4.2 Stochastic Controllers

The cautious and dual stochastic controllers have the VCS general scheme, defined in section 2.3 and figure 2. The equations, which define the updated theta control vector for both the local and global models, are determined by solving the problem defined by equations (2-30) and (2-31). The performance index for the cautious and dual controllers and the theta control vector update equations are defined in sections 2.4.2.1 and 2.4.2.2, respectively.

As in the case of the deterministic controller, provision is made for internal and external limiting in lieu of formal constraints on the theta control vector. Internal limiting can be applied via the second and third terms in the performance index (eq. (2-37)), and external limiting can be imposed by the procedure defined by equations (2-33) through (2-36).

**2.4.2.1 Cautious Controller**—When the local model is used, the performance index assumed for the cautious controller is

$$J = Z_i^T W_Z Z_i + \theta_i^T W_\theta \theta_i + \Delta\theta_i^T W_{\Delta\theta} \Delta\theta_i + [Tr(W_Z)] \Delta\theta_i^T P_i \Delta\theta_i \quad (2-41)$$

The theta control vector is updated according to

$$\theta_i^* = D[(T^T W_Z T + W_{\Delta\theta} + \lambda\{Tr(W_Z)\}P_i)\theta_{i-1} - T^T W_Z Z_{i-1}] \quad \text{for the local model} \quad (2-42)$$

where

$$D = [T^T W_Z T + W_{\theta} + W_{\Delta\theta} + \lambda\{Tr(W_Z)\}P_i]^{-1} \quad \text{for the local model} \quad (2-43)$$

and

- $M$  is the principal dimension of the Theta-Vector, equal to 6
- $P$  is the  $(M \times M)$  covariance matrix of the  $T$ -Matrix row currently being identified, evaluated after the measurement of the  $Z$ -Vector during the current cycle (see section 2.3.2)
- $\lambda$  adjusts the magnitude of the stochastic term relative to the nonstochastic term in the control law defined by equations (2-41), (2-42), and (2-43)
- $*$  denotes that this value of  $\theta$  is the solution to equation (2-32)
- $i$  is the time point number (e.g., number of rotor revolutions)

When the global model is used, the performance index assumed for the cautious controller is

$$J = Z_i^T W_Z Z_i + \theta_i^T W \theta_i + \Delta\theta_i^T W \Delta\theta_i + (Tr(W_Z))\theta_i^T P_i \theta_i \quad (2-44)$$

It is convenient to partition the  $(7 \times 7)$   $P$ -Matrix into four submatrices: the  $(6 \times 6)$   $P_{TT}$  submatrix, the  $(6 \times 1)$   $P_{TZ}$  submatrix, the  $(1 \times 6)$   $P_{ZT}$  submatrix, and the  $(1 \times 1)$   $P_{ZZ}$  submatrix (a scalar). Specifically,

$$P = \begin{bmatrix} P_{TT} & P_{TZ} \\ P_{ZT} & P_{ZZ} \end{bmatrix} \quad (2-45)$$

Note that

$$P_{ZT} = P_{TZ}^T \quad (2-46)$$

The theta control vector for the global model is then updated according to

$$\theta_i^* = D[W_{\Delta\theta}\theta_{i-1} - T^T W_Z Z_0 - \lambda\{Tr(W_Z)\}P_{TZ}] \quad \text{for the global model} \quad (2-47)$$

where

$$D = [T^T W_Z T + W_{\theta} + W_{\Delta\theta} + \lambda\{Tr(W_Z)\}P_{TT}]^{-1} \quad \text{for the global model} \quad (2-48)$$

and

- $M$  is the principal dimension of the Theta-Vector, equal to 7
- $0$  denotes the uncontrolled condition (i.e., evaluated for a zero Theta-Vector)

**2.4.2.2 Dual Controller**—When the local model is used, the performance index assumed for the dual controller is:

$$J = Z_i^T W_Z Z_i + \theta_i^T W_\theta \theta + \Delta \theta_i^T W_{\Delta \theta} \Delta \theta_i - \lambda \Delta \theta_i^T \left( \frac{P_{i-1}}{R} \right) \Delta \theta_i \quad (2-49)$$

The theta control vector is updated according to

$$\theta_i^* = D \left[ \left( T^T W_Z T + W_{\Delta \theta} - \lambda \left\{ \frac{P_{i-1}}{R} \right\} \right) \theta_{i-1} - T^T W_Z Z_{i-1} \right] \quad \text{for the local model} \quad (2-50)$$

where

$$D = \left[ T^T W_Z T + W_\theta + W_{\Delta \theta} - \lambda \left\{ \frac{P_{i-1}}{R} \right\} \right]^{-1} \quad \text{for the local model} \quad (2-51)$$

and

- $M$  is the principal dimension of the Theta-Vector, equal to 6
- $P$  is the  $(M \times M)$  covariance matrix of the  $T$ -Matrix row currently being identified, evaluated after the measurement of the  $Z$ -Vector during the current cycle (see section 2.3.2)
- $R$  is the  $(1 \times 1)$  scalar covariance of the measurement noise
- $\lambda$  is a parameter which is used to adjust the magnitude of the stochastic term relative to the nonstochastic terms in the control law defined by equations (2-49), (2-50), and (2-51)
- $*$  denotes that this value of  $\theta$  is the solution to equation (2-32)
- $i$  is the time point number (e.g., number of rotor revolutions)

When the global model is used, the performance index assumed for the dual controller is:

$$J = Z_i^T W_Z Z_i + \theta_i^T W_\theta \theta_i + \Delta \theta_i^T W_{\Delta \theta} \Delta \theta_i - \lambda \theta_i^T \left( \frac{P_{i-1}}{R} \right) \theta_i \quad (2-52)$$

As in the case of the cautious controller, it is convenient to partition the  $(7 \times 7)$   $P$ -Matrix into four submatrices: the  $(6 \times 6)$   $P_{TT}$  submatrix,  $(6 \times 1)$   $P_{TZ}$  submatrix, the  $(1 \times 6)$   $P_{ZT}$  submatrix, and the  $(1 \times 1)$   $P_{ZZ}$  submatrix (a scalar). The theta control vector for the global model is then updated according to

$$\theta_i^* = D \left[ W_{\Delta \theta} \theta_{i-1} - T^T W_Z Z_0 - \lambda \left( \frac{P_{TZ}}{R} \right) \right] \quad \text{for the global model} \quad (2-53)$$

where

$$D = \left[ T^T W_Z T + W_\theta + W_{\Delta \theta} - \lambda \left( \frac{P_{TT}}{R} \right) \right]^{-1} \quad \text{for the global model} \quad (2-54)$$

and

- $M$  is the principal dimension of the Theta-Vector, equal to 7
- $0$  denotes the uncontrolled condition (i.e., evaluated for a zero Theta-Vector)

## 3 COMPARISON STUDY

The selection and definition of the baseline plant and controller are described in this section, and then the effects of the initial estimate of the  $T$ -Matrix, the plant matrix propagation rate, and the measurement noise on controller performance are defined.

### 3.1 Baseline Controller

The models used to initialize and simulate the plant and its propagation, the actual and measured vibration response, the controllers, and the  $T$ -Matrix identification process are defined in section 2.0 and its subsections. In this section, the selection of the important controller constants and the modes of operation which establish the baseline controller is described. The deterministic controller was used in making this selection.

#### 3.1.1 Initial Random Number Generator Seed

In order to evaluate controller performance, it is desirable that the response to the initially computed control be significantly less than the initial "uncontrolled" condition. (The uncontrolled condition, which corresponds to a zero theta control vector, exists just prior to engaging the controller to compute the first nonzero theta control vector.) The random method used to initialize, then to propagate with time, the numerical values of the  $T$ -Matrix elements defines these numerical values from a sequence of random numbers generated with a random number generator function. A particular starting seed value has a unique sequence of random numbers associated with it. The performance index reduction obtainable at the end of the first controlled step (i.e., the initial decrease in response) is highly dependent on the value of this starting seed. The actual numerical values of this starting seed are not of interest in reporting the results of this study; however, for convenience in identification, starting seed values are presented. A starting seed value of 7391 was arbitrarily selected and used for the checkout computations. The corresponding response for this value, which has an initial decrease of only 19.36%, is shown in figure 3 for the case where there is no limiting and the  $T$ -Matrix is invariant. For all cases investigated, zero theta control is assumed to the initiation of the fourth revolution, at which time the controller is engaged. The response to the first computed nonzero theta control vector occurs at the beginning of the fifth revolution.

In a search for a better starting seed (i.e., one which would yield an acceptable initial decrease in response), 17 different starting seed values were tried (tab. 1). No limiting and an invariant  $T$ -Matrix was assumed for all cases. A starting seed value of 83298 was selected because it yielded the greatest initial decrease; a 66.96%, or slightly better than three-to-one, first-step reduction of the performance index. The corresponding response is shown in figure 4.

#### 3.1.2 Control Limiting

The philosophy and methodology of control limiting as employed by the subject controllers is discussed in section 2.4. Recall that (1) internal limiting applies a limiting "pressure" on the theta control vector applied by adjoining terms containing the theta control vector and its rate to the performance index that is minimized by the optimization process; (2) external limiting, which is applied after the

fact, adjusts the theta control vector to the appropriate constraint circle(s), defined by equations (2-33) and (2-34), in the event that the optimization process yields a theta control vector in violation of a constraint. The use of both external and internal limiting was examined.

**3.1.2.1 External Limiting**—External limiting is applied by specifying the values of the least upper bound (l.u.b.) for the external limiting magnitude constraints ( $[R_{\theta_j}]_{max}$  in equation (2-33)) and/or for the external limiting rate (or incremental) constraints ( $[R_{\Delta\theta_j}]_{max}$  in equation (2-34)). It is assumed that the values of  $[R_{\theta_j}]_{max}$  are the same for  $j = 1, 2, 3$ , and similarly that the values of  $[R_{\Delta\theta_j}]_{max}$  are the same for  $j = 1, 2, 3$ . Using one rotor revolution as the unit of time, the rate (or incremental) constraint functions defined by equation (2-34) are computed using a method that makes them numerically equivalent to the corresponding magnitude constraint functions defined by equation (2-33). Because of this computational methodology, when the values of  $[R_{\theta_j}]_{max}$  are specified to be the same as the corresponding values of  $[R_{\Delta\theta_j}]_{max}$ , the constraints defined by equations (2-33) and (2-34) are equivalent. Furthermore, when a value of  $[R_{\theta_j}]_{max}$  is specified to be different from that of the corresponding value of  $[R_{\Delta\theta_j}]_{max}$ , the constraint corresponding to the smaller value becomes active first, thus dominating the external limiting process. Consequently, under these conditions it is only necessary to specify one of either the magnitude or the rate (or incremental) constraints (i.e., to define either  $[R_{\theta_j}]_{max}$  or  $[R_{\Delta\theta_j}]_{max}$  for  $j = 1, 2, 3$ ) when examining the effect of external limiting. Both were examined, however, in order to check out the computational process.

A summary of the effect of the value of  $[R_{\theta_j}]_{max}$  or  $[R_{\Delta\theta_j}]_{max}$  on the performance index at the end of the first controlled step (i.e., at the initiation of the fifth revolution) when there is no internal limiting is presented in table 2, and the response for selected cases is illustrated in figures 5 through 10. The  $T$ -Matrix is assumed to be invariant for these cases and hence the lowest possible value of the performance index  $J$  (i.e., the greatest lower bound [g.l.b.]) is invariant to revolution. For this case, the g.l.b. has the value 0.0005287. If no external limiting applied, or if external limiting constraints are inactive, the controller will define the Theta-Vector such that its corresponding performance index has the value of the g.l.b. at the end of the first controlled step. A range of values for  $[R_{\theta_j}]_{max}$  (and equivalently for  $[R_{\Delta\theta_j}]_{max}$  which yield nonsaturated active constraints of interest were identified. This range is (1, 40) for both constraints since the unit time is one revolution. The threshold value at which the constraints become active is 36.91; the constraints are active for values below 36.91. The constraints become saturated for values below approximately 1. The value of the performance index at the end of the first controlled step as a function of the constraint limit (i.e.,  $[R_{\theta_j}]_{max}$  or  $[R_{\Delta\theta_j}]_{max}$ ) is shown in figure 11, and the revolution at which steady state is achieved, also as a function of the constraint limit, is shown in figure 12. It was decided to use  $[R_{\theta_j}]_{max} = 40$  and  $[R_{\Delta\theta_j}]_{max} = 10$  to produce a three-per-rev delay to steady state (i.e., steady state is achieved at the initiation of revolution 8) without invoking both constraint limits (fig. 12) for the baseline case that will be used as the standard for comparisons. This baseline case has the same response as that shown in figure 7.

**3.1.2.2 Internal Limiting**—Internal limiting is applied by specifying values of the diagonal element of  $W_{\theta}$  in equation (2-30) ( $\text{Diag}(W_{\theta})$ ) and the diagonal elements of  $W_{\Delta\theta}$  in equation (2-30) ( $\text{Diag}(W_{\Delta\theta})$ ). The effect of internal limiting was evaluated by varying the values of  $\text{Diag}(W_{\theta})$  and  $\text{Diag}(W_{\Delta\theta})$  through several orders of magnitude with no application of external limiting. For this evaluation, it was assumed that each of the elements of  $\text{Diag}(W_{\theta})$  had the same value, and similarly that

each of the elements of  $\text{Diag}(W_{\Delta\theta})$  had the same value. The cases which were examined are defined in table 3, and the response for the selected cases is illustrated in figures 13 through 21.

The first case in this series has no limiting at all, and is provided as a reference for comparison. The response of the nonaugmented  $Z$ -Vector quadratic metric, defined by equation (2-20), is shown in these figures rather than that of the complete performance index, defined by equation (2-37), since it is the  $Z$ -Vector metric which is the measure of helicopter vibration. For these cases, the  $T$ -Matrix was randomly propagated in time according to the procedure defined in section 2.2.3 and by equation (2-4), where a value of 0.001 was assumed for the scaling coefficient  $C_\rho$ . (See section 3.1.3 for a discussion of the selection of the value of  $C_\rho$ , and section 2.2.2 for numerical values of the elements of a typical actual  $T$ -Matrix.)

It can be seen from table 3 and figures 13 through 21 that a change of approximately two orders of magnitude of the value of either an element of  $\text{Diag}(W_\theta)$  or an element of  $\text{Diag}(W_{\Delta\theta})$  is required to go from the limit saturation condition to the no-limiting condition. The selection of the appropriate values for an element of  $\text{Diag}(W_\theta)$  and an element of  $\text{Diag}(W_{\Delta\theta})$  to satisfy the limiting constraints (i.e., the conditions required by equations (2-33) and (2-34)) by means of internal limiting, while minimizing the  $Z$ -Vector metric, is not necessarily a simple matter. Indeed, as was pointed out in section 2.4, external limiting is provided after the fact as a backup means to assure that the solution is feasible (i.e., the limiting requirements are satisfied). It was also pointed out in section 2.4 that the problem which is defined when the  $Z$ -Vector metric has internal limiting terms adjoined to it as per equation (2-30) is not the same problem as minimizing the  $Z$ -Vector metric by itself when constraints are imposed on the theta control vector. This can be illustrated by considering a scalar case (i.e., when  $T$ ,  $Z$ ,  $Z_0$ ,  $\theta$ ,  $\Delta\theta$ ,  $W_Z$ ,  $W_\theta$ , and  $W_{\Delta\theta}$  are all scalar). Two of several possible situations are illustrated in figures 22 and 23. In both of these examples, it is assumed that the performance index specified by equation (2-30) has the form

$$J = J_Z + J_\theta \quad (3-1)$$

where if

$$Z = T\theta + Z_0 \quad \text{and} \quad J_Z = Z^2$$

then  $J_Z$  and  $J_\theta$  can be expressed

$$J_Z = \alpha(\theta - \beta)^2 - \gamma \quad \text{and} \quad J_\theta = \psi\theta^2 \quad (3-2)$$

where  $\alpha$ ,  $\beta$ ,  $\gamma$ , and  $\psi$  are scalar constants.

Constraints on the theta control vector are imposed; specifically

$$\theta \in [0, \theta_{max}] \quad (3-3)$$

For this case,  $J_Z$  is the actual measure of the vibration,  $J_\theta$  is the theta control penalty term, and  $J$  is the augmented performance index that the subject controllers seek to minimize. The unconstrained minimum of  $J_Z$ , for the case illustrated in figure 22, is assumed to occur at  $\theta_{Z_{min}}$ , which is within the constraint limits of equation (3-3). The augmented performance index, which is the sum of  $J_Z$  and  $J_\theta$ , has a minimum which occurs at  $\theta_{min}$ , which in this case is less than  $\theta_{Z_{min}}$  and lies within the constraint limits. The discrepancy in performance between the solutions to the actual problem and the

augmented problem is the difference between the minimum value of  $J_Z$  and the value of  $J_Z$  which occurs at  $\theta_{min}$ . The corresponding discrepancy in the optimal values of  $\theta$  is the difference in value between  $\theta_{Z_{min}}$  and  $\theta_{min}$ .

The case depicted in figure 23 is similar to that illustrated in figure 22 except that the unconstrained minimum of  $J_Z$  is assumed to occur at a  $\theta$  value which exceeds its upper constraint limit,  $\theta_{max}$ . In this case, the minimum feasible value of  $J_Z$  occurs when  $\theta$  is on the  $\theta_{max}$  constraint bound. As in the previous case, the discrepancy in performance between the actual problem and the augmented problem is the difference between the minimum feasible value  $J_Z$  and the value of  $J_Z$  which occurs at  $\theta_{min}$ . In both cases, the minimum feasible value of  $J_Z$  (i.e., the actual measure of performance) is less than that obtained when the theta control penalty term is adjoined to the performance index to form  $J$ . For this reason, it was decided not to apply internal limiting to the remaining cases generated in the comparison studies.

### 3.1.3 Plant Matrix Propagation Rate

Several values of  $C_\rho$ , the random term scaling coefficient of the plant matrix propagation model described in section 2.2.3 and equation (2-4), were examined to determine a baseline value which would produce a significant, but not overly exaggerated, random change in the plant matrix over 100 revolutions. A summary of the cases which were examined is presented in table 4, and the  $T$ -Matrix time histories for  $C_\rho$  values of 0.0005, 0.001, and 0.002 are shown in figures 24, 25, and 26, respectively. A value of 0.001 for  $C_\rho$  was selected for the baseline controller. This value yields a representative and reasonable time propagation of the  $T$ -Matrix.

## 3.2 Effect of the Initial Estimate of the $T$ -Matrix on Controller Performance

The Kalman filter identification scheme, described in section 2.3.2 and used in this study, requires an initial estimate of the  $T$ -Matrix to start the identification algorithm. The ability of the algorithm to converge to a reasonable, identified  $T$ -Matrix greatly depends on the accuracy of this estimate. The method used to select this estimate is an issue which is separate from the evaluation and comparison of the three subject controllers. The real issue here is the sensitivity of controller convergence to the initial estimate. For this reason, this initial estimate was simplified and systematized using the random procedure defined in section 2.2.2 and by equation (2-3). For convenience, equation (2-3) is shown here as well as in section 2.2.2. Specifically, the initial estimate of the  $T$ -Matrix is

$$\hat{T} = T + C_E \xi \quad (2-3)$$

where

- $C_E$  initial estimate of the scaling coefficient for the random increment matrix term (The nominal value of  $C_E$  used in this study is 0.001.)
- $T$  randomly generated reference  $T$ -Matrix (actual  $T$ -Matrix) which represents the actual helicopter plant
- $\hat{T}$  estimate of the  $T$ -Matrix
- $\xi$  matrix composed of uniform distribution random numbers  $\in [0.0, 1.0]$ .  $\xi$  has the same dimension as the  $T$ -Matrix

The numerical values for the elements of  $\xi$  are generated with a random number generator function, which generates a unique sequence of random numbers associated with a starting seed value. In a manner similar to that described in section 3.1.1, a starting seed value of 10691 was selected and used throughout this study.

In a manner similar to that described in section 3.1.3, the values of  $C_E$  were examined for the deterministic controller. A baseline  $C_E$  value of 0.001 was selected because that value yielded an initial estimate of the  $T$ -Matrix which was nearly as inaccurate as possible while still allowing the identification algorithm to reliably converge in a reasonable manner. The principal cases examined are defined in table 5, and the response for selected cases is illustrated in figures 27 through 31. When the baseline values of the starting seed and  $C_E$  are used for the initial  $T$ -Matrix estimate for the deterministic controller, the response is that shown in figure 27. This is the reference case for the  $T$ -Matrix Initial Estimate Study summarized in table 5.

A sufficiently large value of  $C_E$  was selected to ensure that the deterministic controller would not converge to the response of the baseline case shown in figure 27. This value,  $C_E = 1.0$ , was used to test the cautious and dual controllers to see if their stochastic nature would overcome the effects of a bad initial estimate of the  $T$ -Matrix. Specifically, using  $C_E = 1.0$  to define the initial  $T$ -Matrix estimate, the adjoint coefficient,  $\lambda$ , of the stochastic term in the performance index for both stochastic controllers was varied parametrically through several orders of magnitude (see table 5) to see if convergence to the response of the baseline case could be obtained. Figures 32 through 41 show that use of the stochastic controllers in this manner did not enhance convergence for bad initial estimates of the  $T$ -Matrix. Indeed, in some cases it made matters worse. Convergence only occurred for the trivial limiting case when  $\lambda \rightarrow 0$ , or equivalently when the stochastic controllers coalesced with the deterministic controller.

### 3.3 Effect of the Plant Matrix Propagation Rate on Controller Performance

The method used to propagate the  $T$ -Matrix is described in section 2.2.3, specifically by equation (2-4). For convenience, equation (2-4) is shown here as well as in section 2.2.3. Specifically, the reference  $T$ -Matrix, which represents the actual helicopter plant, was propagated in time according to

$$T_i = T_{i-1} + C_p \xi \quad (2-4)$$

where

- $C_p$  plant propagation scaling coefficient for the random increment matrix term
- $T$  randomly generated reference  $T$ -Matrix (actual  $T$ -Matrix) which represents the actual helicopter plant
- $\xi$  matrix composed of uniform distribution random numbers  $\in [0.0, 1.0]$ .  $\xi$  has the same dimension as the  $T$ -Matrix
- $i$  time point number (e.g., number of rotor revolutions)

The numerical values of the  $T$ -Matrix elements are generated with a random number generator function, which generates a unique sequence of random numbers associated with a starting seed value. As a result of the seed study described in section 3.1.1, a starting seed value of 83298 was selected and used throughout this study.

The baseline value of  $C_\rho$ , the random term scaling coefficient in equation (2-4), was selected to be 0.001 to produce a significant, but not over-exaggerated, change in the  $T$ -Matrix over 100 revolutions (section 3.1.3). This case is shown in figure 42. Questions about the ability of the stochastic controllers to converge to the responses obtained with the deterministic controller motivated investigation of the effect of the value of  $C_\rho$  on this convergence. Parametric values of  $C_\rho$  for the deterministic controller were tested to find values of  $C_\rho$  which result in divergence of the  $T$ -Matrix. The cases tested are defined in table 6, and the responses for selected cases are shown in figures 42 through 46. Strong  $T$ -Matrix divergence occurred for  $C_\rho = 0.0026$  (fig. 45), so this value was used when testing the stochastic controllers for performance enhancement.

In a manner similar to that employed for the  $T$ -Matrix Initial Estimate Study, the adjoint coefficient  $\lambda$  of both stochastic controllers was varied parametrically through several orders of magnitude to see if the stochastic controllers would provide better responses than the deterministic controller, or if, indeed, they would converge to the response of the reference deterministic controller for which  $C_\rho = 0.0026$ . The cases examined are defined in table 6. In general, the stochastic controllers did not perform as well as the deterministic controller except for the trivial limiting cases when  $\lambda \rightarrow 0$ , or equivalently when the stochastic controllers coalesced with the deterministic controller. Selected cases of the cautious and dual controllers for  $T$ -Matrix propagation with  $C_\rho = 0.0026$  are shown in figures 47 through 55.

### 3.4 Effect of Measurement Noise on Controller Performance

The  $Z$ -Vector was the only parameter whose measurement uncertainty was considered. This uncertainty (the "measurement noise") is modeled in accordance with the procedure defined in section 2.2.5 by equation (2-6). The measurement noise manifests itself either directly or indirectly in two of the controller computations: (1) identification of the  $T$ -Matrix (section 2.3.2, equation (2-27)), and (2) the performance index (section 2.4, equation (2-30)). The measurement noise is modeled in such a way that it is (1) random with constant limiting envelopes ("random nonperiodic"), (2) random with sinusoidal limiting envelopes ("random periodic"), or (3) constant or sinusoidal with no randomness ("nonrandom constant" or "nonrandom periodic").

#### 3.4.1 Random Nonperiodic Measurement Noise

The method used to simulate the measured vibration response is described in section 2.2.5, by equation (2-6). For convenience, equation (2-6) is shown again here. The measured helicopter vibration response is defined according to

$$\tilde{Z} = Z(1.0 + C_M C_C \nu) \quad (2-6)$$

where

$\tilde{Z}$	measured helicopter vibration response $Z$ -Vector
$Z$	actual helicopter vibration response $Z$ -Vector
$\nu$	vector composed of uniform distribution random numbers $\in [0.0, 1.0]$ . $\nu$ has the same dimension as the $Z$ -Vector
$C_M$	measured response scaling coefficient for the random increment matrix term
$C_C$	$\begin{cases} 1.0 & \text{if } \tau \geq 1.0D + 10 \\ \cos(360.0^\circ[\sigma + t/\tau]) & \text{if } \tau < 1.0D + 10 \end{cases}$

- $\sigma$  phase of the sinusoidal coefficient of the random term expressed in a nondimensional fraction of a rotor revolution
- $t$  time expressed in rotor revolutions
- $\tau$  period of the sinusoidal coefficient of the random term expressed in rotor revolutions

This technique for introducing random noise defines the numerical values for the elements of  $\nu$  using a random number generator function, which generates a unique sequence of random numbers associated with a starting seed value. A starting seed value of 49377 was used throughout this study.

The effect of the  $Z$ -Vector measurement noise was first investigated for random nonperiodic cases for the deterministic controller. For these cases  $C_M$ , the scaling coefficient for the measurement noise term in equation (2-6), was varied parametrically to determine the sensitivity of the response to measurement noise. The cases examined are defined in table 7, and the response for selected cases is shown in figures 56 through 61. The reference no-noise case (the "0% noise level" case) is obtained when  $C_M = 0$ . This case (fig. 56) serves as a reference for comparison with the other cases described in this section. The 20% noise level case (fig. 57) is representative of the lower end of normal noise, and the 120% noise level case (fig. 61) is representative of the situation in which the noise overshadows the  $Z$ -Vector itself.

The stochastic controllers were compared with the deterministic controller for both the 20% and the 120% noise levels for parametric values of the adjoint coefficient  $\lambda$ . As in previous comparisons,  $\lambda$  was varied through several orders of magnitude to see if the stochastic controllers would provide better responses than the deterministic controller. The cases examined are defined in table 7. In general, the stochastic controllers did not perform as well as the deterministic controller except for the trivial limiting cases when  $\lambda \rightarrow 0$ , or equivalently when the stochastic controllers coalesced with the deterministic controller. Selected cases of both the cautious and dual controllers for 20% and 120% noise levels are shown in figures 62 through 79. These results support the contention that the statistical dimension of the stochastic controllers defined for this study was insufficient for the fully random  $T$ -Matrix model with independent rows that was used. Either the full covariance tensor should have been used in the definition of the stochastic controllers, or the rows of the plant model should have had a sufficient degree of linear dependency so that a single lattice of the covariance tensor would suffice.

### 3.4.2 Random Periodic Measurement Noise

The effects of random periodic measurement noise were investigated in a manner similar to that described in section 3.4.1. For these cases, the limiting envelope for the random noise is sinusoidal with a 20-cycle period ( $\tau = 20$  revs in equation (2-6)) and a zero phase angle ( $\sigma = 0.0$  revs in equation (2-6)) rather than constant. As in the case of random nonperiodic measurement noise,  $C_M$  was varied parametrically from 0% noise level to 40% noise level for the deterministic controller, to determine the sensitivity of the response to measurement noise. The cases examined are defined in table 8, and the response for selected cases is shown in figures 80, 81, and 82. The 20% noise case (fig. 81) is representative of the lower end of normal noise. The situation in which the response to the measurement noise by itself is of the same order of magnitude as the response to the  $Z$ -Vector with no measurement noise was not investigated for random periodic measurement noise cases.

The stochastic controllers were compared with the deterministic controller, assuming a 20% noise level, for parametric values of the adjoint coefficient  $\lambda$ . As in previous comparisons,  $\lambda$  was varied through several orders of magnitude to see if the stochastic controllers would provide a better response than the deterministic controller. The cases examined are defined in table 8. In general, the stochastic controllers did not perform as well as the deterministic controller except for the trivial limiting cases when  $\lambda \rightarrow 0$ , or equivalently when the stochastic controllers coalesced with the deterministic controller. Selected cases of the cautious and dual controllers with a 20% measurement noise level are shown in figures 83 through 90. These results also support the contention that the statistical dimension of the stochastic controllers defined for this study was insufficient for the fully random  $T$ -Matrix model with independent rows that was used. Either the full covariance tensor should have been used in the definition of the stochastic controllers, or the rows of the plant model should have had a sufficient degree of linear dependency so that a single lattice of the covariance tensor would suffice.

### 3.4.3 Nonrandom Periodic Measurement Noise

Finally, the effects of nonrandom periodic measurement noise was investigated in a manner similar to that used for random periodic measurement noise. For these cases, the limiting envelope is identically the measurement noise, and is sinusoidal with a 20-cycle period ( $\tau = 20$  revs in equation (2-6)) and a zero phase angle ( $\sigma = 0.0$  in equation (2-6)). The random vector  $\nu$  in equation (2-6) was set to be identically equal to 1 which, correspondingly, bypasses the generation of random elements in the measurement noise. As in the case of random periodic measurement noise, the scaling coefficient  $C_M$  for the measurement noise term in equation (2-6) was varied parametrically from the 0% noise level case to the 40% noise level case for the deterministic controller, to determine the sensitivity of the response to measurement noise. The cases examined are defined in table 9, and the response for selected cases is shown in figures 91, 92, and 93. The 20% noise case (fig. 92) is representative of the lower end of normal noise. The situation in which the response to the measurement noise by itself is of the same order of magnitude as the response to the  $Z$ -Vector with no measurement noise was not investigated for nonrandom periodic measurement noise cases.

Even though it was expected that use of a stochastic controller would not have any advantage in cases having nonrandom noise, the stochastic controllers were compared with the deterministic controller, assuming a 20% noise level, for parametric values of the adjoint coefficient  $\lambda$ . As in previous comparisons,  $\lambda$  was varied through several orders of magnitude. The cases examined are defined in table 9. In general, the stochastic controllers did not perform as well as the deterministic controller except for the trivial limiting cases when  $\lambda \rightarrow 0$ , or equivalently when the stochastic controllers coalesced with the deterministic controller. Selected cases of both the cautious and dual controllers with a 20% measurement noise level are shown in figures 94 through 101.

## 4 RESULTS

The helicopter vibration reduction capability of two stochastic controllers was evaluated and compared with that of the deterministic controller. The first step was to define a baseline deterministic controller. The resulting baseline definition is described in sections 3.1 through 3.4 and is characterized by specific baseline values of parameters in equations (2-3) through (2-6). For convenience these equations are shown here together with the baseline values of these parameters. The initial estimate of the

$T$ -Matrix is defined by

$$\hat{T} = T + C_E \xi \quad (2-3)$$

where

- $C_E$  initial estimate of the scaling coefficient for the random increment matrix term (The nominal value of  $C_E$  used in this study is 0.001.)
- $T$  randomly generated reference  $T$ -Matrix (actual  $T$ -Matrix) which represents the actual helicopter plant
- $\hat{T}$  estimate of the  $T$ -Matrix
- $\xi$  matrix composed of uniform distribution random numbers  $\in [0.0, 1.0]$ .  $\xi$  has the same dimension as the  $T$ -Matrix. The baseline value of its associated starting seed for this study is 10691

The reference  $T$ -Matrix, which represents the actual helicopter plant, was propagated in time according to

$$T_i = T_{i-1} + C_\rho \xi \quad (2-4)$$

where

- $C_\rho$  plant propagation scaling coefficient for the random increment matrix term. The baseline value of  $C_\rho$  used in this study is 0.001
- $T$  randomly generated reference  $T$ -Matrix (actual  $T$ -Matrix) which represents the actual helicopter plant
- $\xi$  matrix composed of uniform distribution random numbers  $\in [0.0, 1.0]$ .  $\xi$  has the same dimension as the  $T$ -Matrix. The baseline value of its associated starting seed used in this study is 83298
- $i$  time point number (e.g., number of rotor revolutions)

The actual helicopter vibration response  $Z$  is defined according to

$$Z = T\theta \quad (2-5)$$

where

- $T$  randomly generated reference  $T$ -Matrix which represents the actual helicopter plant
- $Z$  actual helicopter vibration response  $Z$ -Vector defined by equation (2-5)
- $\theta$  the current and/or most recently defined control Theta-Vector

The measured helicopter vibration response is defined according to

$$\tilde{Z} = Z(1.0 + C_M C_C \nu) \quad (2-6)$$

where

- $\tilde{Z}$  measured helicopter vibration response  $Z$ -Vector
- $Z$  actual helicopter vibration response  $Z$ -Vector
- $\nu$  vector composed of uniform distribution random numbers  $\in [0.0, 1.0]$ .  $\nu$  has the same dimension as the  $Z$ -Vector. The baseline value of its associated starting seed used in this study is 49377
- $C_M$  measured response scaling coefficient for the random increment matrix term. (The baseline value of  $C_M$  used in this study is 0.200.)

$$C_C \begin{cases} 1.0 & \text{if } \tau \geq 1.0D + 10 \\ \cos(360.0^\circ[\sigma + t/\tau]) & \text{if } \tau < 1.0D + 10 \end{cases}$$

$\sigma$  phase of the sinusoidal coefficient of the random term expressed in a nondimensional fraction of a rotor revolution  
 $t$  time expressed in rotor revolutions  
 $\tau$  period of the sinusoidal coefficient of the random term expressed in rotor revolutions

The next step was to define the reference deterministic controllers to be used as the basis of comparison for the investigations of the effects of the initial estimate of the  $T$ -Matrix (sec. 3.2), the  $T$ -Matrix propagation rate (sec. 3.3), and measurement noise (sec. 3.4). To be able to make these definitions, however, it was first necessary to determine the performance degradation of the deterministic controller for each of the comparison conditions to be investigated. Specifically, the performance degradation of the deterministic controller from its baseline configuration was determined for

1. an increasing error in the initial estimate of the  $T$ -Matrix (modeled using the value of  $C_E$ ),
2. an increasing scaling coefficient used for  $T$ -Matrix propagation (modeled using the value of  $C_\rho$ ),
3. an increasing envelope for the measurement noise (modeled using the value of  $C_M$ ).

Using this performance degradation data, the reference deterministic controllers were selected to define conditions which would be relatively more advantageous to the stochastic controllers. These reference deterministic controllers differ from the baseline deterministic controller by the following values:

1.  $C_E = 1.0$  for the initial estimate of the  $T$ -Matrix investigation
2.  $C_\rho = 0.0026$  for the  $T$ -Matrix propagation investigation
3.  $C_M = 0.2000$  for the investigation of measurement noise at the lower end of normal noise levels
4.  $C_M = 1.2000$  for the investigation of measurement noise when it overshadows the  $Z$ -Vector itself

The comparison of the helicopter vibration reduction capability of two stochastic controllers with that of the deterministic controller was then accomplished by assuming the numerical characteristics of the appropriate reference deterministic controller and then parametrically varying the adjoint coefficient  $\lambda$  of the stochastic controller being investigated (secs. 3.2, 3.3, and 3.4).

#### 4.1 Results Obtained from the Comparison Study

In general, the deterministic controller proved to be reliable and robust for the assumed random plant and the conditions which were investigated. The deterministic controller was able to converge to the desired response for (1) large excursions in the initial estimate of the  $T$ -Matrix, (2) large  $T$ -Matrix

propagation rates, and (3) moderately high levels of measurement noise. Aside from minor exceptions which were probably coincidental, and the trivial limiting cases for which  $\lambda \rightarrow 0$ , the stochastic controllers did not perform as well as the deterministic controller for the cases which were investigated. Neither external nor internal limiting was applied in order to ensure that the deterministic solution was optimal. Absence of limiting did not affect these results.

The study of the effect of the initial estimate of the  $T$ -Matrix on controller performance showed (sec. 3.2) that the deterministic controller would converge to the response of the baseline controller even if the  $T$ -Matrix initial estimate scaling coefficient  $C_E$  were increased by two orders of magnitude (figs. 27 through 31), but that the stochastic controllers would not converge to the baseline case for any value of the adjoint coefficient  $\lambda$  (figs. 32 through 41) when the initial estimate of the  $T$ -Matrix was made sufficiently large by setting  $C_E = 1.0$  in equation (2-3). In other words, the statistical characteristics of the stochastic controllers, as defined for this study, did not alleviate the problem posed by a bad initial estimate of the  $T$ -Matrix.

During the study of the effect of the plant matrix propagation rate on controller performance (sec. 3.3) the stochastic controllers, as defined for this study, did not enhance convergence to the reference case when the  $T$ -Matrix propagation rate was made large by setting  $C_p = 0.0026$  in equation (2-4). Convergence did occur, but only when the value of the adjoint coefficient  $\lambda$  (figs. 47 through 55) was small enough that the stochastic terms were negligible. The statistical characteristics of the stochastic controllers not only did not alleviate the problems which occur with high  $T$ -Matrix propagation rates, but they actually exacerbated the situation.

It was seen during the study of the effect of measurement noise on controller performance (secs. 3.4.1 through 3.4.3) that the stochastic controllers, as defined for this study, did not enhance convergence to the reference cases either for relatively low measurement noise (e.g., when  $C_M = 2.000$  in equation (2-6)) or for relatively large measurement noise (e.g., when  $C_M = 1.2000$  in equation (2-6)). As in the other cases, convergence did occur, but only when the value of the adjoint coefficient  $\lambda$  (figs. 62 through 79) was sufficiently small that the stochastic terms were negligible and the controller coalesced to the deterministic controller. The presence of the stochastic terms was actually a hindrance rather than a help to convergence.

## 4.2 Identification of Possible Causes of the Results of this Study

Based on the results of previous studies, it had been anticipated that the stochastic controllers would perform better than the deterministic controller under some conditions. The deterministic controller, however, appeared to perform better than the stochastic controllers for the cases which were examined. Indeed, the statistics and its method of application to stochastic controllers was more of a hindrance than a help to convergence. The stochastic controllers, as defined and tested for this study, would approach the performance of the deterministic controller only when the value of the adjoint coefficient  $\lambda$  was small enough to cause the magnitude of the stochastic terms to become negligible when compared to the deterministic part of the controllers. This apparent lack of performance of the stochastic controllers is most likely due to (1) the use of a random plant model rather than a detailed helicopter simulation, (2) the use of a single lattice (i.e., Matrix) of the covariance tensor for the identification process, (3) the adjoining of a stochastic term to the performance index, which is functionally dependent on a single

lattice of the covariance tensor, or (4) the coalescence of stochastic controllers with the deterministic controller for the assumed measurement noise model.

#### 4.2.1 Random Plant Model Versus Detailed Simulations Used on Previous Studies

The apparent lack of performance by the stochastic controllers could be the result of assuming simplified statistics to define the stochastic performance index. Specifically, it was assumed that a stochastic term defined as a function of a single lattice of the rank three covariance tensor associated with  $T$ -Matrix identification could be adjoined to the performance index so that its inclusion would enhance vibration reduction. The presumption that the identification statistics can be adequately represented by a single covariance lattice has the effect of reducing the statistical dimension by one, and can be made if the identification statistics (e.g., the covariance lattice) for each row of the  $T$ -Matrix is nearly the same. If the helicopter fuselage was a rigid body that pivoted at a point, its associated  $T$ -Matrix would be approximately of rank one and, correspondingly, a single covariance lattice should be adequate for all the rows of the  $T$ -Matrix. The helicopter fuselage is, in general, a nonlinear aeroelastic body with bending modes. How reasonable it is to use a single covariance lattice in the performance index depends on at least three circumstances: (1) to what degree the fuselage approximates a rigid body, (2) whether or not the vibration response as measured by the accelerometers is similar to that which would result if the fuselage were a rigid body, and (3) how much variation exists in the identification statistics (i.e., the covariance lattice) for each  $T$ -Matrix row. The expected values of the rank three covariance tensors (note, each covariance tensor is composed of twelve covariance lattices, each of which is of rank seven) were determined for a number of the cases computed during this study. In none of the cases examined did it appear as if the statistics could be adequately represented by a single lattice of the rank three covariance tensor. This result is undoubtedly due to the random methods employed during this study to generate and propagate the  $T$ -Matrix. The use of a single lattice of the covariance tensor not only affects the definition of the stochastic performance index, but it also affects the  $T$ -Matrix identification process itself.

#### 4.2.2 Plant Matrix Identification

A single lattice of the covariance tensor, rather than the full rank three covariance tensor, was used in the Kalman filter identification process (sec. 2.3.2, equations (2-26) and (2-28)). The "correct" procedure would be to define a Kalman filter gain,  $K_j$ , for each  $T$ -Matrix row,  $T_j$ , being identified. Since the  $T$ -Matrix appears in the control laws of the three controllers (secs. 2.4.1, 2.4.2.1, and 2.4.2.2), it was expected that the use of only a single lattice of the rank three covariance tensor for  $T$ -Matrix identification could significantly affect the corresponding definition of the  $T$ -Matrix. Oddly enough, but not necessarily in contradiction with the apparent difficulties in defining the optimal control with the stochastic controllers, the evidence obtained during this study clearly indicates that this approximation did not significantly adversely affect the  $T$ -Matrix identification. Indeed, the  $T$ -Matrix identification process used in this study appeared to work reasonably well.

#### 4.2.3 Stochastic Term in Performance Index

It was pointed out in section 2.3.1 that typically for the helicopter vibration reduction problem, it was desired to minimize a scalar measure of the vibration (i.e., a vibration metric) subject to the imposition

of inequality constraints on the control. It was also pointed out that the adjoining of nonperformance terms, other than bona fide equality constraint functions adjoined by bona fide Lagrangian multipliers, to the performance index did, in general, result in a suboptimal solution. Indeed, a scalar example of this performance degradation was illustrated in section 3.1.2.2. There is no apparent justification for adding separate stochastic terms to the performance index of the stochastic controllers examined in this study; indeed, it should be expected that the addition of these stochastic terms to the performance index would decrease performance. If the philosophy is to enhance identification by driving the covariance to zero; this should be done in the identification part of the process in conjunction with the covariance update. Even if the addition of a covariance term to the performance index were desirable, this term should, in general, involve the full rank three covariance tensor, not just a single lattice of it, for the  $T$ -Matrix model used in this study.

#### 4.2.4 Coalescence of Stochastic Controllers with the Deterministic Controller

Rather than adding covariance terms to the performance index as was done for the cautious and dual controllers, a more meaningful approach to using the statistics of the process to enhance selection of the control is suggested in part by the minimum variance controller presented by Davis in reference 1. For this approach, the expected value of the quadratic metric of the  $Z$ -Vector defined by equation (2-20) is minimized subject to the inequality constraints defined by equation (2-8):

Minimize

$$J = E[Z^T W_Z Z] \quad (4-1)$$

subject to

$$\psi_k(\theta) \geq 0 \quad \text{for } k = 1, 2, \dots, M \quad (4-2)$$

where

$$E[Z^T W_Z Z] = \int_{-\infty}^{+\infty} \int_{-\infty}^{+\infty} \dots \int_{-\infty}^{+\infty} (Z^T W_Z Z) f(Z) dz_1 dz_2 \dots dz_{2L} \quad (4-3)$$

and  $f(Z)$  is the probability density function.

This stochastic controller should perform as well as or better than the other stochastic controllers which were the subject of this study simply because this controller directly addresses the real problem, that is, minimization of the expected value of the vibration metric. The probability density function for the random modeling used in this study is uniform and is defined by

$$f(Z) \equiv \left\{ \begin{array}{ll} 0 & \text{if } |z_k| > 1 \\ C & \text{if } |z_k| \leq 1 \end{array} \right\} \quad \text{for } k = 1, 2, \dots, 2L \quad (4-4)$$

where  $C$  is a nonzero constant.

Setting the derivative of  $J$  to zero for the uniform probability density function defined by equation (4-4) yields the same conditions for optimal control as those defined for the deterministic controller. In other words, this stochastic controller coalesces with the deterministic controller when the probability density function becomes uniform.

The stochastic part of the controller defined by equations (4-1) through (4-4) only describes the measurement noise statistics; the statistics of the  $T$ -Matrix identification process is not included. This means that the  $T$ -Matrix is assumed to be known identically and, correspondingly, the performance of this stochastic controller should be better than that of stochastic controllers for which the  $T$ -Matrix is identified with statistical errors (e.g., the cautious and dual controllers). If indeed this is true, and it appears reasonable that it is even though it is not readily provable, then the stochastic controllers as defined and modeled in this study cannot be expected to perform any better than the deterministic controller.

### 4.3 Theoretical Limitations of These Controllers

Two principal limitations in the formulation of the subject controllers were identified: (1) the definition of the desired control problem to be solved, and (2) the selection of the  $T$ -Matrix identification algorithm. The desired control problem to be solved is simply to define the control which minimizes a metric of the vibration, subject to the imposition of inequality constraints on the control, and in which the  $T$ -Matrix is identified in an efficient, reliable, and accurate manner. The  $T$ -Matrix identification algorithm determines the quality of the identified  $T$ -Matrix and its associated statistics, which are used by the controller to define the "optimal" control.

#### 4.3.1 Definition of the Optimal Control Problem

The subject controllers of this study appeared not to directly address the desired control problem, defined in equations (2-7) and (2-8). Instead these controllers were formulated to address the different problems defined by (1) equations (2-37) through (2-40), for the deterministic controller, (2) equations (2-41) through (2-48), for the cautious controller, and (3) equations (2-49) through (2-54), for the dual controller. The stochastic controllers included internal limiting in the performance index and external limiting applied after the fact, rather than adjoining the appropriate constraints to the performance index with an adjoint vector composed of Lagrangian multipliers. Furthermore, these stochastic controllers incorporated the statistics as add-on stochastic terms to the performance index. Because of this, it is expected that these controllers could never perform better than a controller designed to solve the desired problem defined by equations (2-7) and (2-8). For convenience in documentation, the limitations of these controllers are grouped according to their applicability to the deterministic and stochastic parts of the controller.

**4.3.1.1 Deterministic Part**—The deterministic part of all three controllers should include only that which is to be minimized. The limitations of optimization theory require that this performance index be a scalar. Furthermore, to facilitate the automation of the process, this performance index should be a function of only one performance parameter. If more than one performance parameter is to be minimized, some parameterization scheme should be employed in which one of the performance parameters is minimized while the others are parametrically varied as appropriate.

The relatively common procedure of simply adding the performance parameters to form a scalar performance index is fraught with peril. In the first place, the minimization of a sum of parameter terms is not the same thing as minimizing the individual terms. It is possible that some of the terms will decrease while others will increase, or that some of the terms will not decrease as much as desired

while others will decrease more than required. The practice of using weighting coefficients for the various terms requires trial-and-error selection and adjustment for example problems and can, in some circumstances, become a problem of sorcery and witchcraft. Even if all the terms decrease in an acceptable manner, a minor change in the problem can cause the individual terms in the solution to have different relative values, thus complicating the interpretation of the results.

The example scalar problems illustrated in figures 22 and 23 clearly show the discrepancy between the solutions to the optimal control for minimization of the vibration metric,  $\theta_{Z_{min}}$ , and the optimal control for minimization of the augmented problem,  $\theta_{min}$ , with a corresponding discrepancy in the attainable vibration reduction. The actual multidimensional helicopter vibration problem examined during this study has similar discrepancies from the actual optimal control vector and its corresponding attainable vibration reduction.

**4.3.1.2 Stochastic Part**—The stochastic terms in the performance index and corresponding control laws for the cautious and dual controllers were assumed to be dependent on only a single lattice of the rank three covariance tensor, rather than on the entire covariance tensor itself. Since the assumed *T*-Matrix models are random in all elements and have no apparent row (or column) linear dependence, there is no apparent justification for assuming that a single lattice (matrix) of the covariance tensor associated with a specific row of the *T*-Matrix adequately describes the statistics of *T*-Matrix identification. A single lattice might suffice if some degree of linear dependence between the *T*-Matrix rows existed.

In general, only the actual single scalar measure to be minimized (or maximized) and the duly adjoined (added with Lagrangian multipliers) proper constraint functions (i.e., constraints of the form defined by equation (2-14)) should be elements of the performance index. There is no advantage to including anything else in the performance index; indeed, the inclusion of anything else will result in a suboptimal solution. For this reason, it should be expected that stochastic controllers whose performance index has the form defined by equation (2-30) will not generally perform as well as either deterministic or stochastic controllers whose performance index has the form defined by equation (2-7) or equation (2-13).

#### **4.3.2 Limitations of the Plant Matrix Identification Algorithm**

The principal limitation of the Kalman filter identification scheme used in this study was the accuracy required for the initial estimate of the *T*-Matrix (sec. 3.2). In general, notwithstanding the use of only a single lattice of the covariance tensor, this identification algorithm appeared to adequately identify the *T*-Matrix for reasonable initial estimates of the *T*-Matrix.

## **5 FUTURE CONTROLLER DEVELOPMENT**

The results of this study suggest that (1) controller performance could be improved by defining the performance index to be the actual vibration measure and expressing the resulting optimal control problem in the classical max/min calculus form with constraints, (2) an improved stochastic controller could be defined by using the classical form, with the performance index defined as the next-cycle-expected-value of the actual vibration measure, (3) other identification schemes should be examined to determine if any of them provide better identification when used with these specific controllers, and

(4) a relatively simple higher harmonic blade pitch control scheme for the cockpit can be defined when the aforementioned controllers are employed.

## 5.1 Theoretical Considerations

The theoretical considerations focused on (1) the deterministic and stochastic parts of the optimal control problem the controller is designed to solve, and (2) the  $T$ -Matrix identification scheme.

### 5.1.1 Deterministic Part

It is strongly contended that both the deterministic and stochastic controllers should be designed to solve the optimal control problem defined by equations (2-7) and (2-8), in which the inequality constraints are transformed to equality constraints and then adjoined to the performance index with an adjoint vector composed of Lagrangian multipliers, rather than the problem defined by equations (2-30) and (2-31), in which the control constraints are treated as part of the performance measure to be minimized instead of constraints to be satisfied. Specifically, only the vibration measure should be used to form the performance index. For the deterministic controller, the performance index should be  $Z^T W_Z Z$  as defined by equation (2-20). For the stochastic controller, the performance index should be the expected value of  $Z^T W_Z Z$ ,  $E(Z^T W_Z Z)$ , as defined by equation (4-1) at the next time step. The next time step is usually the first opportunity to implement the newly determined control vector. The control vector constraints, which are inequality constraints, can easily be transformed to equality constraints by using the slack variable method defined by equations (2-9) through (2-12) so that they can be adjoined to the performance index with Lagrangian multipliers and the problem can be solved using conventional max/min calculus. This methodology is common to the recommended deterministic and stochastic controllers and is referred to herein as the deterministic part of the problem.

A problem similar to the problem addressed in this study, of a lower dimension but with the form defined by equations (2-7) and (2-8), was solved analytically in this manner to demonstrate the feasibility of obtaining an analytic solution to the full problem. A cursory attempt was made to solve the full problem addressed in this study. Although a full analytic solution to this problem has not been derived at this time, the solution process clearly shows that the solution, if it exists, is similar to that obtained for the lower dimensional problem which was solved.

### 5.1.2 Stochastic Part

It is also strongly contended that the stochastic controller should be designed to solve the optimal control problem defined by equations (4-1) through (4-4), in which the performance index is defined to be  $E(Z^T W_Z Z)$  at the next time step, rather than the problems defined by equations (2-30) and (2-31), in which the control constraints are treated as part of the performance measure to be minimized instead of constraints to be satisfied. Specifically, the statistics of the problem should be incorporated into the solution by using the appropriate probability density functions to define the expected value of the vibration measure,  $E(Z^T W_Z Z)$ , that is to be minimized at the next time step, rather than by adding bits and parts of a covariance tensor to a deterministic performance index. This methodology is referred to herein as the stochastic part of the problem and is unique to the stochastic controller.

### 5.1.3 Plant Matrix Identification

Although the Kalman filter identification scheme used in this study adequately identified the *T*-Matrix only for reasonable initial estimates of the *T*-Matrix, no alternative identification schemes were examined. It is noted that the actual scheme employed in this study used only a single lattice of the covariance tensor, and extension of this scheme to use the full covariance tensor only requires a relatively simple and minor modification. It was determined that the initial estimate of the *T*-Matrix does affect controller performance. Alternative identification schemes should be examined, as Jacklin did in his comparison of five identification schemes (ref. 8), to determine if any other schemes offer greater reliability, robustness, simplification, ease in initiation, or other advantages. It would greatly simplify matters if it were not necessary to provide an initial estimate to the *T*-Matrix, and if covariance tensors were not required as part of the identification process.

## 5.2 Cockpit Application

When the optimal control problem is in the form defined by equations (2-7) and (2-8), that is, when the problem is to determine the control that minimizes a metric of the vibration subject to the imposition of inequality constraints on the control, the solution can be exploited to yield a relatively simple higher harmonic blade pitch control device for the cockpit. The definition of the constraint envelopes will, most likely, be based on required maintenance intervals and wear/fatigue/structural limits. Typically, a relationship exists between the level of the operating higher harmonic blade pitch constraint envelopes and the time left before the next required maintenance. It is expected that the higher the operating constraint envelope levels, the shorter the operating time to the next required maintenance. Accordingly, a set of operating constraint envelope limits, characterized by the time to next required maintenance, can be defined. For example, operating constraint levels corresponding to time to next required maintenance values of 1,000 hr (for normal operation), 100 hr (for elevated operation), 10 hr (for higher elevated operation), 1 hr (for still higher elevated operation), and 6-min (for emergency operation) can be defined. Correspondingly, the HHC unit (fig. 102) would include the HHC switch with an OFF position and positions for the time to next required maintenance values specified above. Since the time to next required maintenance is dependent on the operating constraint level, if the HHC switch is set to different positions between consecutive maintenances, then evaluation of the time to next required maintenance requires an integration of the current time to next required maintenance. This integration can be easily accomplished with an integration circuit in the HHC unit. A convenient way to display these results would be to include a digital counter on the HHC unit which displays the "integrated actual" time to next required maintenance.

Operationally, the pilot would set the HHC switch to the 1,000-hr (normal) position when HHC was desired. If an emergency occurred involving a rotor imbalance of some kind, the HHC switch could be turned to its limit at the 6-min (emergency) position. If no improvement occurs, the pilot would have to take other measures including backing the HHC switch down to a lower setting. If satisfactory improvement occurs, the switch would be backed down to a lower, but acceptable, setting after the pilot regains satisfactory control of the helicopter.

## REFERENCES

1. Davis, Mark W.: Refinement and Evaluation of Helicopter Real-Time Self-Adaptive Active Vibration Controller Algorithms. NASA CR-3821, 1984.
2. Lizak, Alfred A.: Design, Operation, and Maintenance Manual for NASA-Ames Rotor Test Apparatus. SER-50988, Sikorsky Aircraft, 1977.
3. Halfman, Robert L.: Dynamics, Systems, Variational Methods, and Relativity. Addison-Wesley Publishing Co., Inc., 1962.
4. Hamming, R. W.: Numerical Methods for Scientists and Engineers. Second ed., Dover Publications, Inc., 1973.
5. Edwards, C. H., Jr.; and Penney, David E.: Calculus and Analytic Geometry. Prentice-Hall, Inc., 1982.
6. Schultz, Donald G.; and Melsa, James L.: State Functions and Linear Control Systems. McGraw-Hill Book Co., 1967.
7. Pontryagin, L. S.; Boltyanskii, V. G.; Gamkrelidze, R. V.; and Mishchenko, E. F.: The Mathematical Theory of Optimal Processes. John Wiley & Sons, Inc., 1962.
8. Jacklin, Stephen A.: Performance Comparison of Five Frequency Domain System Identification Techniques for Helicopter Higher Harmonic Control. 2nd International Conference of Rotorcraft Basic Research, University of Maryland, Feb. 16-18, 1988.

## TABLES

Table 1. The effect of the starting seed on the first-step decrease in  $J$ .

Starting seed value for propagation	Figure number	Percentage decrease in $J$ after the first control step
7391	3	19.356
3962117		56.375
435		42.919
10691		16.931
7398495		31.775
990539		28.594
62117		50.663
49377		64.825
83297		65.800
83293		56.900
83298	4	66.956
27438		28.256
27437		39.706
83299		66.206
83300		48.869
83301		30.175
83296		43.619

**Notes:**

<sup>a</sup>The starting seed value of 7391 for  $T$ -Matrix initialization and propagation was assumed initially during program checkout.

<sup>b</sup>A starting seed value of 83298 for  $T$ -Matrix initialization and propagation yielded the greatest decrease in  $J$  after the first control step.

Table 2. Summary of the external limiting study.

External limiting l.u.b. [ $R_{\theta_j}$ ] $_{max}$ and/or [ $R_{\Delta\theta_j}$ ] $_{max}$	Figure number	Percentage decrease in $J$ after the first control step	Number of revolutions to g.l.b.
100,000,000		66.956	5
1,000		66.956	5
100		66.956	5
80		66.956	5
60		66.956	5
40	5	66.956	5
36.91		66.956	5
36.905		66.950	5
34		66.444	5
31		66.019	5
28		62.681	5
27		61.700	5
20	6	52.006	6
10	7	29.556	8
8		23.850	9
6	8	18.831	11
4		13.644	14
2		7.231	23
1	9	3.569	30+
0.1	10	0.013	30+
0.01		-0.356	30+
0.001		-0.394	30+
0.0001		-0.400	30+
0.0000000001		-0.400	30+

Notes:

<sup>a</sup>The theta control vector is zero at the initiation of the fourth revolution at which time the controller is engaged. The response to the first computed nonzero theta control vector occurs at the beginning of the fifth revolution.

<sup>b</sup>The starting seed value of 83298 for  $T$ -Matrix initialization and propagation was assumed.

<sup>c</sup>The  $T$ -Matrix is invariant.

Table 3. Summary of the internal limiting study.

Internal limiting diag ( $W_\theta$ )	Internal limiting diag ( $W_{\Delta\theta}$ )	Figure number	Remarks
0	0	13	Reference case with no limiting.
0	10,000	14	Saturated, no effective decrease in $J$ .
0	1,000		Saturated, no effective decrease in $J$ .
0	100		Saturated, no effective decrease in $J$ .
0	10		Saturated, no effective decrease in $J$ .
0	1		Saturated, no effective decrease in $J$ .
0	0.3162		Saturated, on verge of a decrease in $J$ .
0	0.1	15	Saturated, some decrease in $J$ .
0	0.03162		Slow convergence, minimum $J$ by 40 revs.
0	0.01	16	Slow convergence, minimum $J$ by 20 revs.
0	0.003162		Convergence to minimum $J$ by 20 revs.
0	0.001	17	Nearly the same as the no-limiting case.
0	0.0001		Nearly the same as the no-limiting case.
100	0	18	Saturated, no effective decrease in $J$ .
10	0		Saturated, no effective decrease in $J$ .
1	0		Saturated, no effective decrease in $J$ .
0.1	0		Saturated, no effective decrease in $J$ .
0.01	0	19	Saturated, on verge of a decrease in $J$ .
0.003162	0		Saturated, some decrease in $J$ .
0.001	0	20	Saturated, significant decrease in $J$ .
0.0003162	0		Closer to the no-limiting case.
0.0001	0	21	Nearly the same as the no-limiting case.
0.00003162	0		Nearly the same as the no-limiting case.
0.00001	0		Nearly the same as the no-limiting case.
0.000001	0		Nearly the same as the no-limiting case.

Notes:

<sup>a</sup>The theta control vector is zero at the initiation of the fourth revolution at which time the controller is engaged. The response to the first computed nonzero theta control vector occurs at the beginning of the fifth revolution.

<sup>b</sup>The starting seed value of 83298 for  $T$ -Matrix initialization and propagation was assumed.

<sup>c</sup>The  $T$ -Matrix was propagated with the propagation scaling coefficient  $C_\rho = 0.001$  (see sections 2.2.3 and 3.1.3).

Table 4. Summary of the baseline plant matrix propagation rate study.

$T$ -Matrix propagation scaling coefficient $C_\rho$	Figure	Remarks
0.0005	24	Flat and unexciting.
0.0007		Reasonable, but somewhat too flat.
0.0010	25	Reasonable and representative, selected to be the baseline.
0.0013		Reasonable, but excursions slightly too high.
0.0020	26	Excursions too high.
0.0030		Excursions too high.
0.0100		Excursions way too high!

Notes:

<sup>a</sup>The theta control vector is zero at the initiation of the fourth revolution at which time the controller is engaged. The response to the first computed nonzero theta control vector occurs at the beginning of the fifth revolution.

<sup>b</sup>The starting seed value of 83298 for  $T$ -Matrix initialization and propagation was assumed.

Table 5. Summary of the  $T$ -Matrix initial estimate study.

Controller type	$T$ -Matrix initial estimate scaling coefficient $C_E$	Adjoint coefficient $\lambda$	Figure
Deterministic	0.001	0	27
Deterministic	0.01	0	28
Deterministic	0.1	0	29
Deterministic	0.69897	0	
Deterministic	1.0	0	30
Deterministic	6.98970	0	
Deterministic	10.0	0	31
Cautious	1.0	0.00001	
Cautious	1.0	0.0001	32
Cautious	1.0	0.001	
Cautious	1.0	0.01	33
Cautious	1.0	0.1	34
Cautious	1.0	1.0	
Cautious	1.0	10.0	35
Cautious	1.0	100.0	
Dual	1.0	0.0000001	
Dual	1.0	0.000001	36, 37
Dual	1.0	0.00001	
Dual	1.0	0.0001	38
Dual	1.0	0.001	39
Dual	1.0	0.01	40
Dual	1.0	0.1	41
Dual	1.0	1.0	

Notes:

<sup>a</sup>The theta control vector is zero at the initiation of the fourth revolution at which time the controller is engaged. The response to the first computed nonzero theta control vector occurs at the beginning of the fifth revolution.

<sup>b</sup>The starting seed value of 83298 for  $T$ -Matrix initialization and propagation was assumed.

<sup>c</sup>The  $T$ -Matrix was propagated with the propagation scaling coefficient  $C_p = 0.001$  (sections 2.2.3 and 3.1.3), with 20% random nonperiodic measurement noise ( $C_M = 0.200$ ), with no limiting, and for parametric values of the initial  $T$ -Matrix estimate scaling coefficient  $C_E$ .

Table 6. Summary of the  $T$ -Matrix propagation rate study.

Controller type	$T$ -Matrix propagation scaling coefficient $C_p$	Adjoint coefficient $\lambda$	Figure
Deterministic	0.0010	0	42
Deterministic	0.0020	0	43
Deterministic	0.0022	0	
Deterministic	0.0024	0	44
Deterministic	0.0026	0	45
Deterministic	0.0028	0	
Deterministic	0.0030	0	46
Cautious	0.0026	0.00001	
Cautious	0.0026	0.0001	47, 48
Cautious	0.0026	0.001	49
Cautious	0.0026	0.01	50
Cautious	0.0026	0.1	
Cautious	0.0026	1.0	
Cautious	0.0026	10.0	
Cautious	0.0026	100.0	
Dual	0.0026	0.0000001	
Dual	0.0026	0.000001	51, 52
Dual	0.0026	0.00001	53
Dual	0.0026	0.0001	54
Dual	0.0026	0.001	55
Dual	0.0026	0.01	
Dual	0.0026	0.1	
Dual	0.0026	1.0	

Notes:

<sup>a</sup>The theta control vector is zero at the initiation of the fourth revolution at which time the controller is engaged. The response to the first computed nonzero theta control vector occurs at the beginning of the fifth revolution.

<sup>b</sup>The starting seed value of 83298 for  $T$ -Matrix initialization and propagation was assumed.

<sup>c</sup>The  $T$ -Matrix was propagated with parametric values of the propagation scaling coefficient  $C_p$  (sections 2.2.3 and 3.1.3), with 20% random nonperiodic measurement noise ( $C_M = 0.200$ ), with no limiting, and for the initial  $T$ -Matrix estimate scaling coefficient  $C_E = 0.001$ .

Table 7. Summary of the random nonperiodic measurement noise level study study.

Controller type	Measurement noise scaling coefficient $C_M$	Adjoint coefficient $\lambda$	Figure
Deterministic	0.0000	0	56
Deterministic	0.1000	0	
Deterministic	0.2000	0	57
Deterministic	0.3000	0	
Deterministic	0.4000	0	58
Deterministic	0.5000	0	
Deterministic	0.6000	0	59
Deterministic	0.7000	0	
Deterministic	0.8000	0	
Deterministic	0.9000	0	60
Deterministic	1.0000	0	
Deterministic	1.1000	0	
Deterministic	1.2000	0	61
Deterministic	1.3000	0	
Cautious	0.2000	0.00001	62
Cautious	0.2000	0.0001	
Cautious	0.2000	0.001	63
Cautious	0.2000	0.01	64
Cautious	0.2000	0.1	65
Cautious	0.2000	1.0	
Cautious	0.2000	10.0	
Dual	0.2000	0.0000001	66
Dual	0.2000	0.000001	
Dual	0.2000	0.00001	67
Dual	0.2000	0.0001	68
Dual	0.2000	0.001	69
Dual	0.2000	0.01	
Dual	0.2000	0.1	

Table 7. Concluded.

Controller type	Measurement noise scaling coefficient $C_M$	Adjoint coefficient $\lambda$	Figure
Cautious	1.2000	0.000001	
Cautious	1.2000	0.00001	70
Cautious	1.2000	0.0001	71
Cautious	1.2000	0.001	72
Cautious	1.2000	0.01	
Cautious	1.2000	0.1	73
Cautious	1.2000	1.0	
Dual	1.2000	0.000000001	
Dual	1.2000	0.00000001	74
Dual	1.2000	0.0000001	
Dual	1.2000	0.000001	75, 76
Dual	1.2000	0.00001	77
Dual	1.2000	0.0001	78
Dual	1.2000	0.001	79
Dual	1.2000	0.01	

Notes:

<sup>a</sup>The theta control vector is zero at the initiation of the fourth revolution at which time the controller is engaged. The response to the first computed nonzero theta control vector occurs at the beginning of the fifth revolution.

<sup>b</sup>The starting seed value of 83298 for  $T$ -Matrix initialization and propagation was assumed.

<sup>c</sup>The  $T$ -Matrix was propagated with the propagation scaling coefficient  $C_\rho = 0.001$  (sections 2.2.3 and 3.1.3), for parametric values of the random nonperiodic measurement noise coefficient  $C_M$ , with no limiting, and for the initial  $T$ -Matrix estimate scaling coefficient  $C_E = 0.001$ .

Table 8. Summary of the random 20-cycle periodic measurement noise level study.

Controller type	Measurement noise scaling coefficient $C_M$	Adjoint coefficient $\lambda$	Figure
Deterministic	0.0000	0	80
Deterministic	0.1000	0	
Deterministic	0.2000	0	81
Deterministic	0.3000	0	
Deterministic	0.4000	0	82
Cautious	0.2000	0.00001	83
Cautious	0.2000	0.0001	
Cautious	0.2000	0.001	84
Cautious	0.2000	0.01	85
Cautious	0.2000	0.1	86
Cautious	0.2000	1.0	
Dual	0.2000	0.0000001	87
Dual	0.2000	0.000001	
Dual	0.2000	0.00001	88
Dual	0.2000	0.0001	89
Dual	0.2000	0.001	90
Dual	0.2000	0.01	

Notes:

<sup>a</sup>The theta control vector is zero at the initiation of the fourth revolution at which time the controller is engaged. The response to the first computed nonzero theta control vector occurs at the beginning of the fifth revolution.

<sup>b</sup>The starting seed value of 83298 for  $T$ -Matrix initialization and propagation was assumed.

<sup>c</sup>The  $T$ -Matrix was propagated with the propagation scaling coefficient  $C_p = 0.001$  (sections 2.2.3 and 3.1.3), for parametric values of the random 20-cycle periodic measurement noise coefficient  $C_M$ , with no limiting, and for the initial  $T$ -Matrix estimate scaling coefficient  $C_E = 0.001$ .

Table 9. Summary of the nonrandom 20-cycle periodic measurement noise level study.

Controller type	Measurement noise scaling coefficient $C_M$	Adjoint coefficient $\lambda$	Figure
Deterministic	0.0000	0	91
Deterministic	0.1000	0	
Deterministic	0.2000	0	92
Deterministic	0.3000	0	
Deterministic	0.4000	0	93
Cautious	0.2000	0.00001	94
Cautious	0.2000	0.0001	
Cautious	0.2000	0.001	95
Cautious	0.2000	0.01	96
Cautious	0.2000	0.1	97
Cautious	0.2000	1.0	
Dual	0.2000	0.0000001	98
Dual	0.2000	0.000001	
Dual	0.2000	0.00001	99
Dual	0.2000	0.0001	100
Dual	0.2000	0.001	101
Dual	0.2000	0.01	

Notes:

<sup>a</sup>The theta control vector is zero at the initiation of the fourth revolution at which time the controller is engaged. The response to the first computed nonzero theta control vector occurs at the beginning of the fifth revolution.

<sup>b</sup>The starting seed value of 83298 for  $T$ -Matrix initialization and propagation was assumed.

<sup>c</sup>The  $T$ -Matrix was propagated with the propagation scaling coefficient  $C_\rho = 0.001$  (sections 2.2.3 and 3.1.3), for parametric values of the nonrandom 20-cycle periodic measurement noise coefficient  $C_M$ , with no limiting, and for the initial  $T$ -Matrix estimate scaling coefficient  $C_E = 0.001$ .

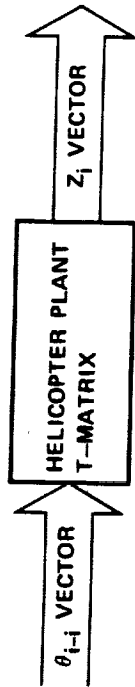


Figure 1. Controlled vibration response.

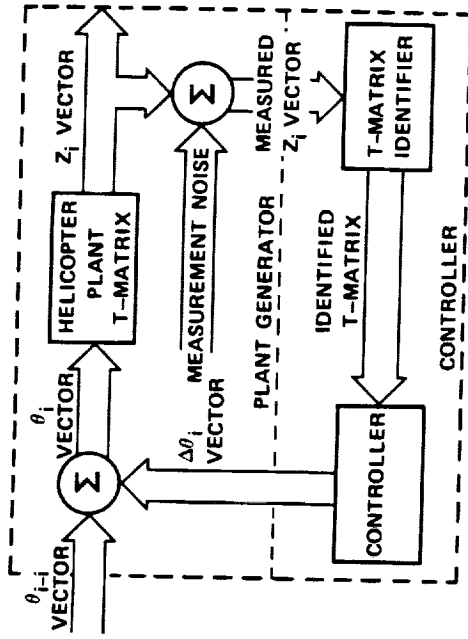


Figure 2. General scheme for the closed-loop vibration control system.

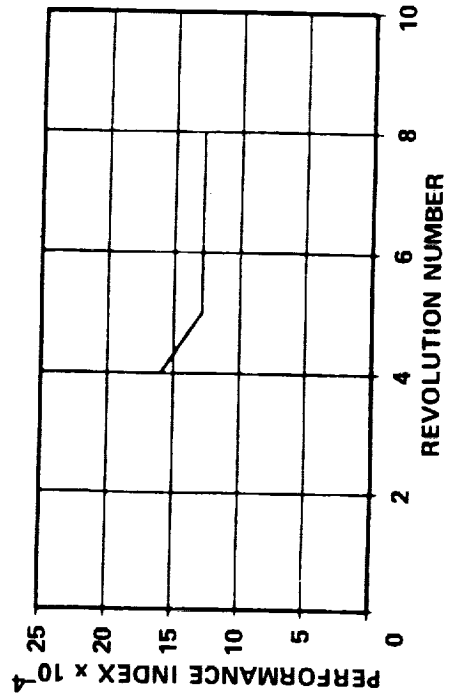


Figure 3. Initial response for starting seed value = 7391.

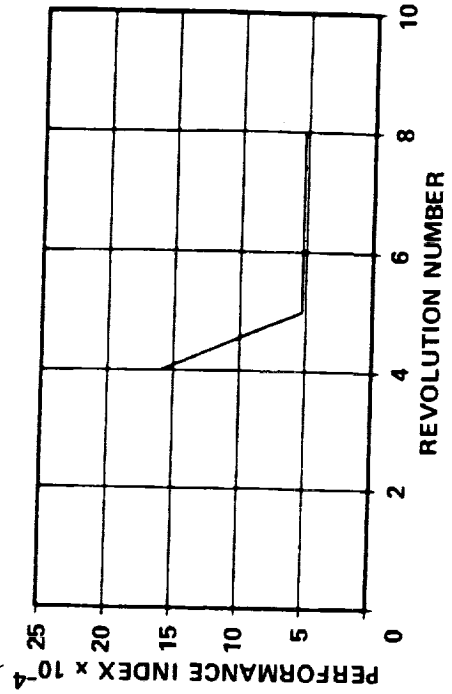


Figure 4. Initial response for starting seed value = 83298.

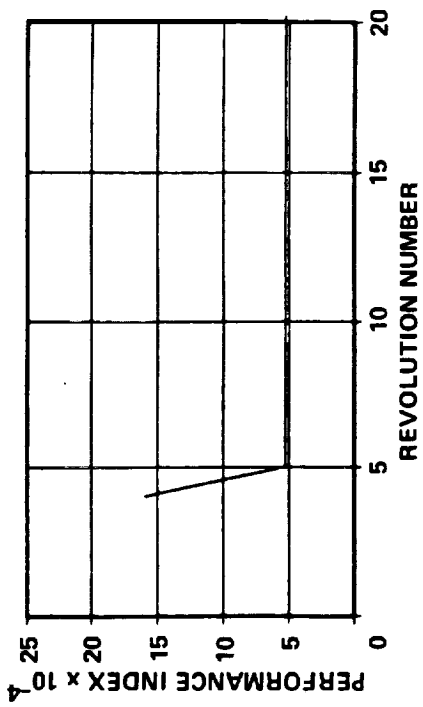


Figure 5. Response when external limiting  
l.u.b. = 40.

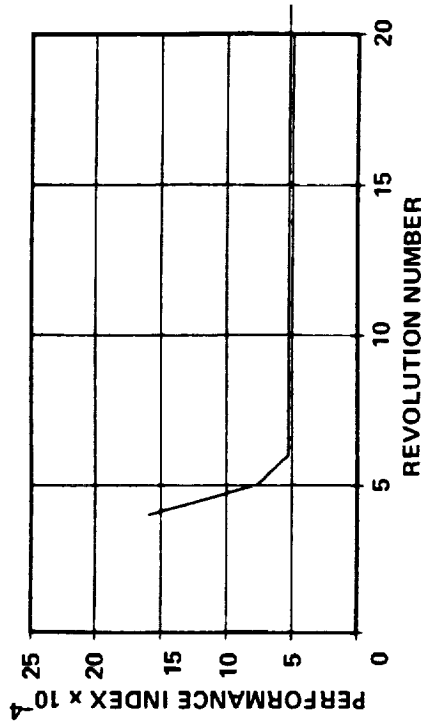


Figure 6. Response when external limiting  
l.u.b. = 20.

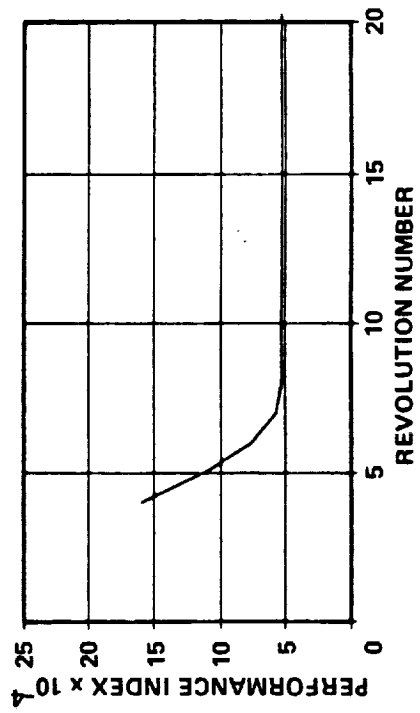


Figure 7. Response when external limiting  
l.u.b. = 10.

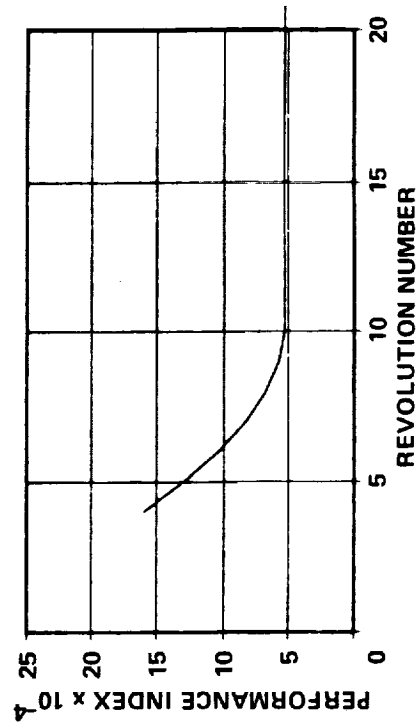


Figure 8. Response when external limiting  
l.u.b. = 6.

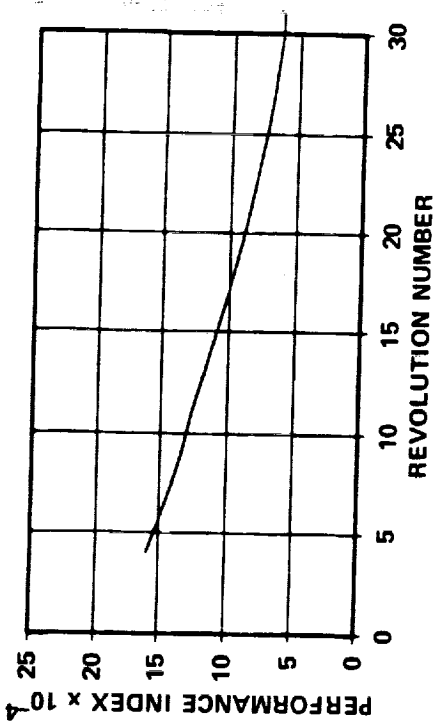


Figure 9. Response when external limiting l.u.b. = 1.

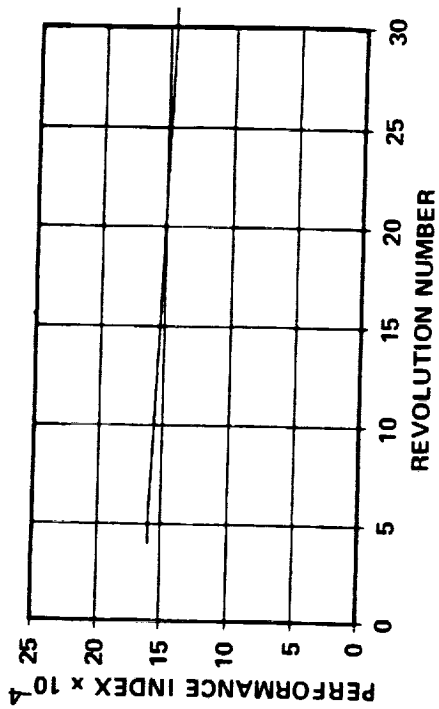


Figure 10. Response when external limiting l.u.b. = 0.1.

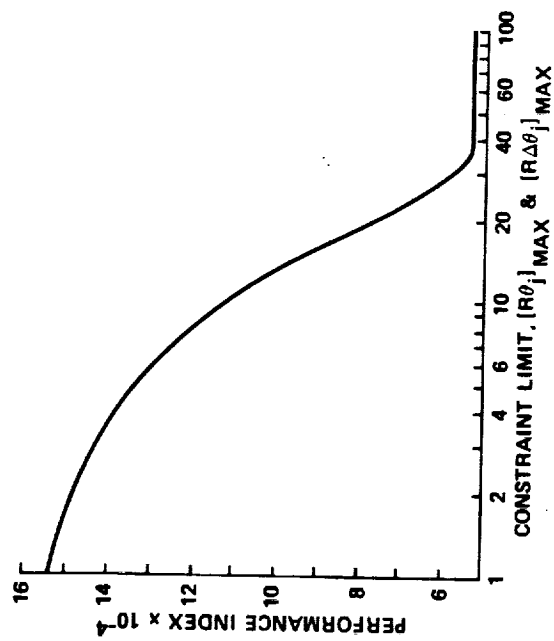


Figure 11. Performance index after first controlled step.

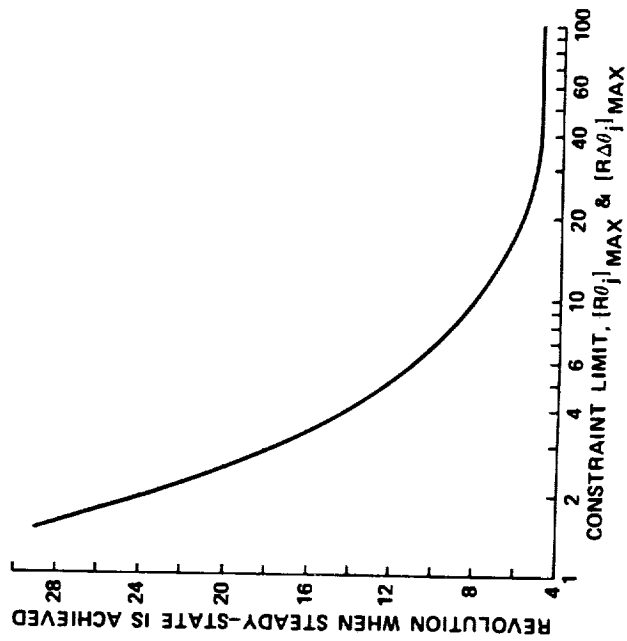


Figure 12. Revolution when steady state is achieved.

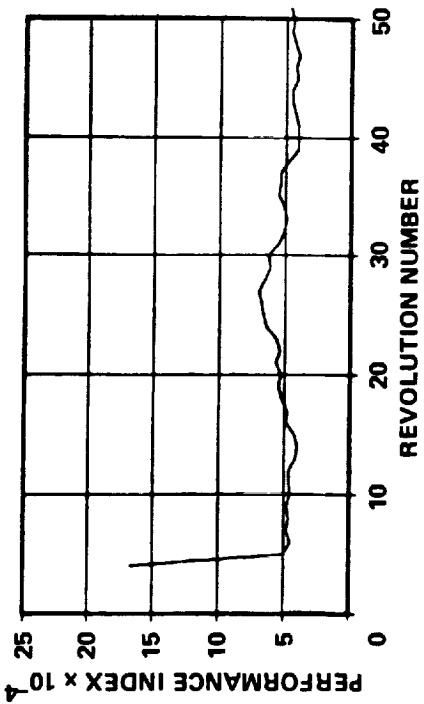


Figure 13. Response when there is no limiting.

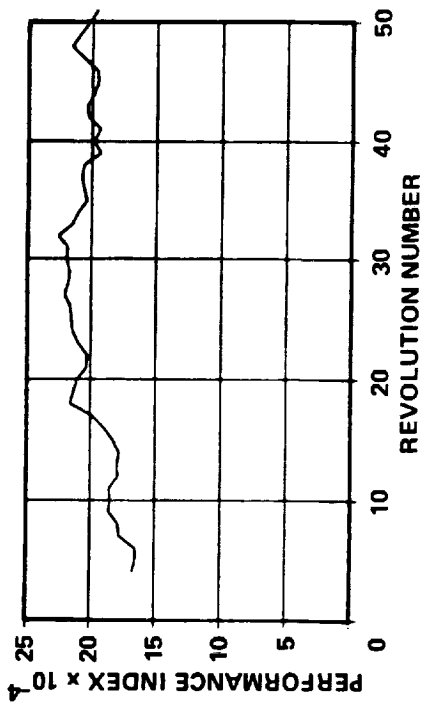


Figure 14. Response when internal limiting is applied with  $W_{\Delta\theta} = 10,000$ .

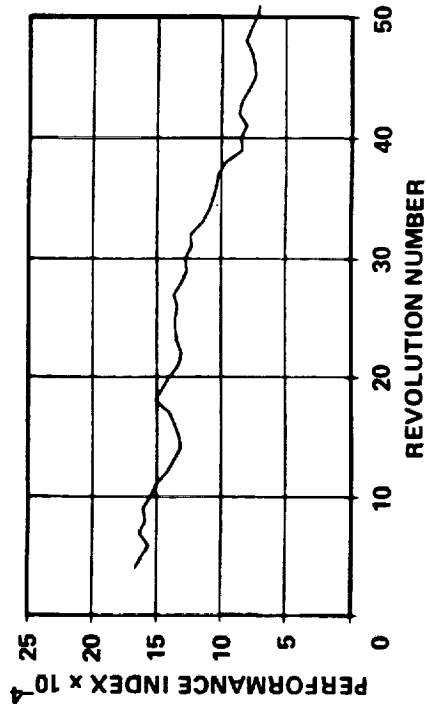


Figure 15. Response when internal limiting is applied with  $W_{\Delta\theta} = 0.1$ .

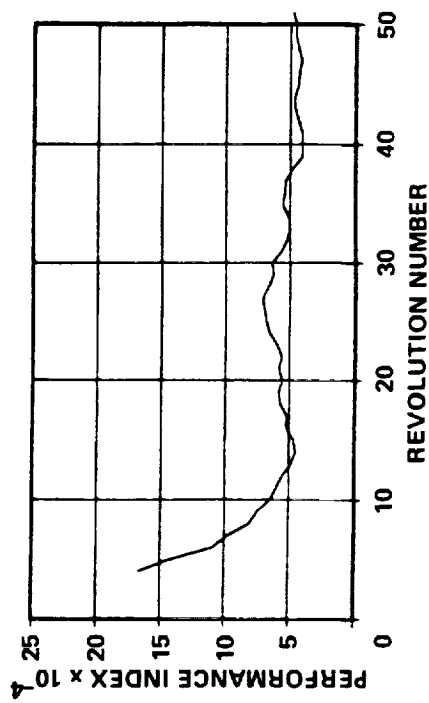


Figure 16. Response when internal limiting is applied with  $W_{\Delta\theta} = 0.01$ .

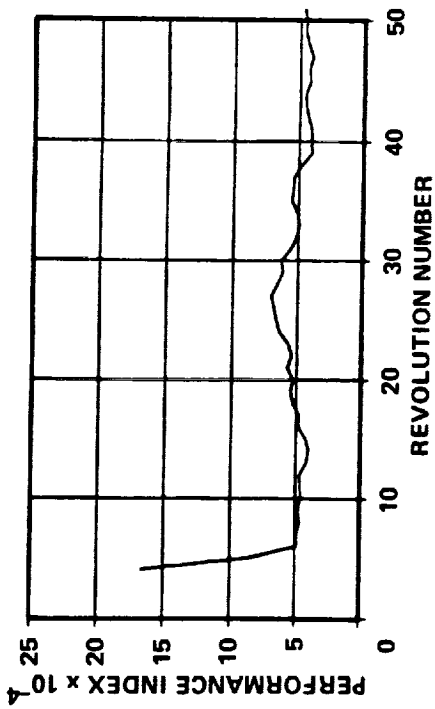


Figure 17. Response when internal limiting is applied with  $W_{\Delta\theta} = 0.001$ .

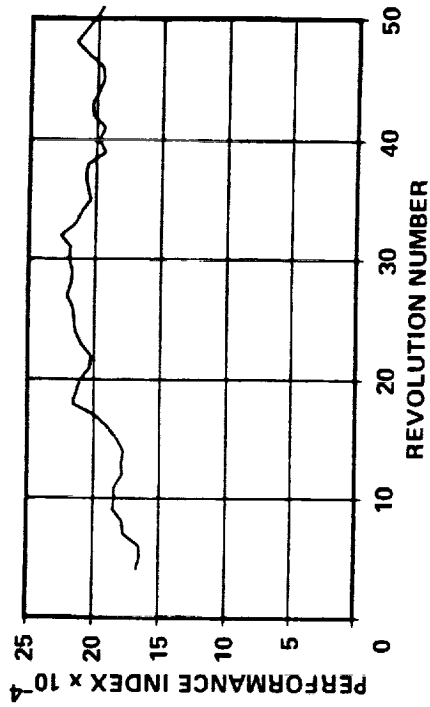


Figure 18. Response when internal limiting is applied with  $W_{\theta} = 100$ .

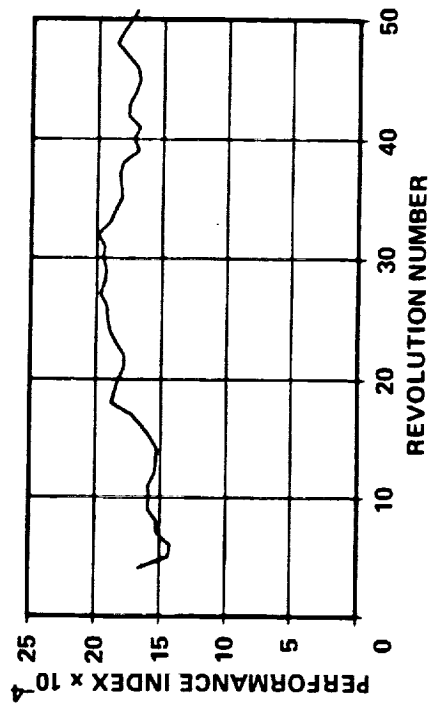


Figure 19. Response when internal limiting is applied with  $W_{\theta} = 0.01$ .

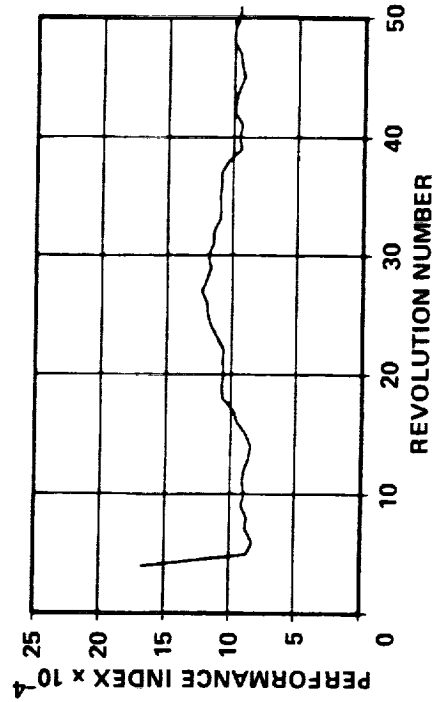


Figure 20. Response when internal limiting is applied with  $W_{\theta} = 0.001$ .

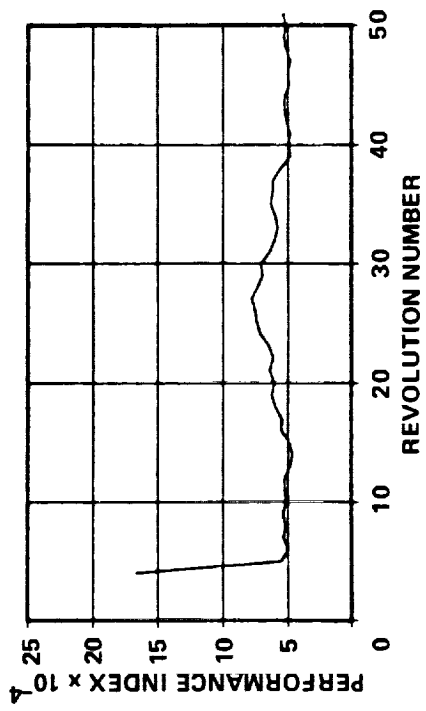


Figure 21. Response when internal limiting is applied with  $W_{\theta} = 0.0001$ .

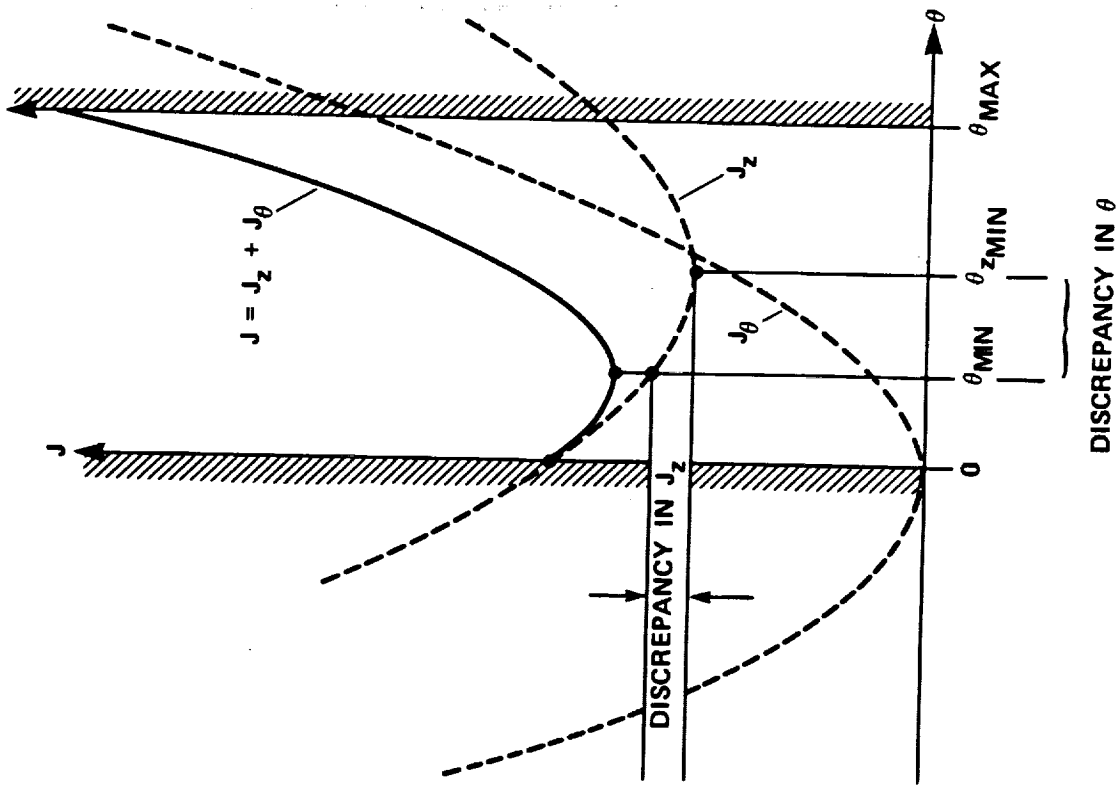


Figure 22. First scalar case showing discrepancy in the minimum vibration metric  $J_z$  for minimized  $J$ .

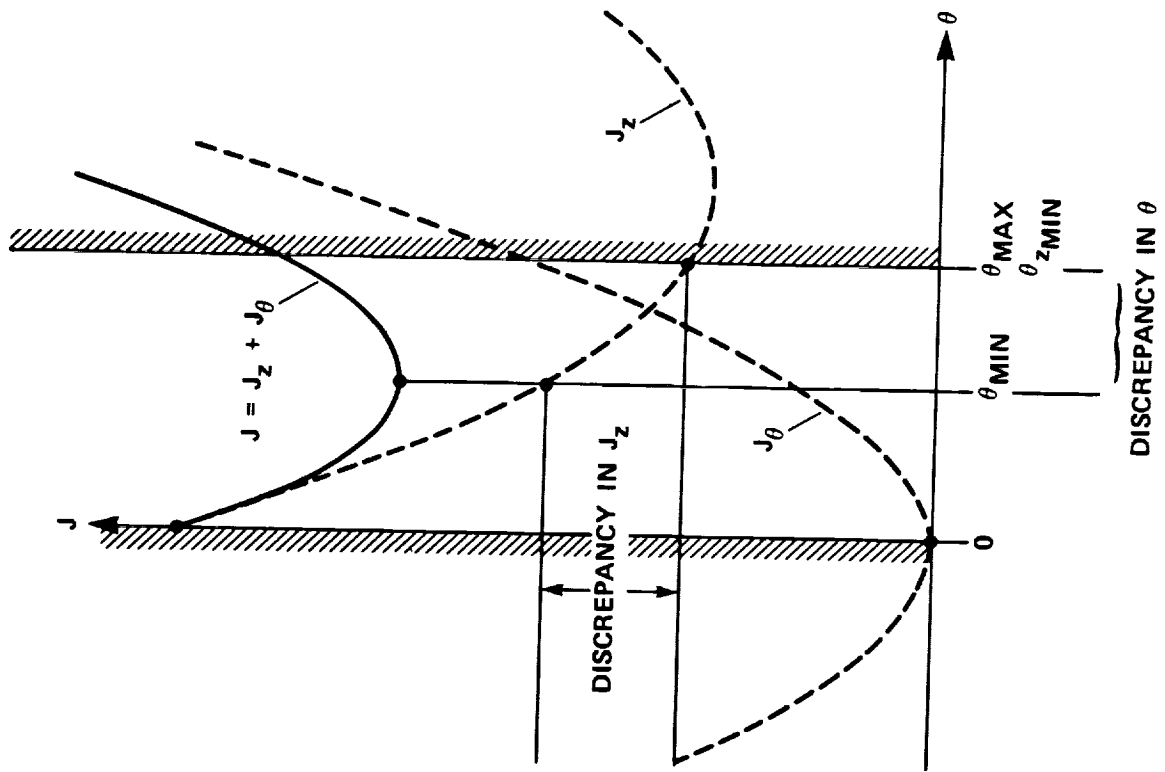


Figure 23. Second scalar case showing discrepancy in the minimum vibration metric  $J_z$  for minimized  $J$ .

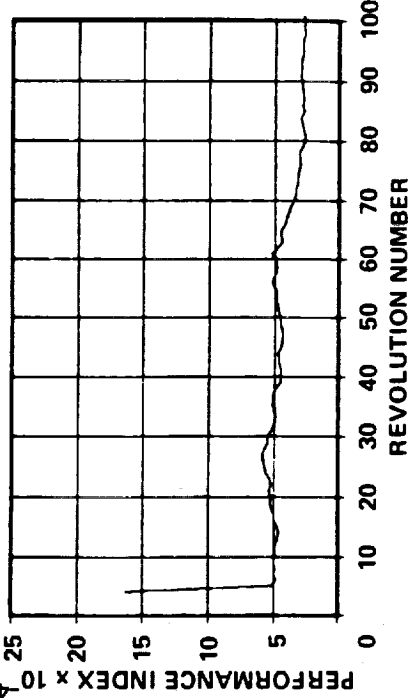


Figure 24. Response when propagation rate scaling coefficient  $C_p = 0.0005$ .

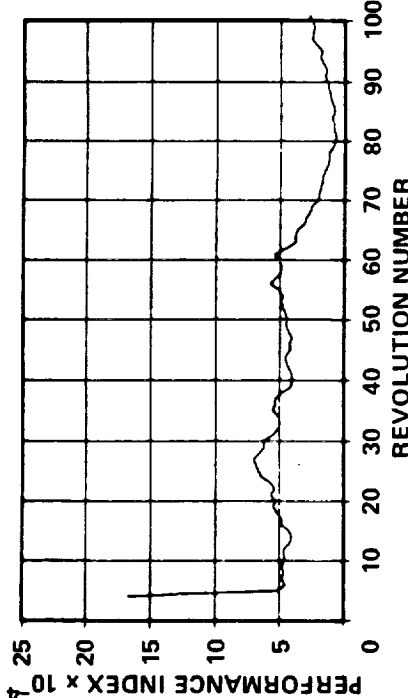


Figure 25. Response when propagation rate scaling coefficient  $C_p = 0.001$ .

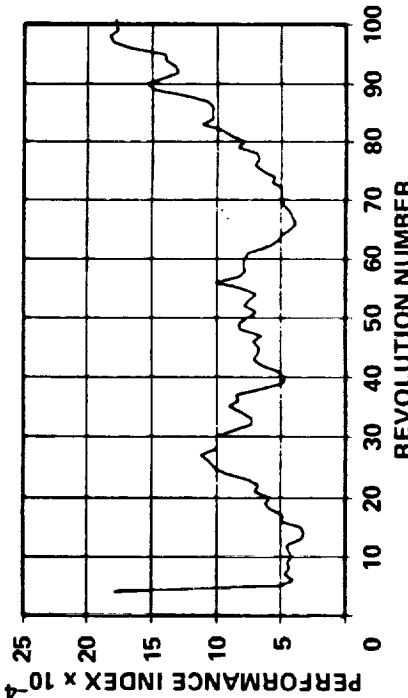


Figure 26. Response when propagation rate scaling coefficient  $C_p = 0.002$ .

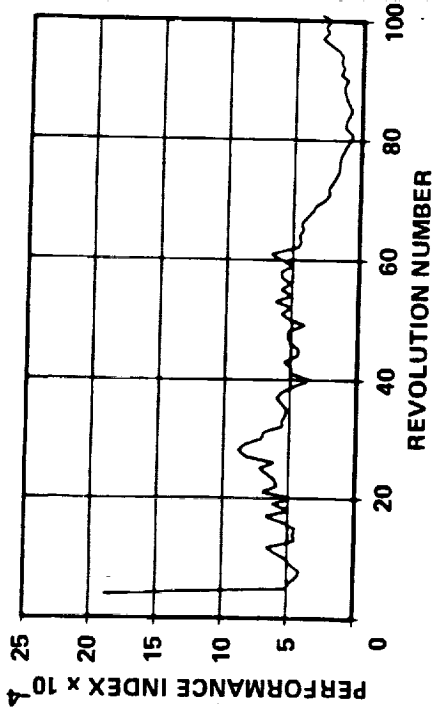


Figure 27. Deterministic controller response for initial  $T$ -matrix estimate defined by  $C_E = 0.001$ .

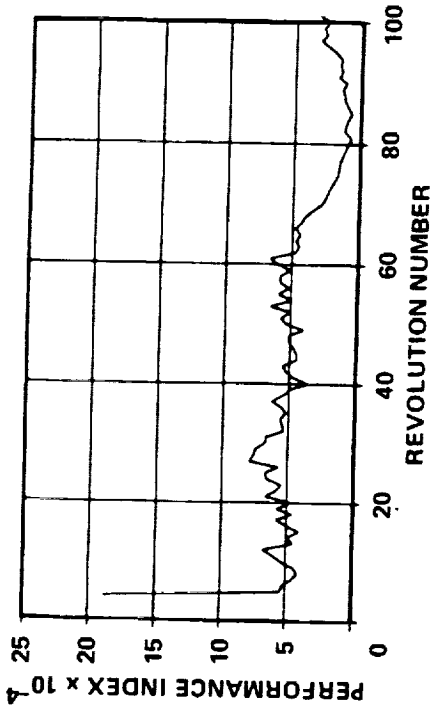


Figure 28. Deterministic controller response for initial  $T$ -matrix estimate defined by  $C_E = 0.01$ .

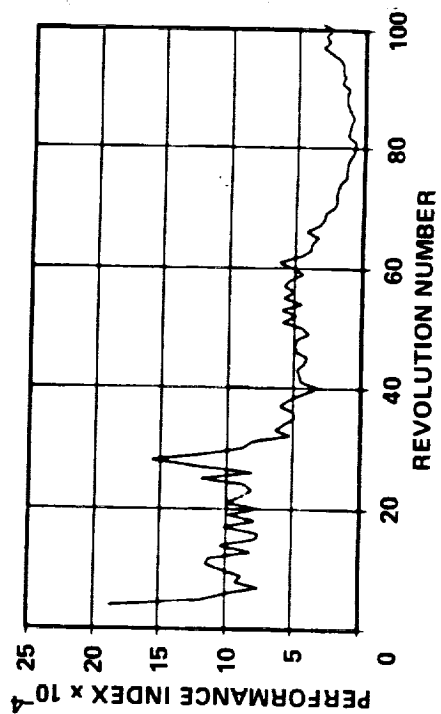


Figure 29. Deterministic controller response for initial  $T$ -matrix estimate defined by  $C_E = 0.1$ .

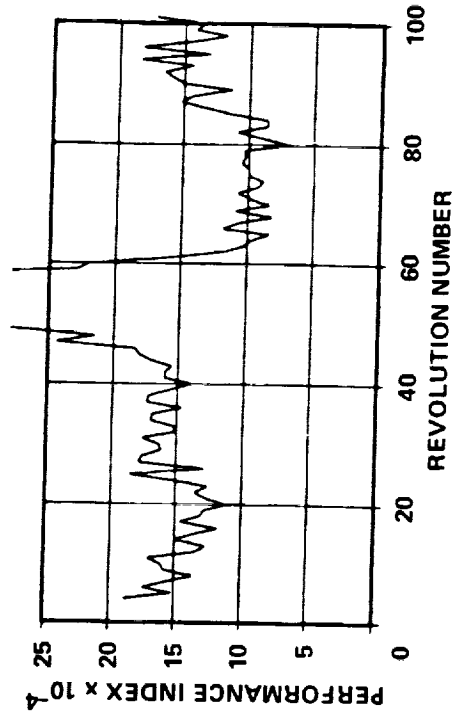


Figure 30. Deterministic controller response for initial  $T$ -matrix estimate defined by  $C_E = 1.0$ .

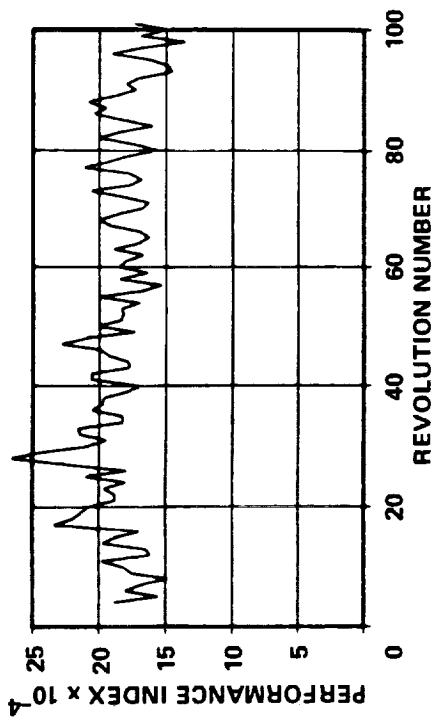


Figure 31. Deterministic controller response for initial  $T$ -matrix estimate defined by  $C_E = 10.0$ .

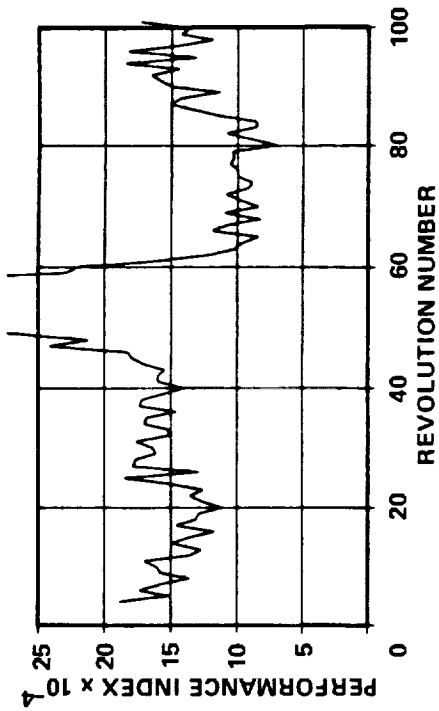


Figure 32. Cautious controller response for initial  $T$ -matrix estimate defined by  $C_E = 1.0$  and  $\lambda = 0.0001$ .

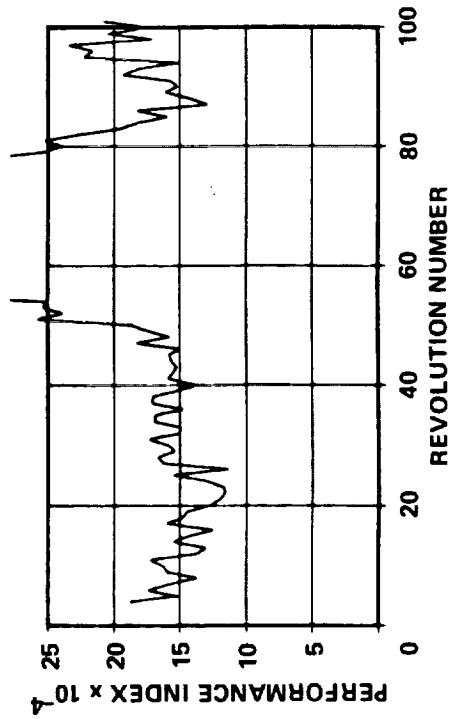


Figure 33. Cautious controller response for initial  $T$ -matrix estimate defined by  $C_E = 1.0$  and  $\lambda = 0.01$ .

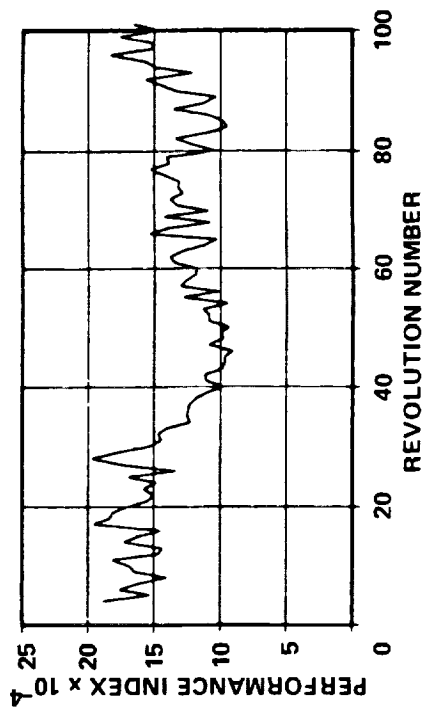


Figure 34. Cautious controller response for initial  $T$ -matrix estimate defined by  $C_E = 1.0$  and  $\lambda = 0.1$ .

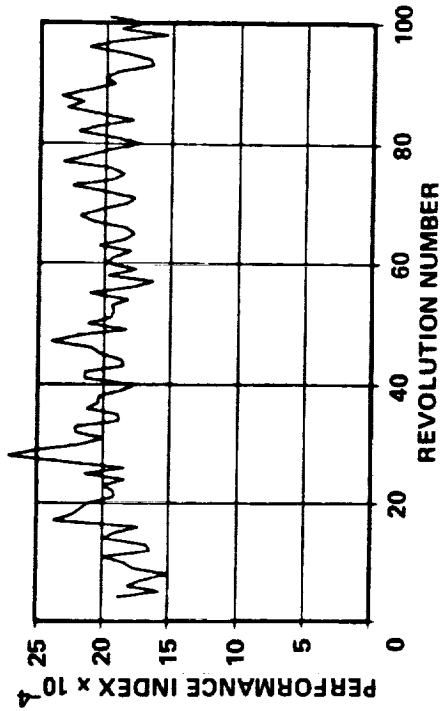


Figure 35. Cautious controller response for initial  $T$ -matrix estimate defined by  $C_E = 1.0$  and  $\lambda = 10.0$ .

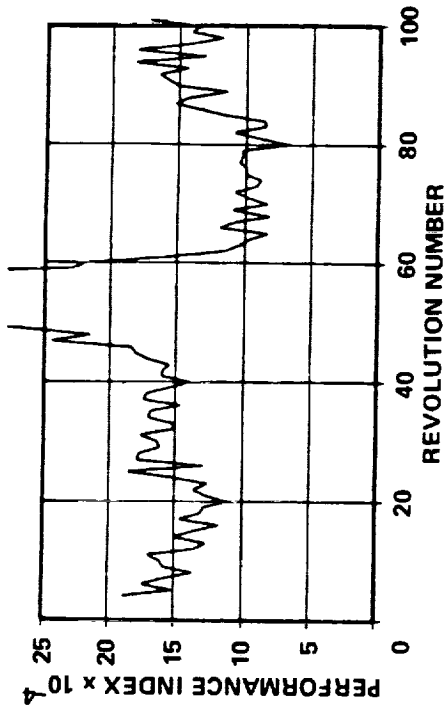


Figure 36. Dual controller response for initial  $T$ -matrix estimate defined by  $C_E = 1.0$  and  $\lambda = 0.000001$ .

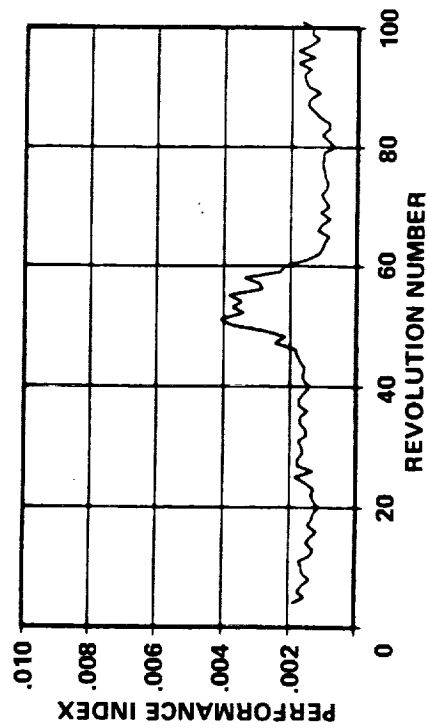


Figure 37. Dual controller response for initial  $T$ -matrix estimate defined by  $C_E = 1.0$  and  $\lambda = 0.000001$ .

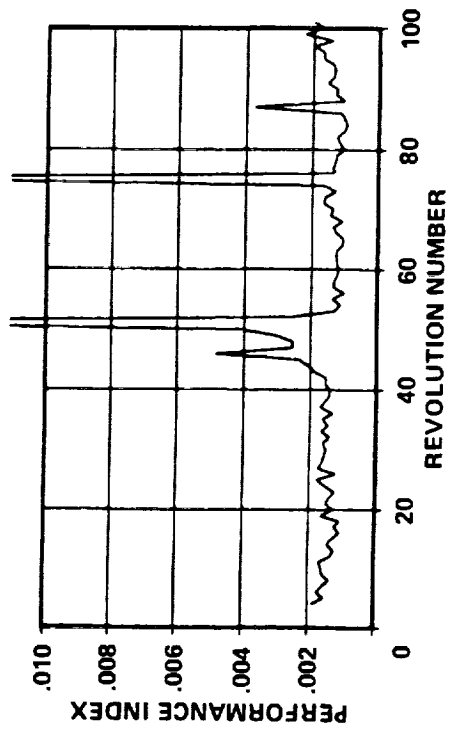


Figure 38. Dual controller response for initial  $T$ -matrix estimate defined by  $C_E = 1.0$  and  $\lambda = 0.0001$ .

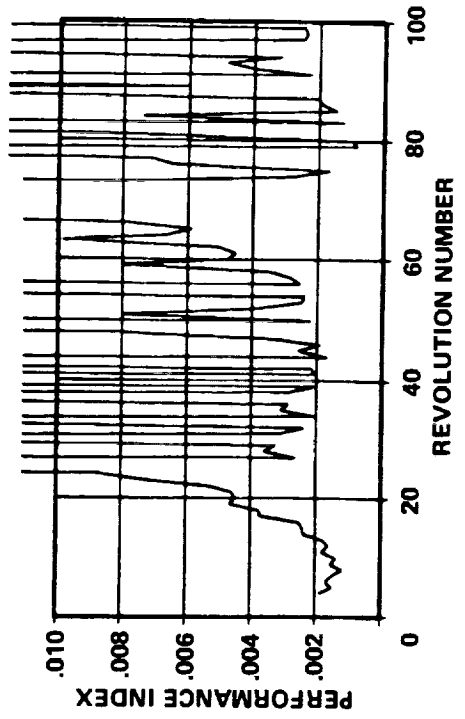


Figure 39. Dual controller response for initial  $T$ -matrix estimate defined by  $C_E = 1.0$  and  $\lambda = 0.001$ .

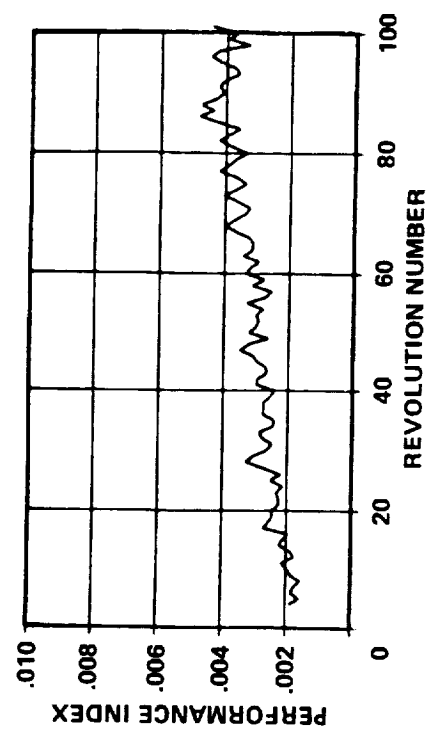


Figure 40. Dual controller response for initial  $T$ -matrix estimate defined by  $C_E = 1.0$  and  $\lambda = 0.01$ .

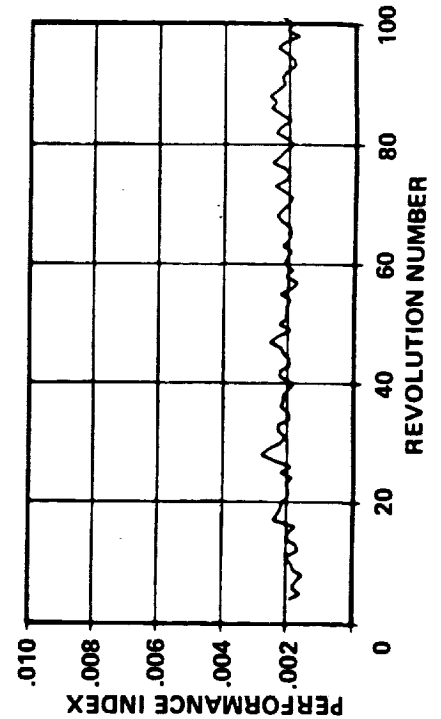


Figure 41. Dual controller response for initial  $T$ -matrix estimate defined by  $C_E = 1.0$  and  $\lambda = 0.1$ .

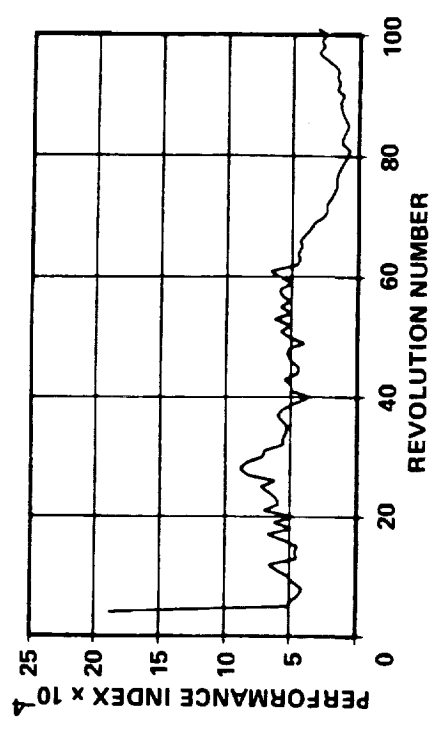


Figure 42. Deterministic controller response for  $T$ -matrix propagation rate defined by  $C_p = 0.0010$ .

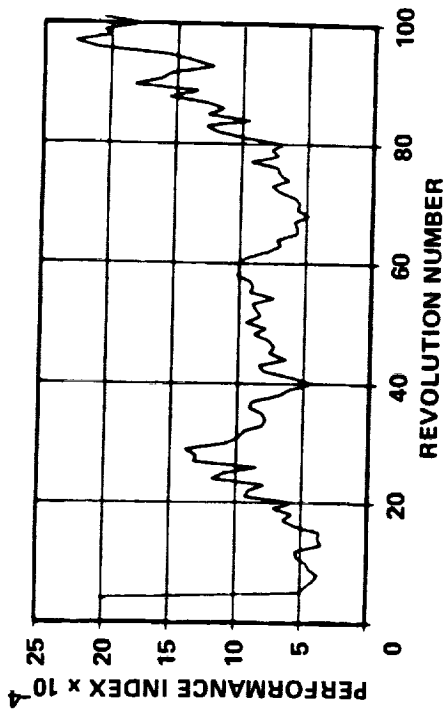


Figure 43. Deterministic controller response for  $T$ -matrix propagation rate defined by  $C_p = 0.0020$ .

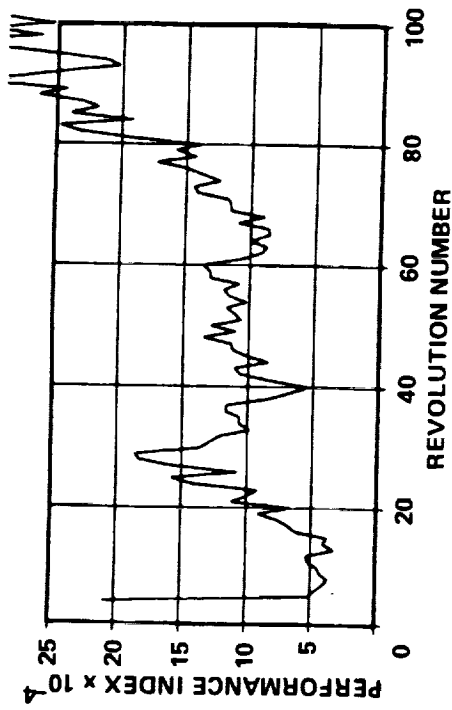


Figure 44. Deterministic controller response for  $T$ -matrix propagation rate defined by  $C_p = 0.0024$ .

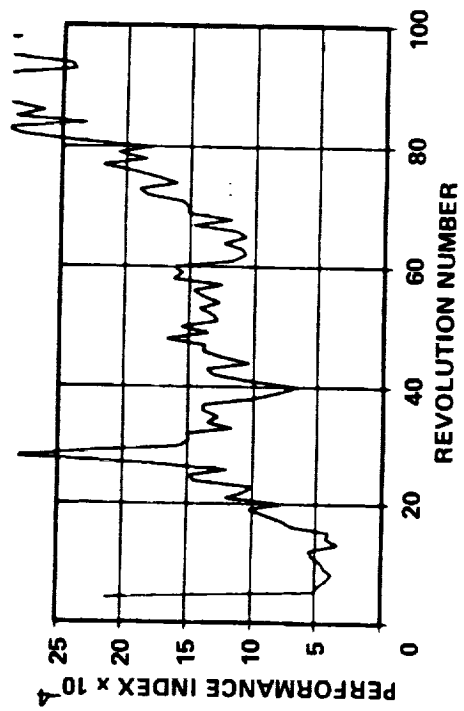


Figure 45. Deterministic controller response for  $T$ -matrix propagation rate defined by  $C_p = 0.0026$ .

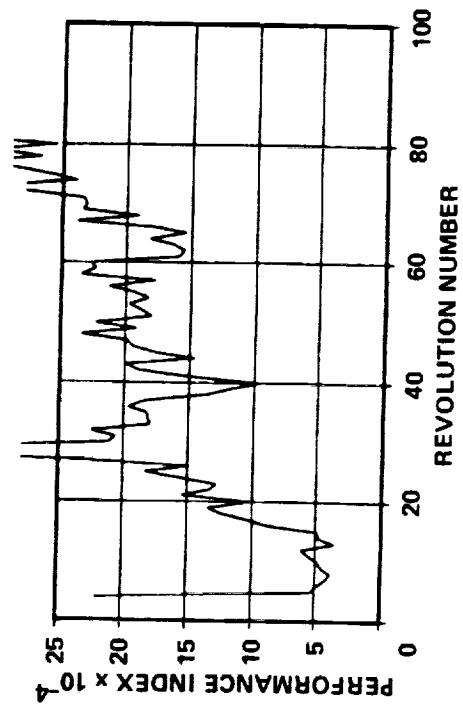


Figure 46. Deterministic controller response for  $T$ -matrix propagation rate defined by  $C_p = 0.0030$ .

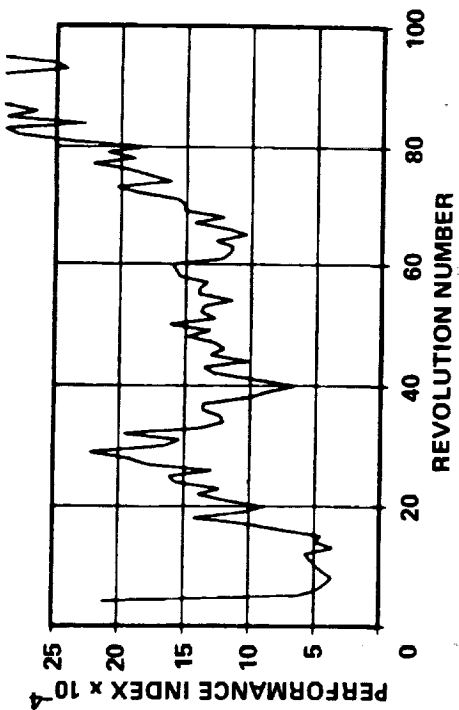


Figure 47. Cautious controller response for  $T$ -matrix propagation rate defined by  $C_p = 0.0026$  and  $\lambda = 0.0001$ .

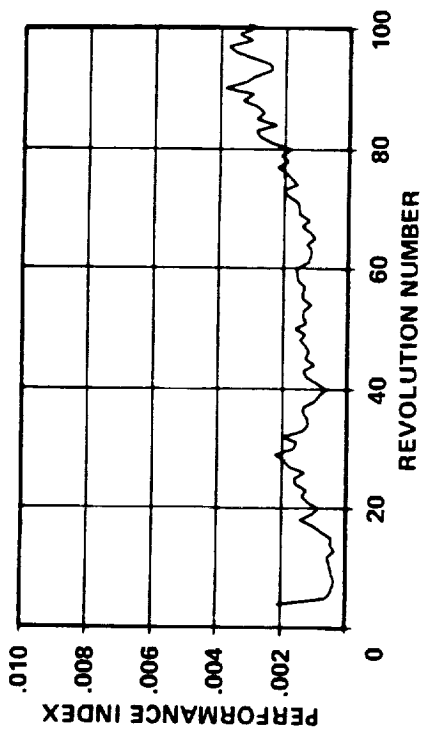


Figure 48. Cautious controller response for  $T$ -matrix propagation rate defined by  $C_p = 0.0026$  and  $\lambda = 0.0001$ .

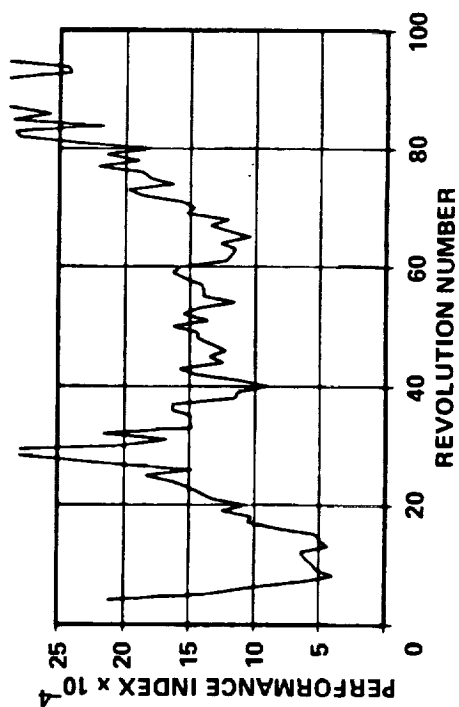


Figure 49. Cautious controller response for  $T$ -matrix propagation rate defined by  $C_p = 0.0026$  and  $\lambda = 0.001$ .

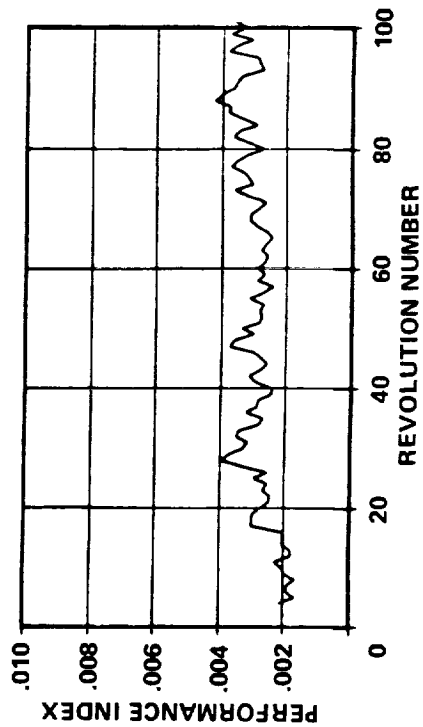


Figure 50. Cautious controller response for  $T$ -matrix propagation rate defined by  $C_p = 0.0026$  and  $\lambda = 0.01$ .

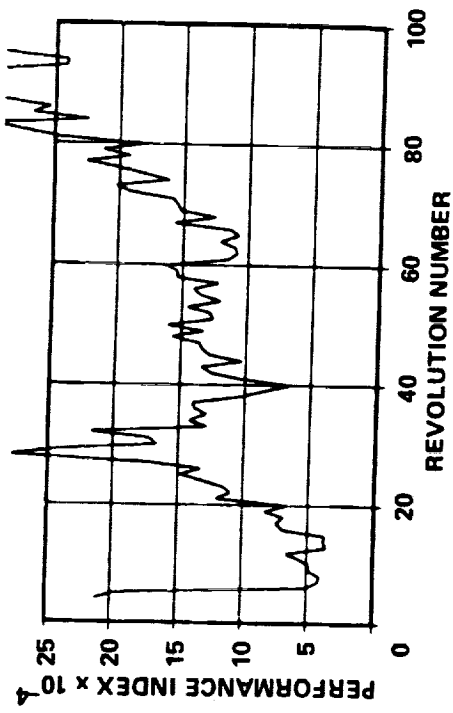


Figure 51. Dual controller response for  $T$ -matrix propagation rate defined by  $C_p = 0.0026$  and  $\lambda = 0.000001$ .

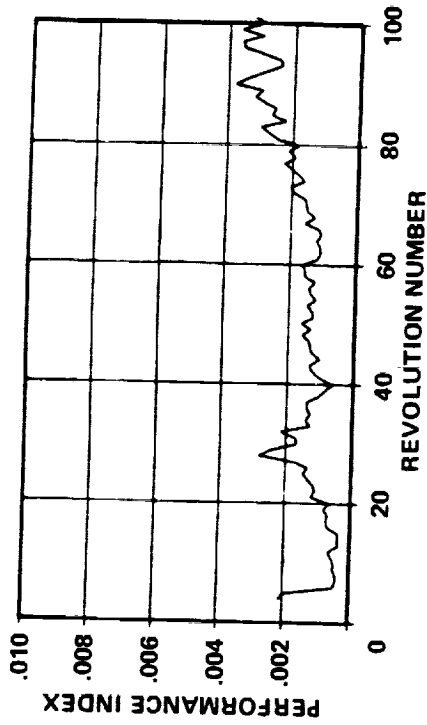


Figure 52. Dual controller response for  $T$ -matrix propagation rate defined by  $C_p = 0.0026$  and  $\lambda = 0.000001$ .

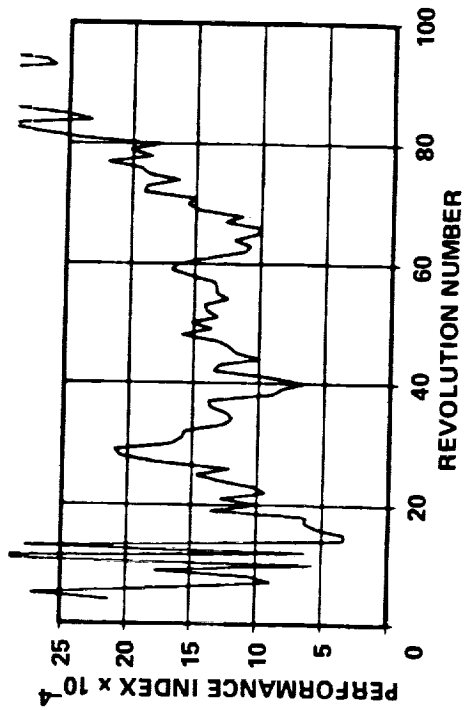


Figure 53. Dual controller response for  $T$ -matrix propagation rate defined by  $C_p = 0.0026$  and  $\lambda = 0.00001$ .

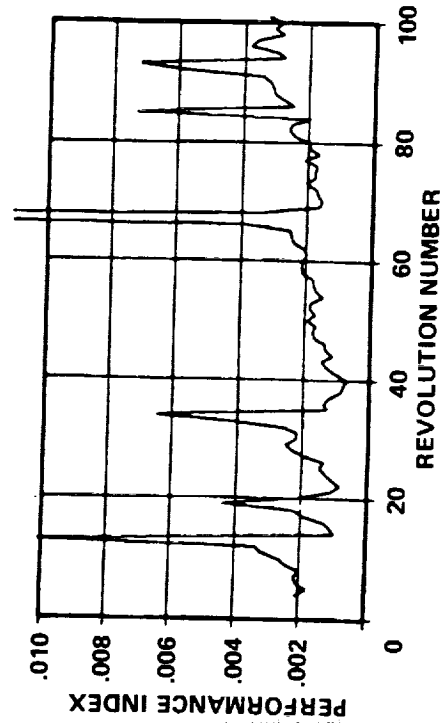


Figure 54. Dual controller response for  $T$ -matrix propagation rate defined by  $C_p = 0.0026$  and  $\lambda = 0.0001$ .

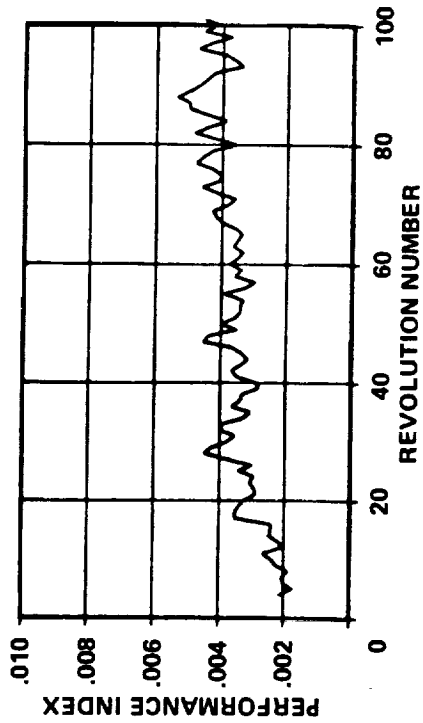


Figure 55. Dual controller response for  $T$ -matrix propagation rate defined by  $C_p = 0.0026$  and  $\lambda = 0.001$ .

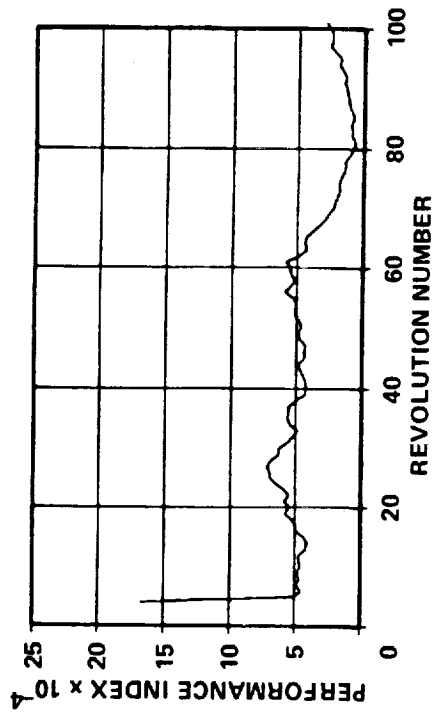


Figure 56. Deterministic controller response for no measurement noise ( $C_M = 0.0000$ ).

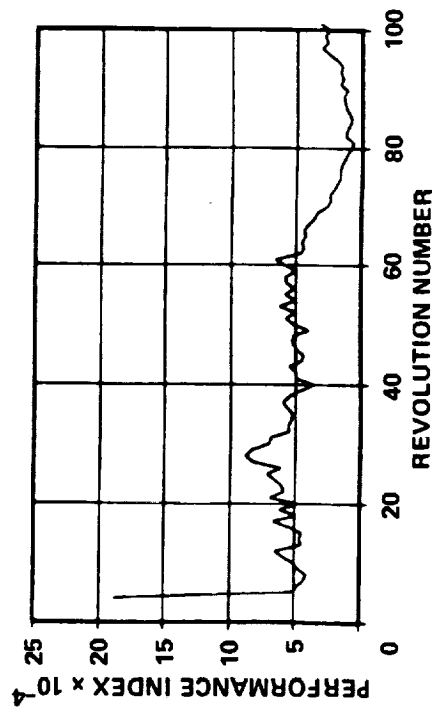


Figure 57. Deterministic controller response for measurement noise defined by  $C_M = 0.2000$ .

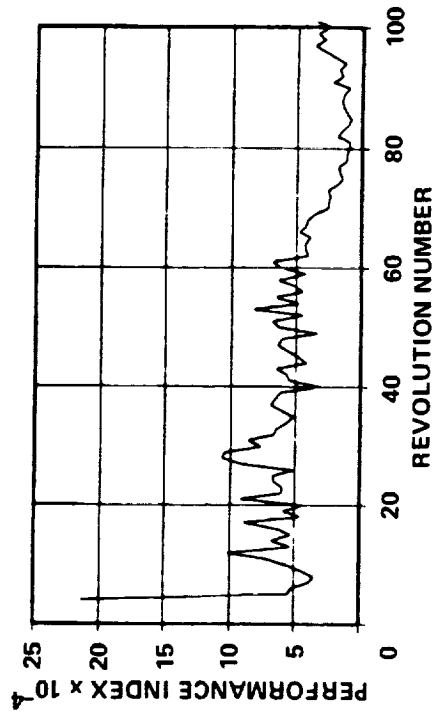


Figure 58. Deterministic controller response for measurement noise defined by  $C_M = 0.4000$ .

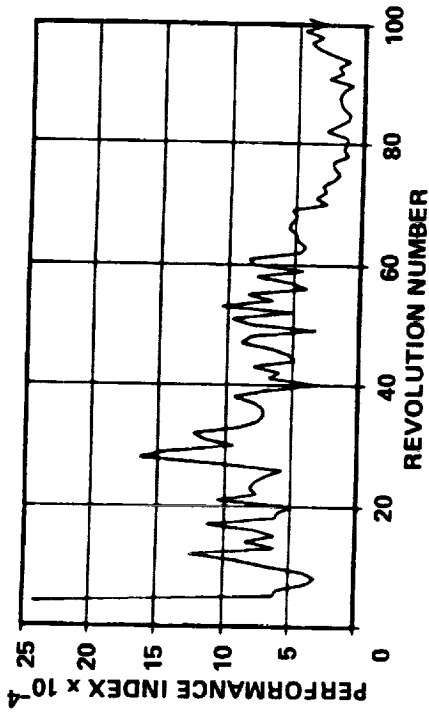


Figure 59. Deterministic controller response for measurement noise defined by  $C_M = 0.6000$ .

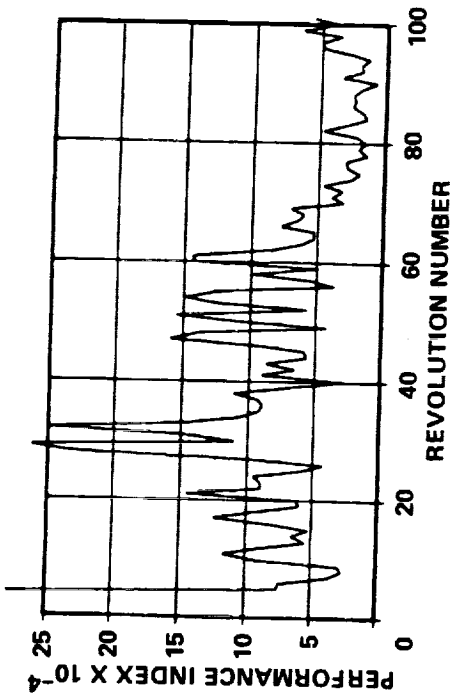


Figure 60. Deterministic controller response for measurement noise defined by  $C_M = 0.9000$ .

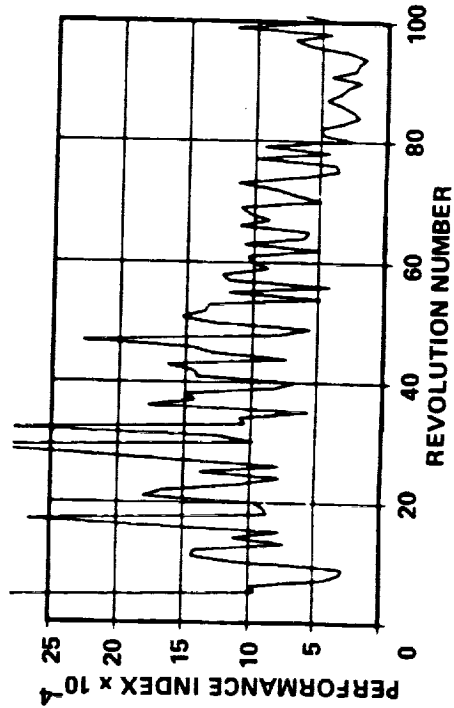


Figure 61. Deterministic controller response for measurement noise defined by  $C_M = 1.2000$ .

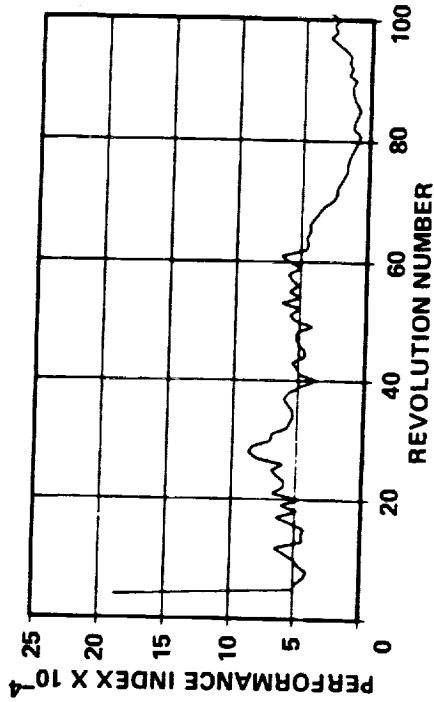


Figure 62. Cautious controller response for measurement noise defined by  $C_M = 0.2000$  and  $\lambda = 0.00001$ .

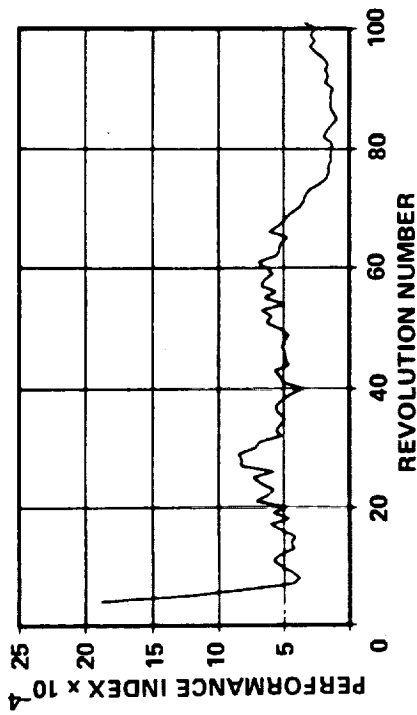


Figure 63. Cautious controller response for measurement noise defined by  $C_M = 0.2000$  and  $\lambda = 0.001$ .

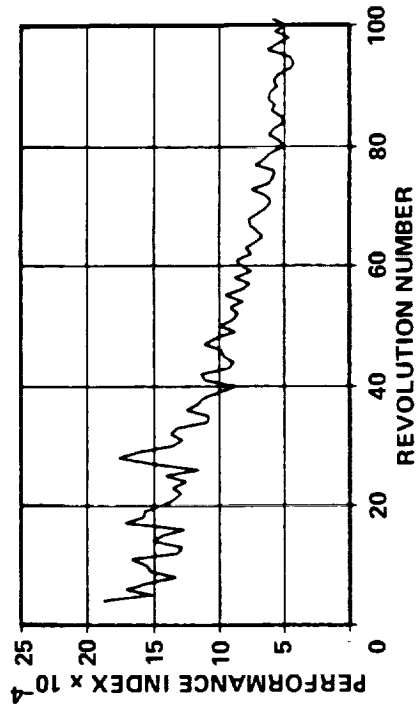


Figure 64. Cautious controller response for measurement noise defined by  $C_M = 0.2000$  and  $\lambda = 0.01$ .

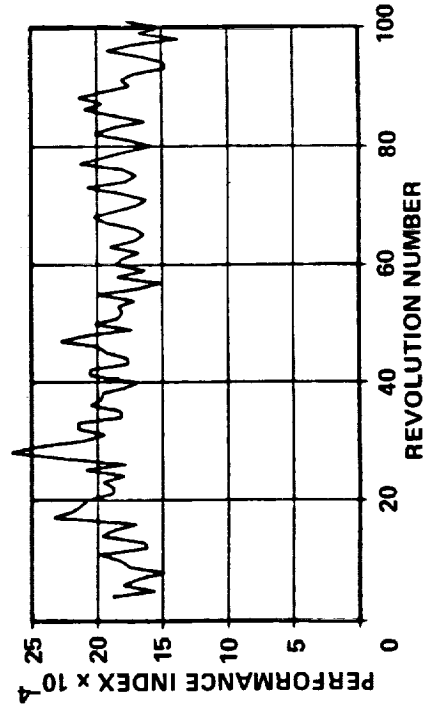


Figure 65. Cautious controller response for measurement noise defined by  $C_M = 0.2000$  and  $\lambda = 0.1$ .

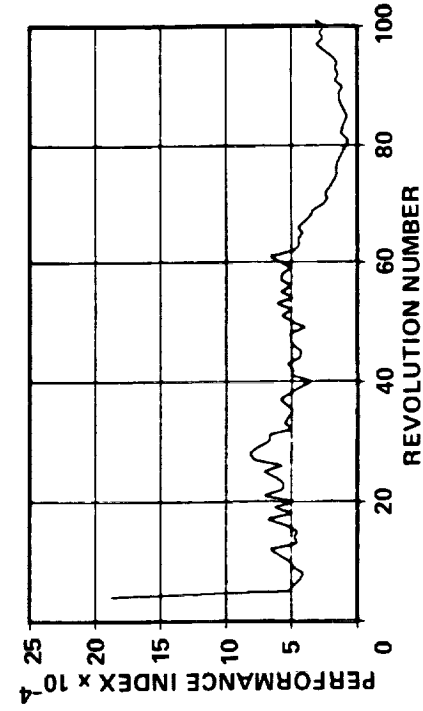


Figure 66. Dual controller response for measurement noise defined by  $C_M = 0.2000$  and  $\lambda = 0.0000001$ .

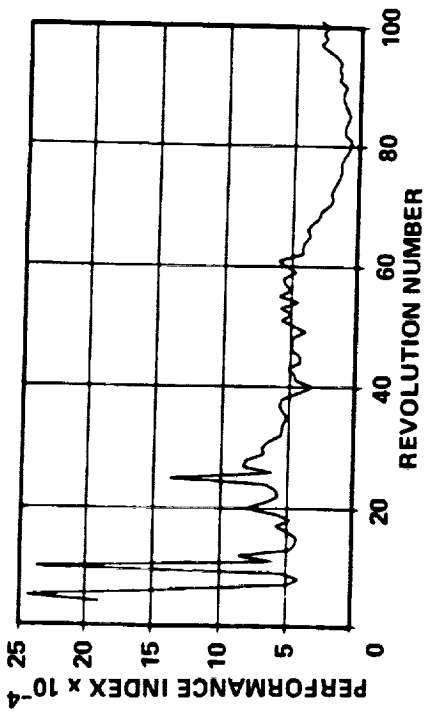


Figure 67. Dual controller response for measurement noise defined by  $C_M = 0.2000$  and  $\lambda = 0.00001$ .

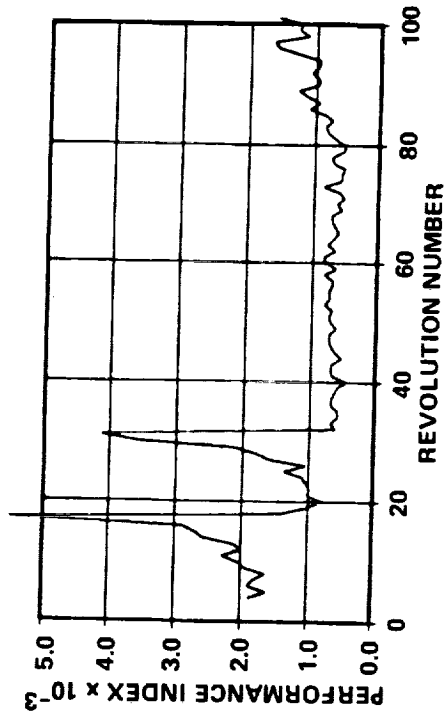


Figure 68. Dual controller response for measurement noise defined by  $C_M = 0.2000$  and  $\lambda = 0.0001$ .

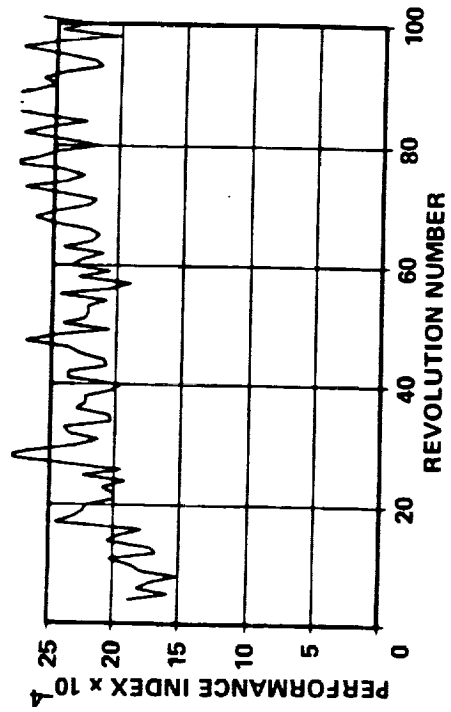


Figure 69. Dual controller response for measurement noise defined by  $C_M = 0.2000$  and  $\lambda = 0.001$ .

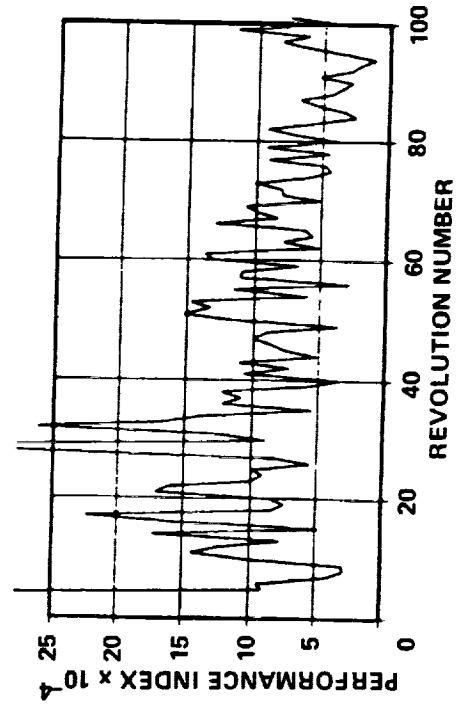


Figure 70. Cautious controller response for measurement noise defined by  $C_M = 1.2000$  and  $\lambda = 0.00001$ .

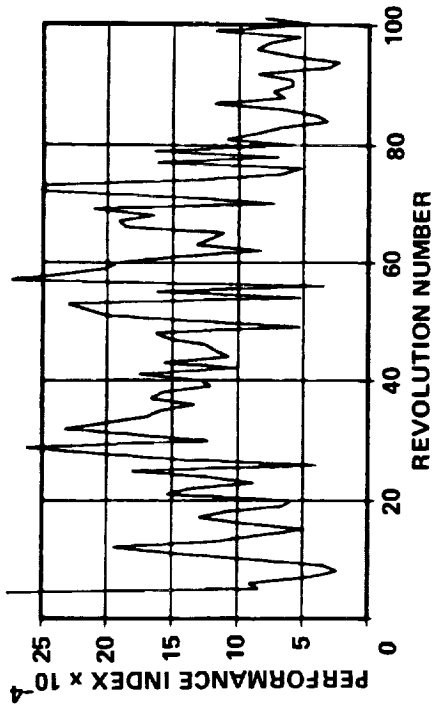


Figure 71. Cautious controller response for measurement noise defined by  $C_M = 1.2000$  and  $\lambda = 0.0001$ .

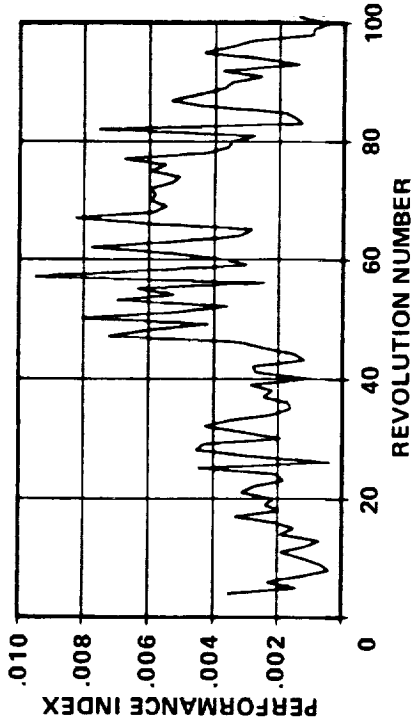


Figure 72. Cautious controller response for measurement noise defined by  $C_M = 1.2000$  and  $\lambda = 0.001$ .

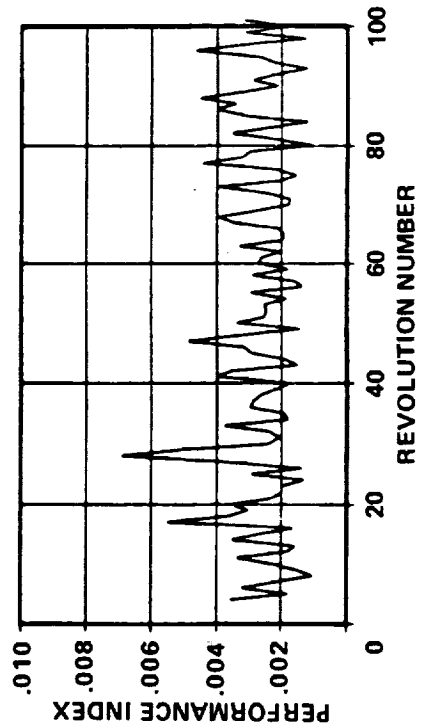


Figure 73. Cautious controller response for measurement noise defined by  $C_M = 1.2000$  and  $\lambda = 0.1$ .

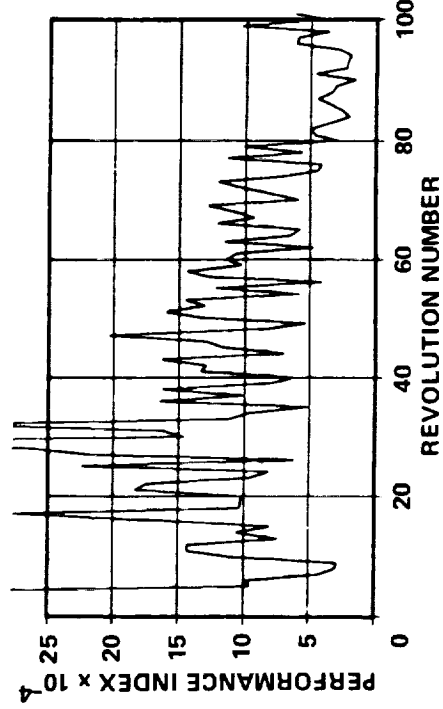


Figure 74. Dual controller response for measurement noise defined by  $C_M = 1.2000$  and  $\lambda = 0.00000001$ .

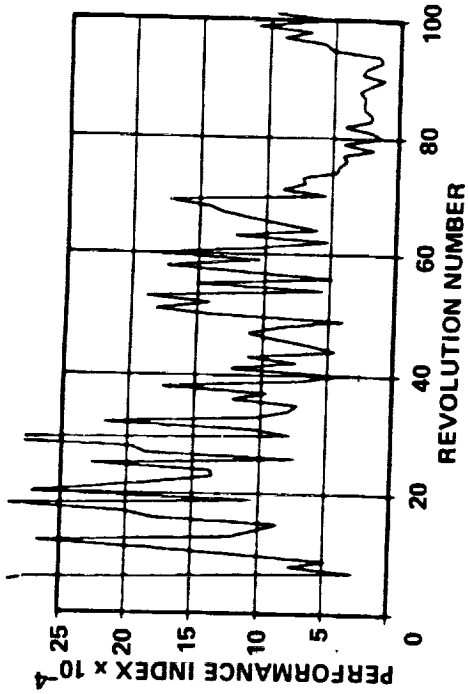


Figure 75. Dual controller response for measurement noise defined by  $C_M = 1.2000$  and  $\lambda = 0.000001$ .

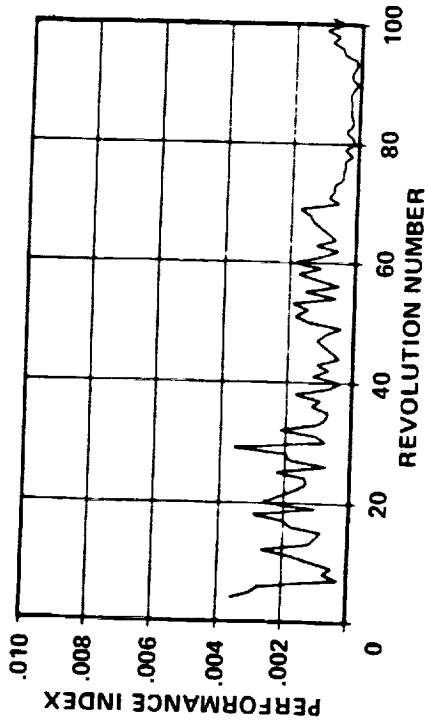


Figure 76. Dual controller response for measurement noise defined by  $C_M = 1.2000$  and  $\lambda = 0.000001$ .

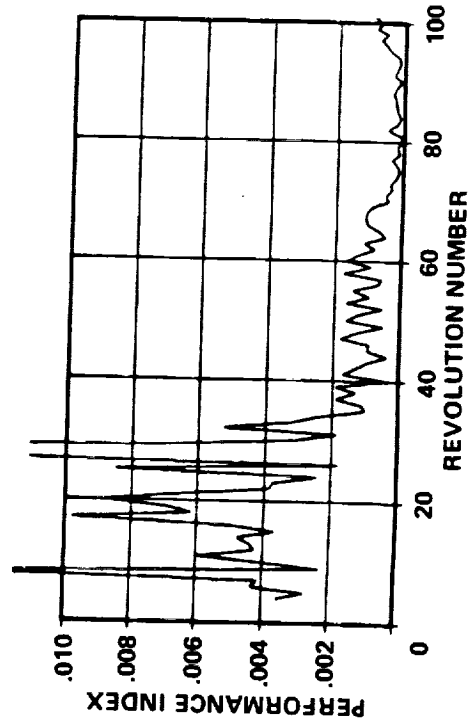


Figure 77. Dual controller response for measurement noise defined by  $C_M = 1.2000$  and  $\lambda = 0.00001$ .

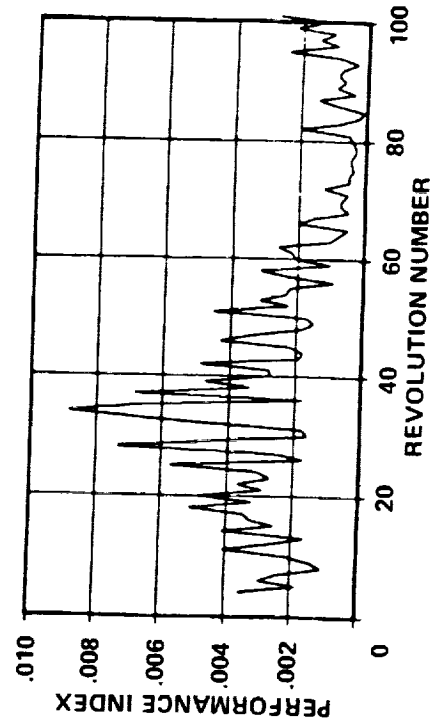


Figure 78. Dual controller response for measurement noise defined by  $C_M = 1.2000$  and  $\lambda = 0.0001$ .

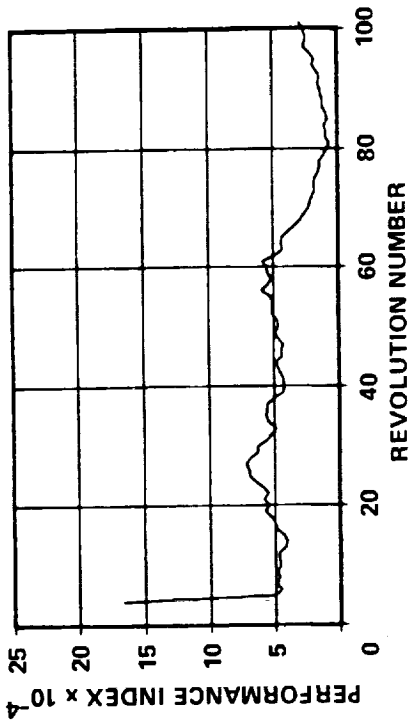


Figure 80. Deterministic controller response for no measurement noise ( $C_M = 0.0000$ ).

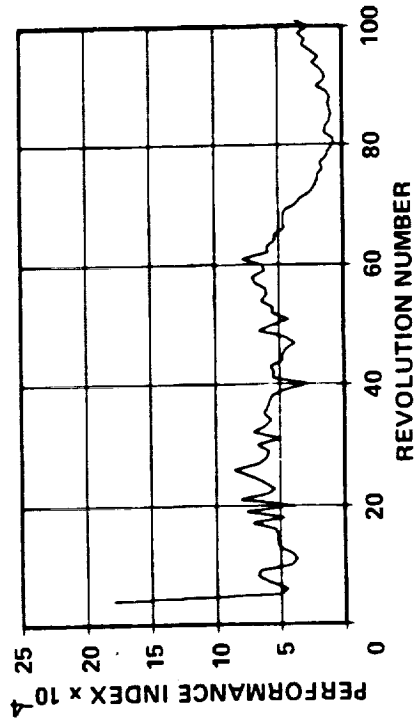


Figure 82. Deterministic controller response for random 20-cycle periodic measurement noise defined by  $C_M = 0.4000$ .

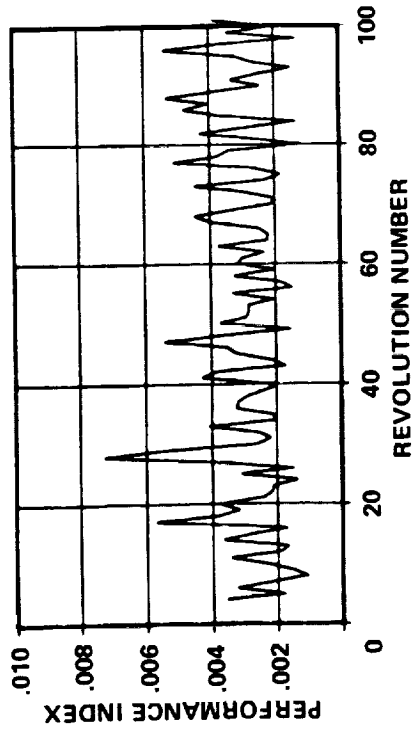


Figure 79. Dual controller response for measurement noise defined by  $C_M = 1.2000$  and  $\lambda = 0.001$ .

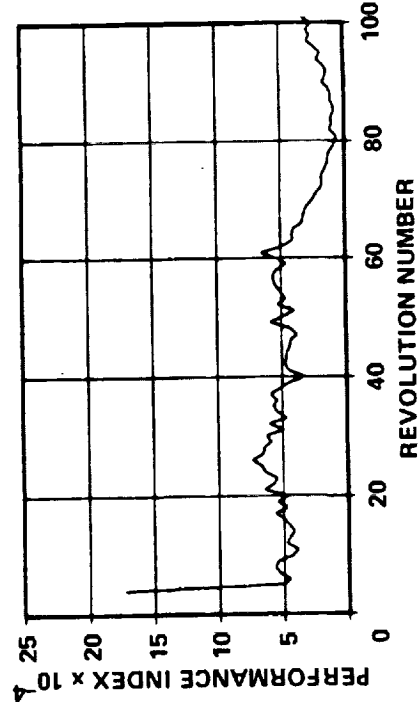


Figure 81. Deterministic controller response for random 20-cycle periodic measurement noise defined by  $C_M = 0.2000$ .

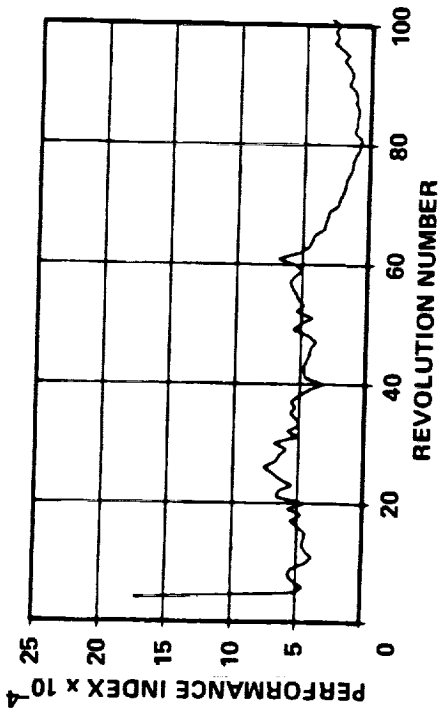


Figure 83. Cautious controller response for random 20-cycle periodic measurement noise defined by  $C_M = 0.2000$  and  $\lambda = 0.00001$ .

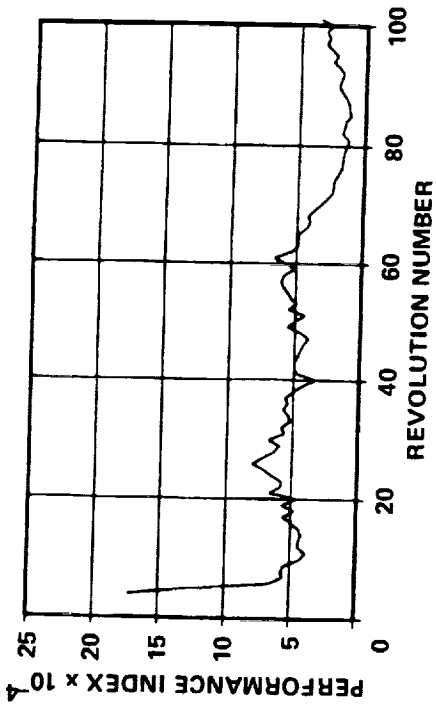


Figure 84. Cautious controller response for random 20-cycle periodic measurement noise defined by  $C_M = 0.2000$  and  $\lambda = 0.001$ .

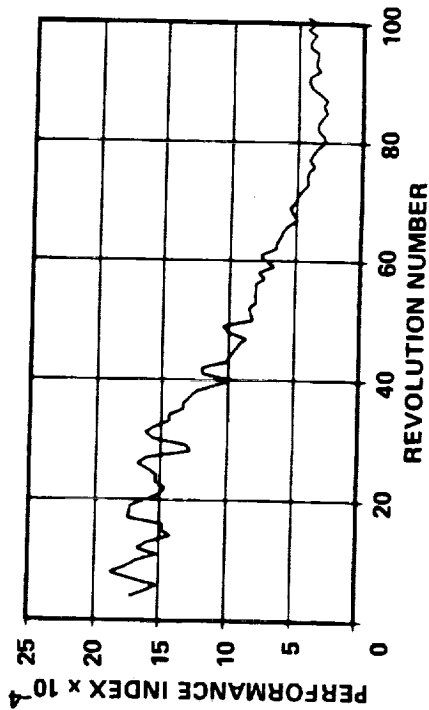


Figure 85. Cautious controller response for random 20-cycle periodic measurement noise defined by  $C_M = 0.2000$  and  $\lambda = 0.01$ .

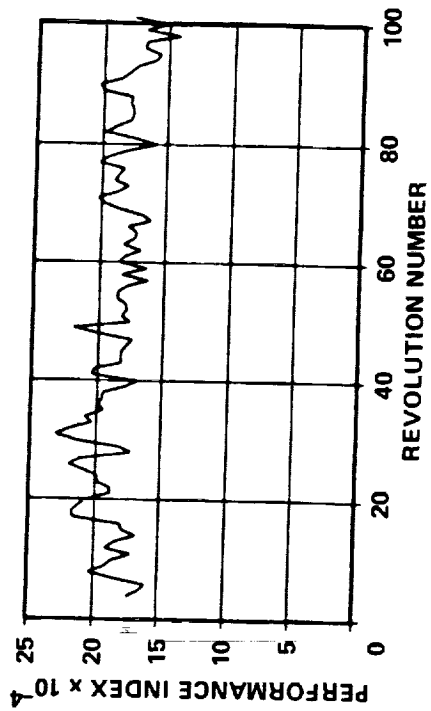


Figure 86. Cautious controller response for random 20-cycle periodic measurement noise defined by  $C_M = 0.2000$  and  $\lambda = 0.1$ .

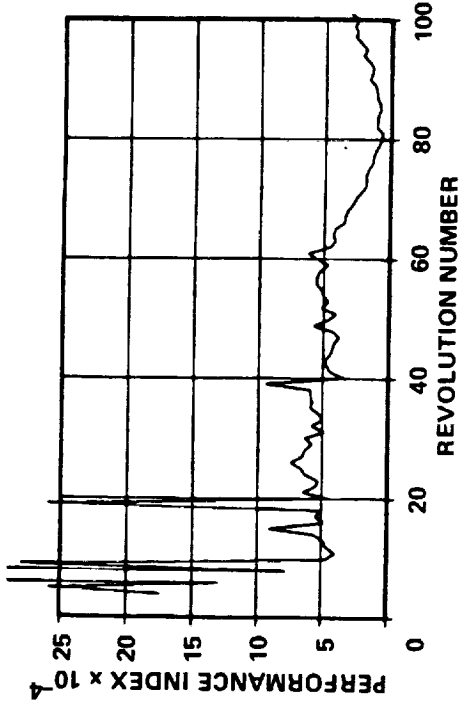


Figure 87. Dual controller response for random 20-cycle periodic measurement noise defined by  $C_M = 0.2000$  and  $\lambda = 0.00000001$ .

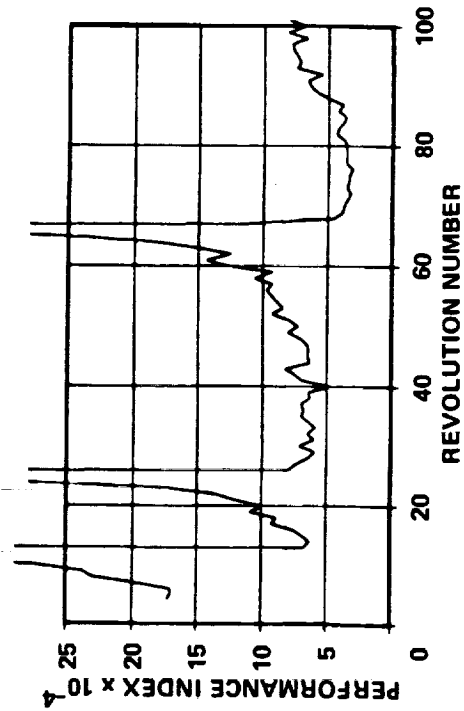


Figure 88. Dual controller response for random 20-cycle periodic measurement noise defined by  $C_M = 0.2000$  and  $\lambda = 0.000001$ .

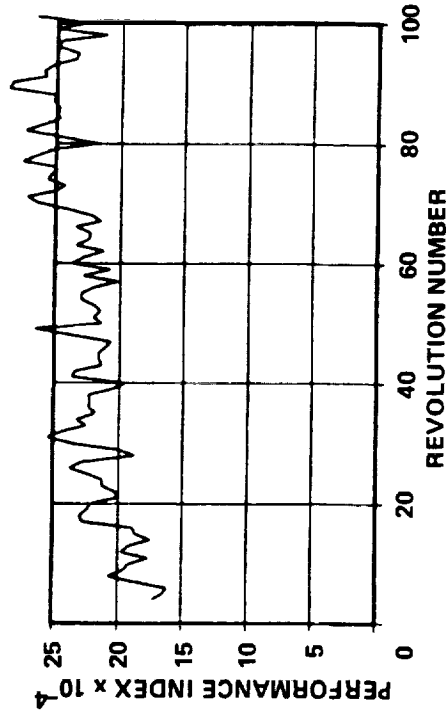


Figure 89. Dual controller response for random 20-cycle periodic measurement noise defined by  $C_M = 0.2000$ , and  $\lambda = 0.00001$ .

Figure 90. Dual controller response for random 20-cycle periodic measurement noise defined by  $C_M = 0.2000$  and  $\lambda = 0.001$ .

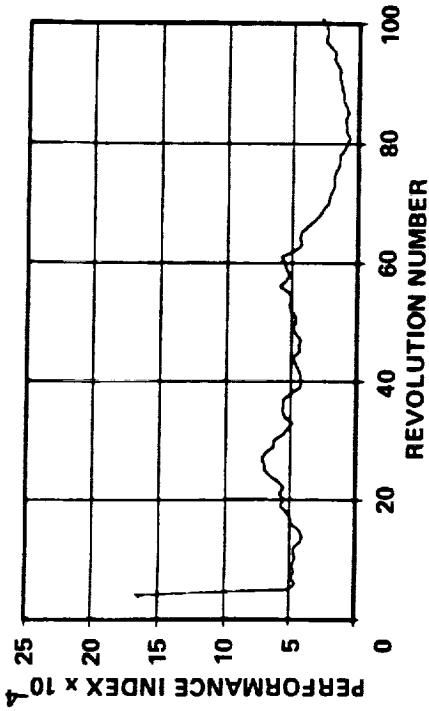


Figure 91. Deterministic controller response for no measurement noise ( $C_M = 0.0000$ ).

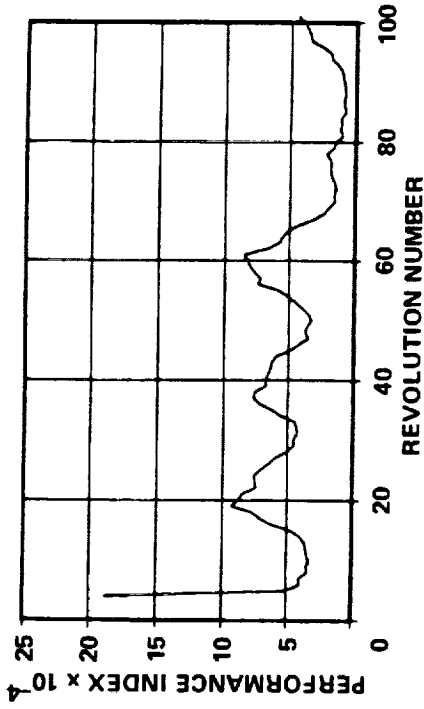


Figure 92. Deterministic controller response for nonrandom 20-cycle periodic measurement noise defined by  $C_M = 0.2000$ .

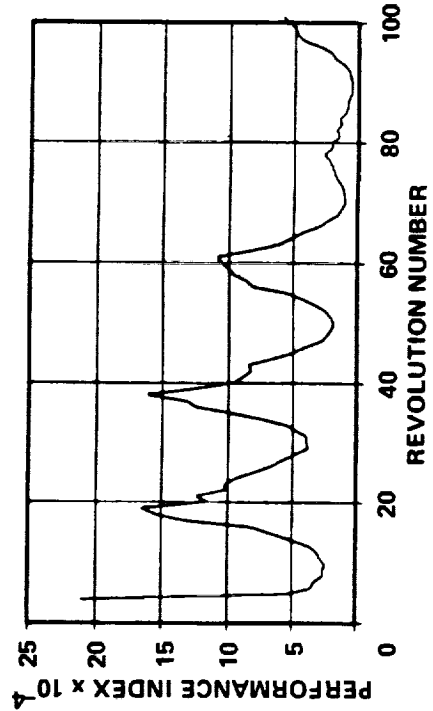


Figure 93. Deterministic controller response for nonrandom 20-cycle periodic measurement noise defined by  $C_M = 0.4000$ .

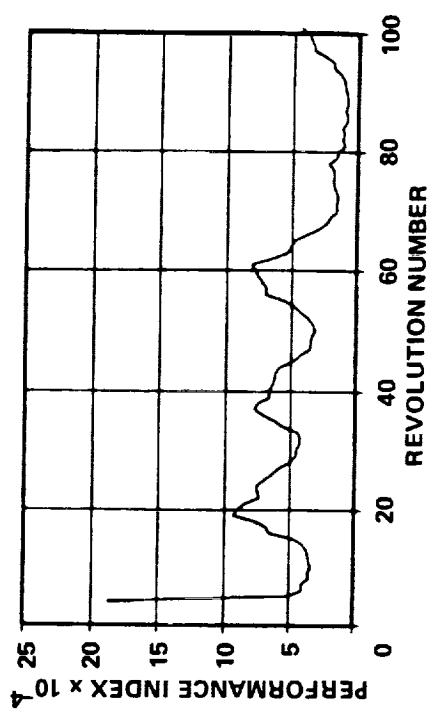


Figure 94. Cautious controller response for nonrandom 20-cycle periodic measurement noise defined by  $C_M = 0.2000$  and  $\lambda = 0.00001$ .

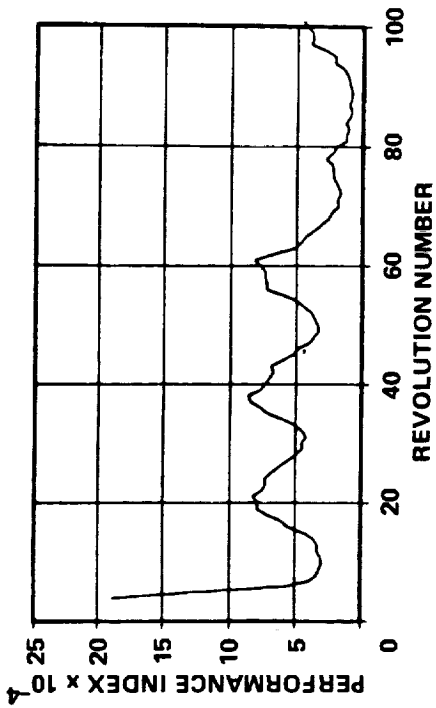


Figure 95. Cautious controller response for non-random 20-cycle periodic measurement noise defined by  $C_M = 0.2000$  and  $\lambda = 0.001$ .

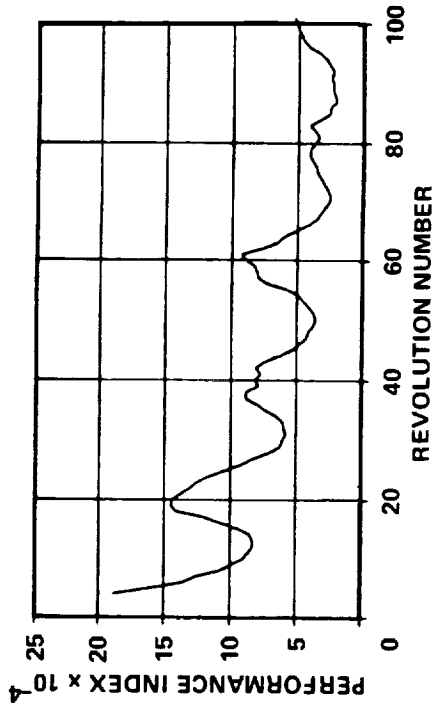


Figure 96. Cautious controller response for non-random 20-cycle periodic measurement noise defined by  $C_M = 0.2000$  and  $\lambda = 0.01$ .

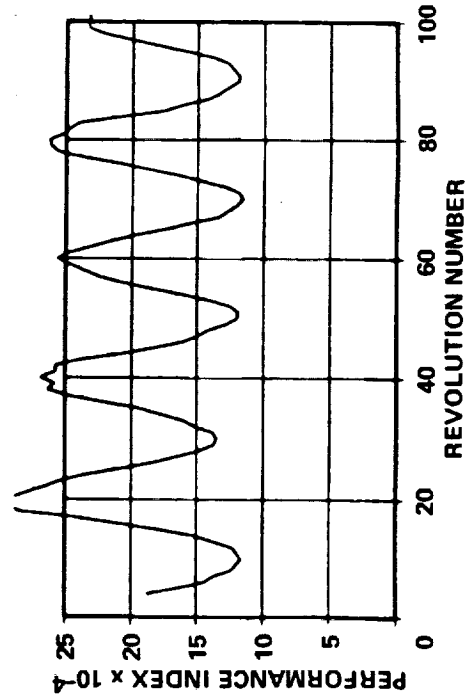


Figure 97. Cautious controller response for non-random 20-cycle periodic measurement noise defined by  $C_M = 0.2000$  and  $\lambda = 0.1$ .

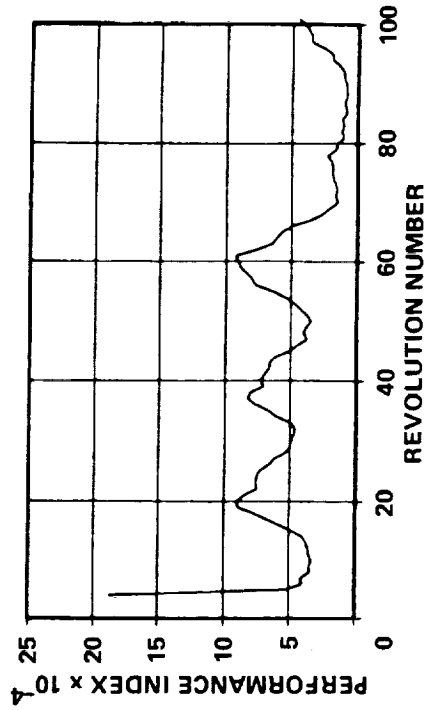


Figure 98. Dual controller response for non-random 20-cycle periodic measurement noise defined by  $C_M = 0.2000$  and  $\lambda = 0.0000001$ .

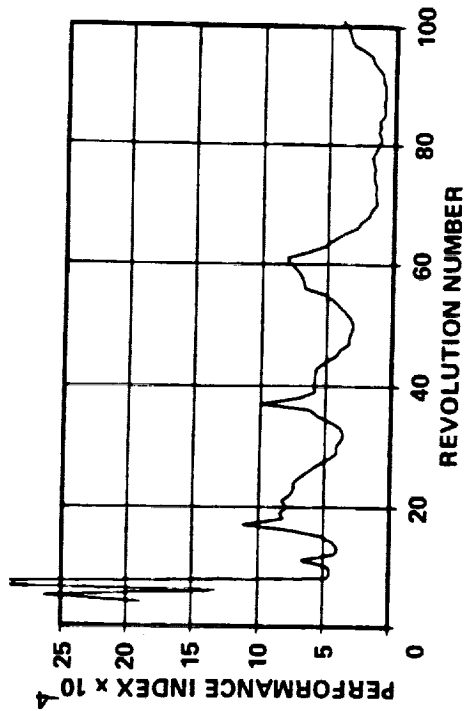


Figure 99. Dual controller response for nonrandom 20-cycle periodic measurement noise defined by  $C_M = 0.2000$  and  $\lambda = 0.00001$ .

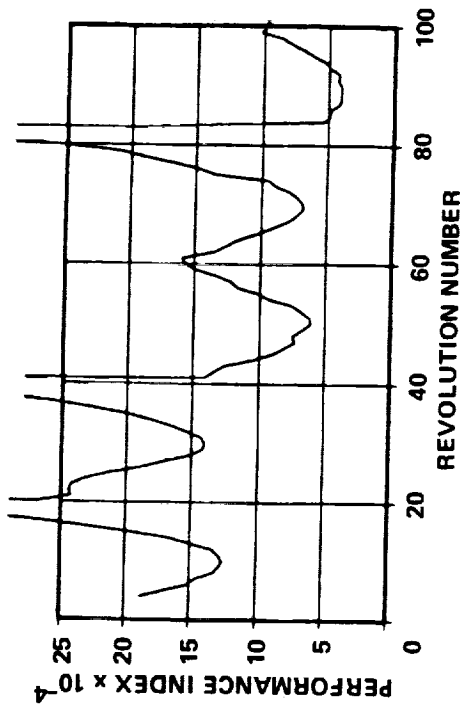


Figure 100. Dual controller response for nonrandom 20-cycle periodic measurement noise defined by  $C_M = 0.2000$  and  $\lambda = 0.0001$ .

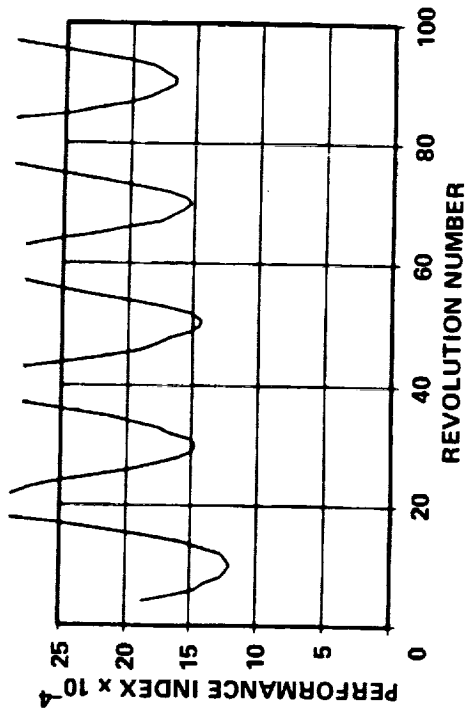


Figure 101. Dual controller response for nonrandom 20-cycle periodic measurement noise defined by  $C_M = 0.2000$  and  $\lambda = 0.001$ .

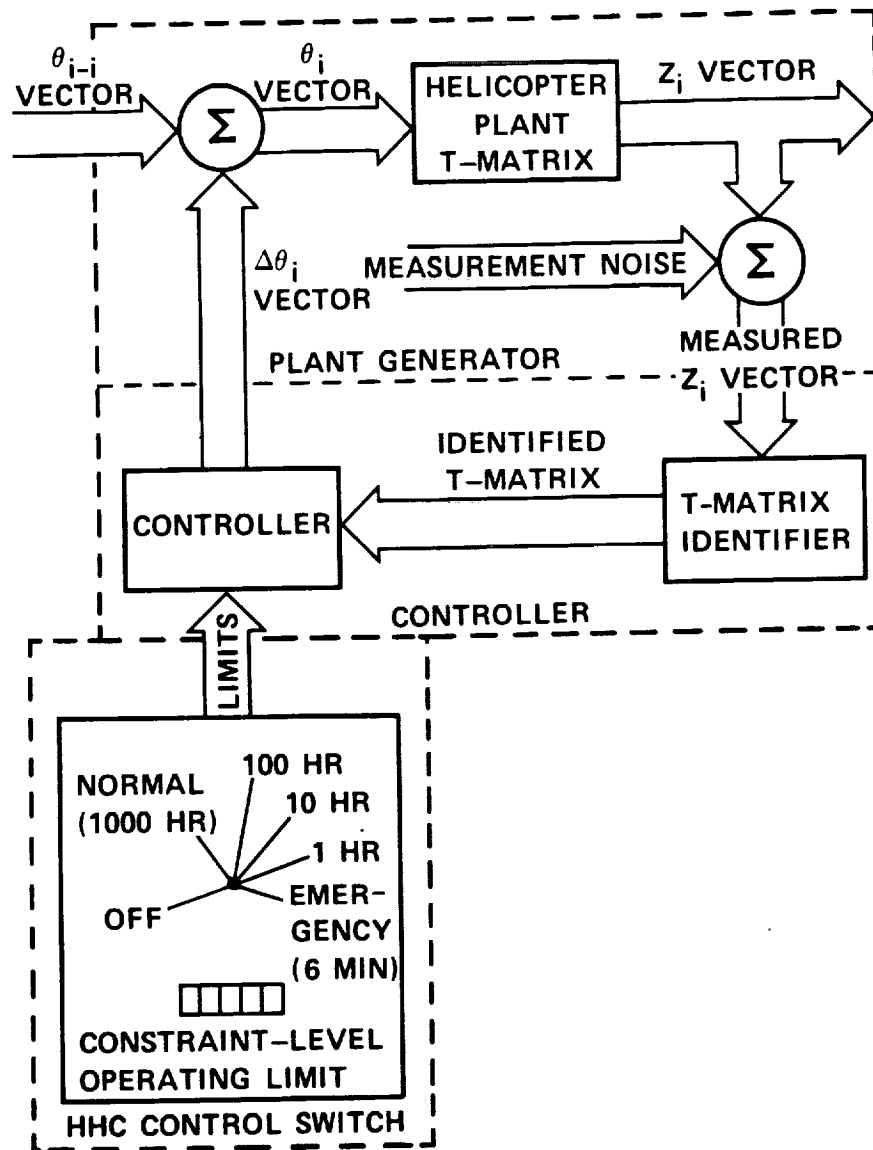


Figure 102. HHC controller with control switch.

# REPORT DOCUMENTATION PAGE

Form Approved  
OMB No. 0704-0188

Public reporting burden for this collection of information is estimated to average 1 hour per response, including the time for reviewing instructions, searching existing data sources, gathering and maintaining the data needed, and completing and reviewing the collection of information. Send comments regarding this burden estimate or any other aspect of this collection of information, including suggestions for reducing this burden, to Washington Headquarters Services, Directorate for Information Operations and Reports, 1215 Jefferson Davis Highway, Suite 1204, Arlington, VA 22202-4302, and to the Office of Management and Budget, Paperwork Reduction Project (0704-0188), Washington, DC 20503.

1. AGENCY USE ONLY (Leave blank)		2. REPORT DATE May 1992	3. REPORT TYPE AND DATES COVERED Technical Memorandum	
4. TITLE AND SUBTITLE Comparison of Three Controllers Applied to Helicopter Vibration			5. FUNDING NUMBERS 505-61-51	
6. AUTHOR(S) Jane A. Leyland			7. PERFORMING ORGANIZATION NAME(S) AND ADDRESS(ES) Ames Research Center Moffett Field, CA 94035-1000	
7. PERFORMING ORGANIZATION NAME(S) AND ADDRESS(ES) Ames Research Center Moffett Field, CA 94035-1000			8. PERFORMING ORGANIZATION REPORT NUMBER A-89130	
9. SPONSORING/MONITORING AGENCY NAME(S) AND ADDRESS(ES) National Aeronautics and Space Administration Washington, DC 20546-0001			10. SPONSORING/MONITORING AGENCY REPORT NUMBER NASA TM-102192	
11. SUPPLEMENTARY NOTES Point of Contact: Jane A. Leyland, Ames Research Center, MS T042, Moffett Field, CA 94035-1000 (415) 604-3092 or FTS 464-3092				
12a. DISTRIBUTION/AVAILABILITY STATEMENT Unclassified — Unlimited Subject Category 08			12b. DISTRIBUTION CODE	
13. ABSTRACT (Maximum 200 words) A comparison was made of the applicability and suitability of the deterministic controller, the cautious controller, and the dual controller for the reduction of helicopter vibration by using higher harmonic blade pitch control. A randomly generated linear plant model was assumed and the performance index was defined to be a quadratic output metric of this linear plant. A computer code, designed to check out and evaluate these controllers, was implemented and used to accomplish this comparison. The effects of random measurement noise, the initial estimate of the plant matrix, and the plant matrix propagation rate were determined for each of the controllers. With few exceptions, the deterministic controller yielded the greatest vibration reduction (as characterized by the quadratic output metric) and operated with the greatest reliability. Theoretical limitations of these controllers were defined and appropriate candidate alternative methods, including one method particularly suitable to the cockpit, were identified.				
14. SUBJECT TERMS Helicopter vibration control, Higher harmonic control, Helicopter controller			15. NUMBER OF PAGES 90	
			16. PRICE CODE A05	
17. SECURITY CLASSIFICATION OF REPORT Unclassified	18. SECURITY CLASSIFICATION OF THIS PAGE Unclassified	19. SECURITY CLASSIFICATION OF ABSTRACT	20. LIMITATION OF ABSTRACT	